IAEA-TECDOC-1262

Radiotracer technology as applied to industry

Final report of a co-ordinated research project 1997–2000

INTERNATIONAL ATOMIC ENERGY AGENCY IAEA

December 2001

The originating Section of this publication in the IAEA was:

Industrial Applications and Chemistry Section
International Atomic Energy Agency
Wagramer Strasse 5
P.O. Box 100
A-1400 Vienna, Austria

RADIOTRACER TECHNOLOGY AS APPLIED TO INDUSTRY
IAEA, VIENNA, 2001
IAEA-TECDOC-1262
ISSN 1011–4289

Printed by the IAEA in Austria
December 2001

FOREWORD

The Co-ordinated Research Project (CRP) on Radiotracer Technology for Engineering Unit Operation Studies and Unit Process Optimization was carried out by the International Atomic Energy Agency (IAEA) from December 1997 until December 2000. The project developed and validated procedures and protocols for investigation of major industrial processes, including fluidized beds, sugar crystallizers, trickle bed reactors, cement rotary kilns, flotation cells, grinding mills, incinerators, wastewater treatment units and interwell communications in oil fields.

Over the years, the IAEA has contributed substantial funding and effort to industrial applications of radiotracer technology. Significant progress has been made, enabling IAEA Member States to introduce the technology in well defined industrial processing fields and establish national and private radiotracer groups with the indigenous capacity to sustain and further develop the technology. There are currently more than 50 radiotracer groups in the developing Member States of the IAEA applying radiotracers in routine service to end users.

This publication is the output of the above mentioned CRP. It provides the principles and state of the art of radiotracer methodology and technology as applied to industry and environment. It is expected to provide wider interest for further development of skills and confidence prior to carrying out field work. It facilitates transfer of technology from developed to developing countries and from nuclear research institutions to industrial end users. The publication could be a suitable guide for radiotracer applications in almost all types of process investigations. The case studies described in this publication deal with typical problems in industry and environment common to all countries. It is intended for radiotracer groups as well as for end engineers and managers from chemical and petrochemical industries, mineral ore and raw material processing, wastewater treatment plants, and other industrial sectors.

The IAEA wishes to thank the participants in the CRP for their valuable contributions. The IAEA officer responsible for this publication was J. Thereska of the Division of Physical and Chemical Sciences.

EDITORIAL NOTE

The use of particular designations of countries or territories does not imply any judgement by the publisher, the IAEA, as to the legal status of such countries or territories, of their authorities and institutions or of the delimitation of their boundaries.

The mention of names of specific companies or products (whether or not indicated as registered) does not imply any intention to infringe proprietary rights, nor should it be construed as an endorsement or recommendation on the part of the IAEA.

CONTENTS

1. INTRODUCTION

The major objective of the Co-ordinated Research Project (CRP) on Radiotracer Technology for Engineering Unit Operation Studies and Unit Processes Optimization was the establishment of the residence time distribution (RTD) as the main universal tool for tracer investigation of industrial unit processes. RTD software for tracer data modelling and interpretation was developed and validated for problem solving purposes in major industrial processes, including fluidized beds, sugar crystallizers, trickle bed reactors, cement rotary kilns, flotation cells, grinding mills, incinerators, wastewater treatment unit and interwell communications in oil fields. Under the framework of this CRP, demonstrative and didactic experiments were undertaken to validate the RTD software and protocols.

The basic radiotracer methodology consists of accurate formulation of the RTD experimental curve and its utilization for system analysis. It is a well established method with universal applications, standard software and hardware. It is also safe, cost effective and competitive.

The RTD method comprises four interrelated aspects, namely: experimental design, data acquisition, processing and interpretation. The technique deals with tools to prepare adequate radiotracers, inject them properly, measure the radioactivity in field or through sampling in laboratory, treat data with specific software, and extract the maximum of information about the process under investigation.

Relevant target areas for radiotracer applications are defined. Though the technology is applicable across a broad industrial spectrum, the petroleum and petrochemical industries, mineral processing and wastewater treatment sectors are identified as the most appropriate target beneficiaries of radiotracer applications. These industries are widespread internationally and are of considerable economic and environmental importance.

Applications of radiotracer technology are prevalent throughout oil refineries worldwide, and this industry is one of the main users and beneficiaries of the technology. Radioactive tracers have been used to a great extent in enhancing oil production in oil fields.

Chemical and petrochemical plants are generally continuously operating and technically complex where the radiotracer techniques are very competitive and largely applied for troubleshooting inspection and process analysis.

Minerals processing plants, in one form or another, are to be found in practically every country in the world. In many cases they are major contributors to national economies. Though the range of minerals that are extracted and processed is extremely wide, there are certain processes found throughout the industry, i.e. comminution, classification, flotation, and homogenization. These processes involve two phase flow (or in some cases, three) and are notoriously difficult to control. Radiotracer technology has proved to contribute to the understanding of these processes.

Radiotracers are tools of choice for efficiency testing of wastewater treatment installations, aiding both their design and performance optimization.

2. RADIOTRACER METHODOLOGY

2.1. RTD FORMULATION AND MODELLING

The principle of the tracer experiment consists in a common impulse-response method: injection of a tracer at the inlet of a system and recording the concentration-time curve at the outlet. The function obtained C(t) is presented in Fig. 1(a). In case the tracer is not Dirac pulse the concentration-time curves at the input $C_i(t)$ and at the output $C_o(t)$ should be recorded, Fig. 4(b).

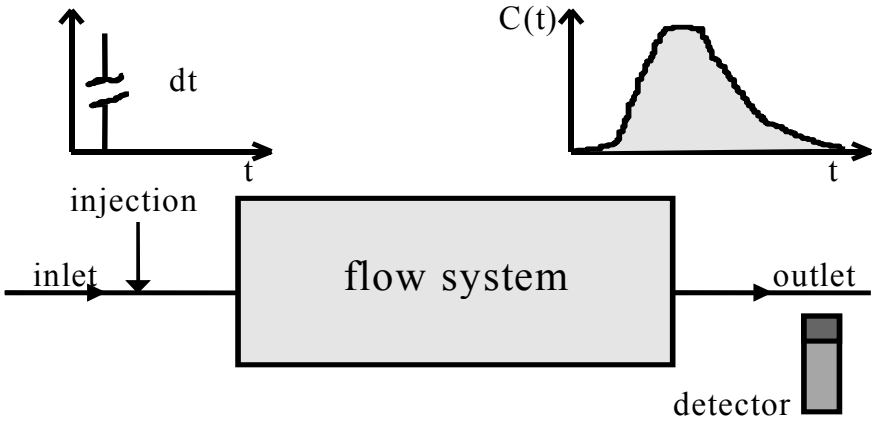

1(a)

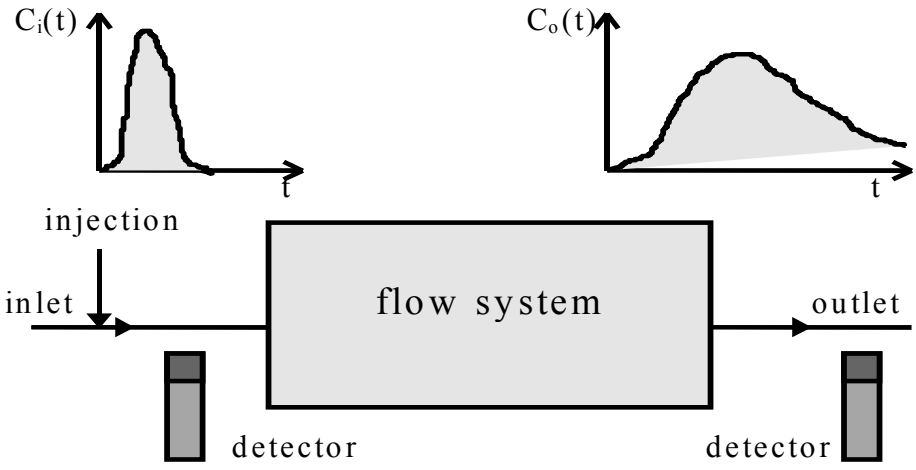

1 (b)

FIG. 1. RTD principle.

The RTD function, so-called exit age distribution function E(t), is represented mathematically by Equation (Eq.) 1:

$$E(t)=\frac{c(t)}{\int_0^\infty c(t)\,dt} \qquad \text{or} \qquad \int_0^\infty E(t)\,dt=1 \tag{1}$$

where

C(t) is the tracer concentration versus time at the outlet of the system,
E(t) is the experimental RTD.

E(t) is calculated from the count rate distribution at the outlet of the system I(t), cps or cpm.

There are physical flow parameters that can be obtained directly by experimental RTD. The experimental RTD: $E_{exp}(t)$ is measured as a series of numerical values. This experimental RTD is used for the diagnosis of reactor troubleshooting — like parallel flows, dead space, bypass or hold-up. The direct calculation of the experimental mean residence time (MRT), the mean velocity or tracer balance is quite useful to determine some process parameters. More data about the hydrodynamics (flow patterns, mixing) of the system can be extracted only through modelling of the RTD curve [1, 2].

The moments method is the simplest method of estimating the distribution parameters. Let us assume probability distribution with m parameters p $f(x,p_1,p_2,.....,p_m)$, where x is random variable. Having the empirical probability distribution one can evaluate the estimator of parameters by estimating the first m moments:

$$\mu_n = \int_0^\infty x^n f(x)dx$$

Fig. 5 presents the exemplary E(t) function. MRT and its standard deviation (SD) are depicted.

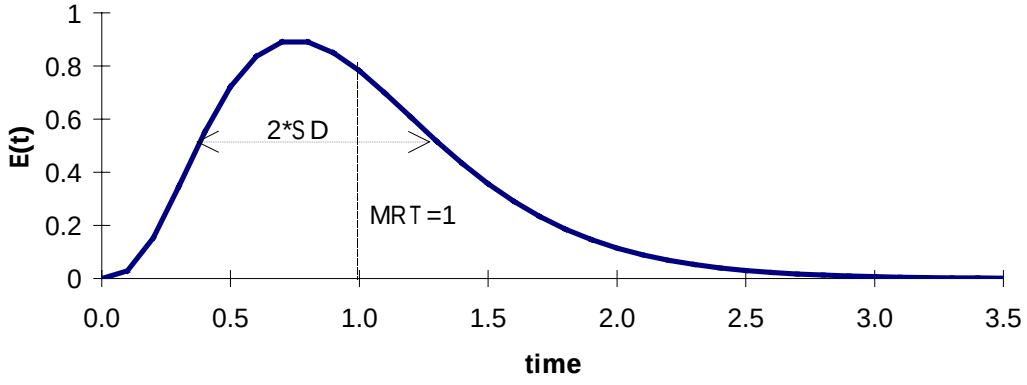

FIG. 2. The exemplary E(t) function showing MRT and SD parameters.

MRT and SD have the following physical interpretation in relation to flow systems:

MRT is directly related to the flow rate and effective flow volume of the system (Eq. 2):

$$\bar{t} = \frac{V}{Q} \tag{2}$$

where

V is the effective volume of the system,
Q is the constant, volumetric flow rate,
SD characterizes the mixing rate of the given medium in the system.

In case of lack of mixing (plug flow) SD equals zero. The higher is mixing rate, the grater value of SD. For perfect mixing system E(t) is exponential function.

Fig. 3 presents E(t) functions having the same MRT values but different SD, i.e. different mixing rates.

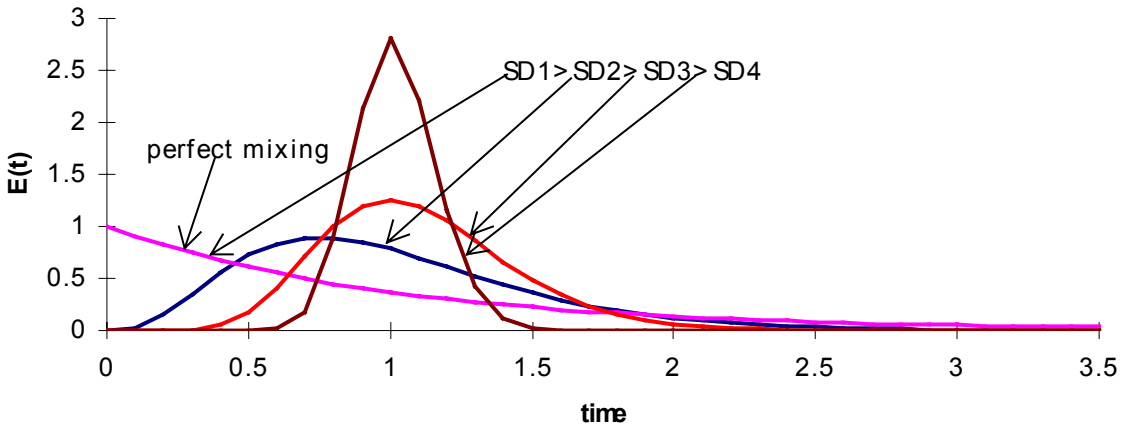

FIG. 3. E(t) functions for different mixing rate systems.

Experimental RTD is basic information for further treatment. Throughout its modelling the optimal parameters for process simulation and control could be determined. Modelling is realized in general by mathematical equations involving empirical or fundamental parameters, such as axial dispersion coefficients or arrangement of ideal mixers.

Evaluation of the dynamic parameters of continuous flows in vessels by optimizing (best fit) of the experimental RTD $E_{exp}(t)$ with the theoretical model (or theoretical RTD) $E^*(t,p_i)$, where p_i- are the process parameters, is almost common approach in field experiments (parametric approach or grey box principle). The fitting coefficient is found by using the method of least squares. Always knowing some features of the reactor performance, parametric modelling can be used to find the dynamic parameters.

Two classes of classical well known models are mostly used: N, of equal size, fully mixed tanks in series, and axial dispersion model with Peclet number P as parameter of axial

dispersion. In practice, however, above ideal conditions are rarely achieved and the situation is usually somewhere between the two.

The axial dispersion model is used when the material that passes through a vessel moves along the longitudinal direction by advection as it tends to mix in the transverse direction. The differential equation representing the unidirectional dispersion model is

$$\frac{\partial \mathrm{C}}{\partial \mathrm{t}} = \mathrm{D} \cdot \frac{\partial^2 \mathrm{C}}{\partial \mathrm{x}^2} - \mathrm{u} \cdot \frac{\partial \mathrm{C}}{\partial \mathrm{x}} \tag{3}$$

where

C is the concentration at a distance x at time t,
D is the axial dispersion coefficient,
u is the mean velocity of advective transport.

For an instantaneous and planar injection at, t=0 and x=0, the solution is:

$$\mathrm{C(x,t)} = \frac{\mathrm{M}}{\mathrm{A}\sqrt{4\pi \mathrm{Dt}}} . \mathrm{e}^{-(\mathrm{x}-\mathrm{ut})^2 / 4\mathrm{Dt}} \tag{4}$$

where

M is the mass of tracer injected into the cross-section at the inlet.

The model parameter normally used as index of mixing is the non-dimensional Peclet number, $P_e = ux/D$ (P_e = infinite for plug flow, while $P_e = 0$ for completely mixed flow).

Ideal stirred tanks connected in series model is frequently used to describe the systems where it is assumed that injected tracer is immediately (in comparison to flow rate) mixed with the entire volume of the system as a result of either mechanical mixing or some circulation. In such a case, the concentrations of the tracer at the inlet and the outlet are equal. Then, the time-concentration function for the outlet is:

$$\frac{dC_o(t)}{dt} = \frac{1}{\bar{t}}\left[C_o(t) - C_i(t)\right]$$

As the $C_i(t)$ function is usually a Dirac pulse $\delta(t)$, normalized $C_o(t)$ represents RTD, which in time domain is equivalent to:

$$E(t) = \frac{1}{\bar{t}} \exp\left(-\frac{t}{\bar{t}}\right)$$

It is common practice to present the system as an arrangement of perfect mixers connected in series.

For such a model E(t) is:

$$E(t) = \frac{1}{(k-1)!} \cdot \frac{1}{t_o} \cdot \left(\frac{t}{t_o}\right)^{k-1} \exp\left(-\frac{t}{\bar{t}}\right) \tag{5}$$

where

t_o is the MRT for a single mixer,
k is the number of mixers.

Total MRT time is then:

$$\bar{t} = k \cdot t_o$$

In order to compare E(t) curves for different flow conditions and mixing efficiency, normalization to dimensionless time θ is performed:

$$\theta = \frac{t}{\bar{t}}$$

Then the equation forms:

$$E(t) = \frac{k^k}{(k-1)!} \cdot \theta^{k-1} \exp(-k \cdot \theta) \tag{6}$$

where,

k (or N) is infinite, for plug flow, and is equal to 1, and for completely mixed flow.

For continuous process vessels with high dispersion, the best model is the cascade of mixers in series. When dispersion is low, either the axial dispersion or the cascade of mixers in series models follows well the material transfer. In the latter case, both models are equivalent (Villermaux) [2]:

$$P = 2 * (N - 1)$$

The cascade of mixers in a series model describes quite well all the simple flows with partial dispersion. Moreover, the cascade of mixers in a series model offers the possibility to build up more complicated models, combining the mixer units in various arrangements as well as adding into them several cells or zones with different flow regimes, i.e. plug flow, stagnant zone, dead volume, bypass, recirculations, etc.

TABLE 1. PARAMETERS OF EACH ELEMENTARY REACTOR

Elementary reactor	Parameters
Perfect mixing cell	MRT: E
Plug flow reactor	MRT: E
Perfect mixing cells in series	MRT: E Number of mixing-cells: N
Perfect mixing cells in series Exchanging with a dead zone	MRT: E Number of mixing-cells: N Exchange time constant: t_m Volume ratio: K
Perfect mixing cells in series with back-mixing	MRT: E Number of mixing-cells: N Back flow-rate ratio: α
Plug flow reactor with axial dispersion Closed to the diffusion	MRT: E Peclet number: Pe
Plug flow reactor with axial dispersion Half closed to the diffusion	MRT: E Peclet number: Pe
Plug flow reactor with axial dispersion Open to the diffusion	MRT : E Peclet number: Pe

Models derived from tracer experiments are often limited to simple elementary reactors, such as perfect mixing cells in series or plug flow with axial dispersion. Information obtained is not sufficient for the understanding of complex processes. Better understanding may be obtained by creating complex networks of interconnected elementary reactors. However, complex models contain so many parameters that two different models may give the same result or the same model may give an identical result with different sets of parameters [3–6].

2.2. RTD SOFTWARE

Throughout RTD modelling it is possible to determine optimal parameters for process simulation and control. Modelling is realized in general by mathematical equations involving empirical or fundamental parameters such as axial dispersion coefficients or arrangement of ideal mixers. The experimental data can be treated further through RTD compartment modelling only when they represent the RTD function. Tracer response curves obtained by the detection system can be different from the RTD function if experiments are not properly conducted. This means that experimental design and execution to obtain reliable and accurate RTD curve is essential.

There are commercial and homemade RTD softwares for data processing. In fact, the results of RTD modelling do not depend on the performance of a particular software, but different softwares facilitate extraction of information and interpretation, in particular for complex process analysis.

Obviously, an RTD software is just a tool. Whatever the proposed model is the software can give an answer, but can never tell whether the model has physical sense or not. RTD software may likewise be used to determine the parameters of different models giving the same response. Only careful examination of physical soundness of these parameters leads to the choice of a realistic model.

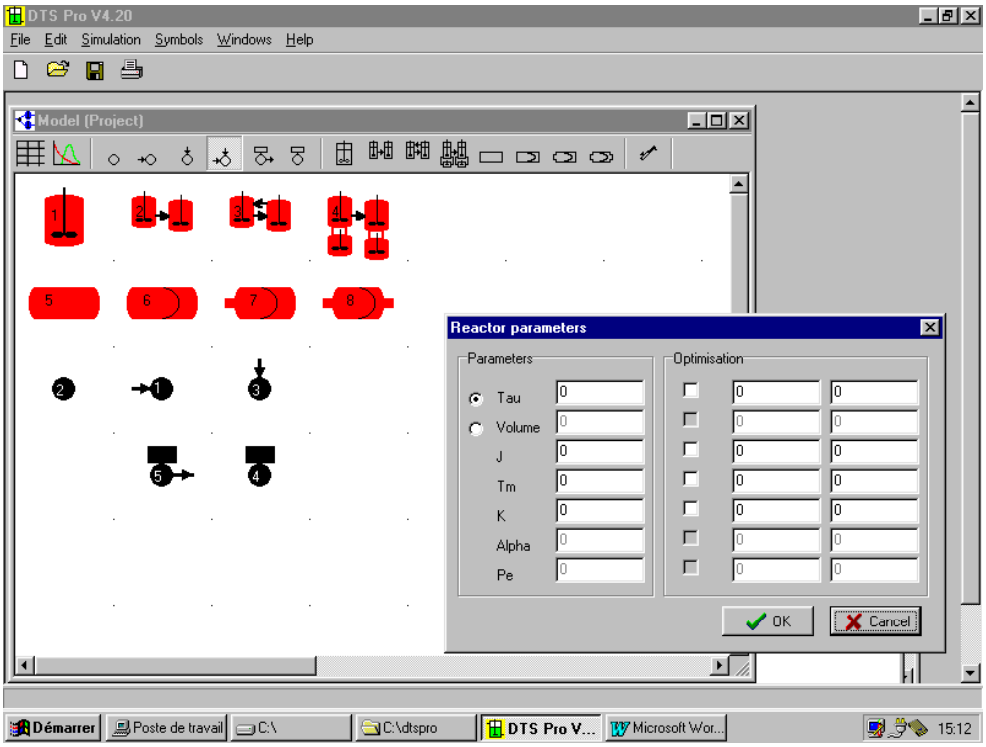

FIG. 4. Combination of elementary reactions in the Progepi RTD software.

Two RTD softwares were validated under the CRP, which can be considered as available standards in routine tracer work.

(1) Progepi DTS software produced by the Laboratory of Chemical Engineering Sciences, Nancy, France [7]

Progepi RTD software is intended for researchers and engineers to simulate the outlet of flow compartment models to an injection of tracer. It allows the user to simulate the response to any input of any complex network of elementary interconnected basic flow patterns.

Preliminary treatment of the tracer experimental curve, including background correction, exponential extrapolation, and normalization, are performed by the software. The software automatically estimates moments of both experimental and theoretical curves. This software is mainly useful in determining compartment models on the basis of the hydrodynamic flow behaviour of complex reactors as well as in simulating and estimating the mass balance in processes with multiple recirculations.

(2) CTU RTD software prepared by the Department of Process Engineering of the Czech Technical University of Prague, Czech Republic the last version of which was completed under the IAEA support [8]

The CTU software is based on more than 30 years of experience of the tracer group and chemical engineers in the Czech Republic. It contains many specific models. The software is described in the manual entitled RTD Software Analysis, Computer Manual Series 11, IAEA, (1996).

The RTD package consists of three independent programs. RTD0 is used for RTD formulation and simple moment calculation. It imports experimental data from data loggers in different formats and performs transformation of non-equidistant data, radioactive decay correction, filtration of noise, smoothing of radioactive fluctuations, background raise subtraction. RTD1 is a tool for "black box" analysis (deconvolution, convolution, and correlation) using splines, FFT, or Laguerre functions. This program is applied mostly for RTD identification and system response prediction. RTD2 is a simulation program for analysis of systems described by differential equations. Models should be created based on physical consideration about the system ("grey box" analysis).

In general both softwares are useful for evaluation and processing of tracer experiments. The Progepi software has a modern front/end (Windows) and is more user friendly than the CTU, which is MS DOS based.

Formulation and adjustment of RTD experimental curve obtained by radiotracer are better done by CTU's RTD0, e.g. interactive graphics, advanced and verified procedures of corrections, flexible import of data from data loggers.

Progepi software is more user friendly. It has the advantage of being useable without the mathematical description of the models. Models can be created and combined to fit better with experimental data directly on the display. Progepi software is preferred for processing complex models that can be described by Fourier transformation, including parameter identification. Definition of the flow sheet is easy, user friendly and reliable. But the physical meaning of the best model still remains the concern of specialists of both softwares.

For more specific operating conditions, e.g. identification of models having more than one output by fitting simultaneously the several experimental outlets, variable flows, responses detected by wall detectors, batch processes, the RTD1 and RTD2 programs are recommended.

Some tracer groups working with radiotracers in different countries also have elaborated individual programs for RTD data treatment. As an example, INCT Warsaw is using Matlab commercial software for RTD data treatment, processing and modelling. Use of this software requires good background in programming.

However, other software tools may also find their application in interpretation of RTD functions in order to give additional insight into investigative flow process, e.g. z-transform as a complementary tool of Laplace and Fourier transforms.

A simple industrial mixer cascade was selected for comparing RTD software. The process is presented schematically in Fig. 5. The mixer cascade consists of three successive compartments separated from each other by perforated walls. On the basis of mechanical flow the process can be seen as three ideal mixers with back mixing.

RTD and DTS softwares were used to model the RTD experimental data. The best fitted model consisted of three ideal mixers with back mixing. Both softwares gave identical results as expected. The experimental RTD, three ideal mixers model and the back mixing model are presented in Fig. 6.

Recommendations for some industrial process models are shown on Table 2 [5].

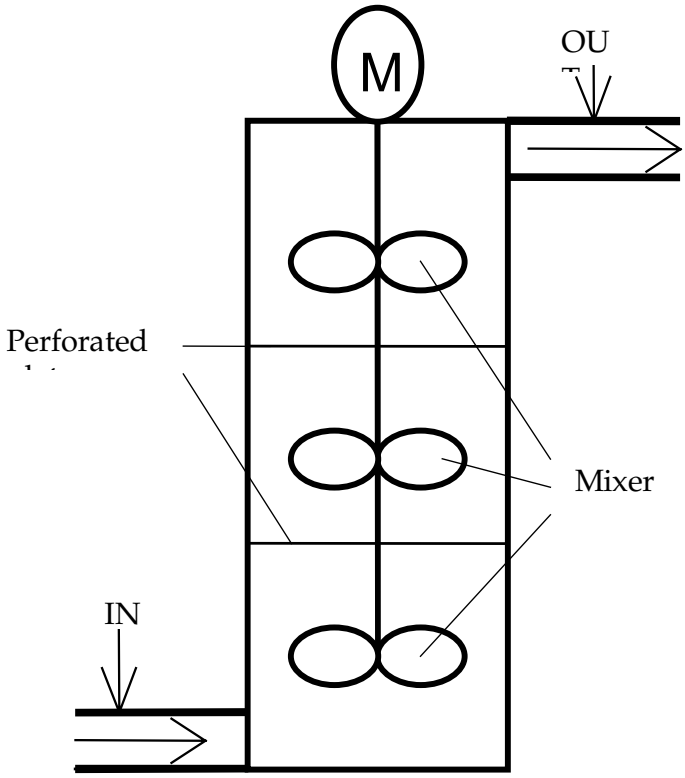

FIG. 5. Industrial mixer.

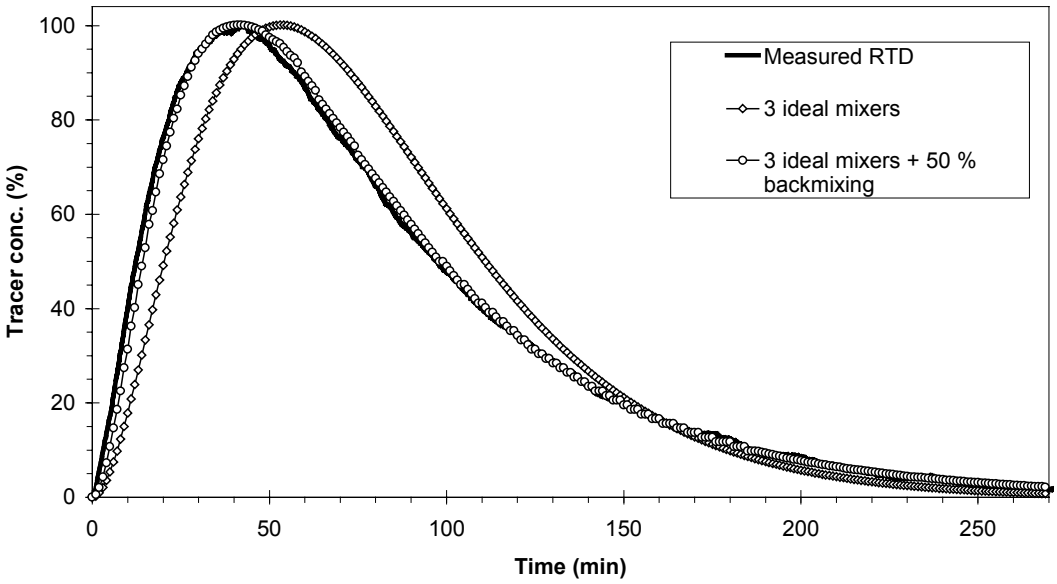

FIG. 6. Experimental RTD and its models.

TABLE 2. RELATIONSHIPS BETWEEN PROCESSES AND EXISTING MODELS DESCRIBING THESE PROCESSES

Industrial processes	Recommended model
Aeration sludge channel reactor	Perfect mixing cells in series (The number of the mixing cells is a function of both gas and liquid flow-rates).
Processes with endless screws (extruders, mixers, spiral classifiers)	Perfect mixing cells in series exchanging with a dead volume (the number of cells is a function of both inlet flow-rate and speed of rotation)
Multiphase fixed-bed reactors : RTD of liquid phase	Two perfect mixing cells in series model in parallel
Classified bed crystallizers	Perfect mixing cells in series with back-mixing

2.3. RADIOSOTOPES USED AS RADIOTRACERS

2.3.1. Applications of radioisotope generators for remote tracer experiments

Radioisotope generators are very important in tracer work in developing countries that do not have nuclear reactors. There are three useful radioisotope generators for remote tracer experiments mostly in liquid phase: Mo-^{99m}Tc, Sn-^{113m}In, Cs-^{137}Ba. Only Mo-^{99m}Tc, which is largely used in nuclear medicine, is available in the market. It has rather limited applications in industry due to short life and low gamma energy.

There are a few suppliers of Sn-^{113m}In generator. It has longer life and larger gamma energy in comparison with ^{99m}Tc, but is two to three times more expensive. It can be used to complement ^{99m}Tc for covering other tracer applications in industry. It has been largely used for water like liquid flow rate calibration as EDTA compound.

Cs-^{137}Ba generator produces very short life radiotracer but has practically very long applicability (for several years at least). This is a very useful radiotracer generator for routine service to end users, in particular for liquid flow rate measurement and calibration because of its high gamma energy which can be easily detected from outside pipes, and of its safety. The Cs-generator is not available in the market. There are some private tracer companies that produce homemade Cs generator for their own use, but they do not disclose their know-how.

These three generators make tracer groups of developing countries independent on radiotracers and can cover large spectrum of tracer applications related with liquid and solid phase flow rate measurement and RTD troubleshooting.

^{137}Cs/^{137m}Ba isotope generators

Cs/Ba generator is well suited for liquid flow measurement with transit time method. In principle it provides an unlimited amount of tracer injection and makes it possible to use radioactive tracer techniques without access to irradiation facilities. Their use is limited since they are not commercially available, except the ones with very low activity for demonstration purposes. The main reason for this is that a durable construction has not been designed. Also, the market for generators would be limited to industrial tracer applications, which can be considered rather small. Another reason for the limited amount of possible applications is the

short half-life of ^{137m}Ba, i.e. 2.5 minutes (min). This has led to the present situation where homemade generators are produced and used.

Under the CRP activities a study of Cs/Ba isotope generators was performed. Main concerns were two practical factors affecting their usability: mechanical durability and Cs residual in elutes.

The purpose of the ion exchange resin in the generator is to chemically retain Cs atoms while the Ba ions are released to the elution liquid. The resin chosen for the first Cs-Ba generator, after an extensive prestudy, was potassium cobalt ferrocyanide (KCoFCn). The poor mechanical durability is mainly due to the fact that the ion-exchange resin used is mechanically very fragile. This results in the clogging of the generator — normally within a year.

Cs residual in the elutes is unsuitable not only in terms of radiation safety, but also on the basis of its effect on generator lifetime. A typical ^{137}Cs/^{137m}Ba ratio was 10^{-5}–10^{-4}. Improvement was achieved under the CRP.

A commercial resin was purchased and used under the framework of the CRP to build new Cs/Ba generators. The new resin proved to possess superior capability to retain Cs atoms. Using the previous compound, ^{137}Cs/^{137m}Ba ratio was of the order of 10^{-4}. Using the new commercial resin, the ratio became of order of $10^{-6}10^{-5}$. Promises of better mechanical durability were anticipated but not realized. Also, new generators experienced clogging.

Clear improvement in the homemade generator technology was achieved in the decreased amount of Cs residual, but availability of a generator for commercial production was not made due to clogging problems. It was suggested to use similar exchangeable column as in Tc generator for clinical work. Such construction would involve lesser loss of valuable mechanical parts, making the generator still usable, needing minimal time to make it operable again.

New tracers

As for the Cs/Ba generator, use of commercial tracers provides the advantage of being independent from local irradiation facilities. Flow measurement of gaseous flow by transit time method was an important application, but lacking of a suitable tracer. ^{41}Ar can sometimes be used but its applicability is delimited by its short half-life of 1.8 h.

^{127}Xe is used for clinical work. Low radiation energy and relatively high price limit its applicability in routine applications. However, usage of Xe has been tested in several locations, which proved to be suitable for several applications. The main limitation is the need to use very high activity for large flows.

Another tracer tested for the detection of wood pulp flow was ^{99m}Tc. As wood pulp is flowing, behaviour of liquid phase becomes less important compared with solid phase transport. In some conditions most of the tracer tends to follow the liquid phase instead of the solid phase. Comparison with irradiated glass fibres (good solid phase tracer) vs. ^{99m}Tc marked pulp was made. The resulting RTDs were identical. This is strong evidence of the fact that Tc follows the flow of solid phase.

Major radioisotopes used as radiotracers in industry are listed in Table 3.

TABLE. 3. MOST COMMONLY USED RADIOTRACERS IN INDUSTRY

Isotope	Half-life	Radiation and energy (MeV)	Chemical form	Tracing of phase
tritium (hydrogen-3)	12.6 y	Beta: 0.018 (100%)	tritiated water	aqueous
sodium-24	15 h	Gamma: 1.37(100%) 2.75(100%)	sodium carbonate	aqueous
bromine-82	36 h	Gamma: 0.55 (70%) 1.32 (27%)	ammonium bromide p-dibrom-benzene dibrobiphenyl	aqueous organic organic
lanthanum-140	40 h	Gamma: 1.16 (95%) 0.92 (10%) 0.82(27%) 2.54 (4%)	lanthanum chloride	solids (absorbed)
gold-198	2.7 d	Gamma: 0.41 (99%)	chloroauric acid	solids (absorbed)
mercury-197	2.7 d	Gamma: 0.077(19%)	mercury metal	mercury
mercury-203	46.6 d	Gamma: 0.28 (86%)	mercury metal	mercury
iodine-131	8.04 d	Gamma: 0.36 (80%) 0.64 (9%)	potassium or sodium iodide, iodobenzene	aqueous organic
molybdenum-99	67 h	Gamma: 0.18(4.5%) 0.74(10%) 0.78(4%)	sodium molybate	aqueous
technetium-99m	6 h	Gamma : 0.14 (90%)	sodium technetate	aqueous
scandium-46	84 d	Gamma: 0.89(100%) 1.84(100%)	scandium oxide	solids (particles)
krypton-85	10.6 y	Gamma: 0.51(0.7%)	krypton	gases
krypton-79	35 h	Gamma: 0.51 (15%)	krypton	gases
argon-41	110 min	Gamma: 1.29(99%)	argon	gases

2.4. FACTORS AFFECTING RTD MEASUREMENT

The formulation of RTD and its utilization for systems analysis are well established. Accurate RTD formulation can be affected by tracer mixing length and detector response.

2.4.1. Tracer mixing length

Good mixing of the tracer into the flowing system is a precondition for formulating the RTD.

The mixing length in duct flows is defined as the distance beyond which the tracer concentration in the cross-section is almost constant. An accurate way to determine the mixing length is the use of a computational fluid dynamics (CFD) code to model both the bulk flow and tracer injection. Fig. 7 illustrates typical CFD concentration maps as a function of time. It clearly shows the influence of initial tracer jet and its dispersion in mixing length [6].

There are a few theoretical formulae to calculate mixing length for various velocity and turbulent diffusion coefficient profiles as a function of injection configuration (central injection and annular injection). These formulae are known to underestimate by a wide margin experimentally observed mixing lengths, probably because simulation of the injection is too simplistic. Values for good mixing length determined experimentally in a straight pipe of circular cross-section with central tracer injection are about twice as large as theoretical values. The main reason for this discrepancy is the difference between actual and postulated flow conditions. These formulae should therefore be used with some caution.

In general, good tracer mixing may require as many as 200 pipe diameters to achieve. It is often not possible to inject the tracer at such a distance upstream to the measurement section. Every singularity in the pipe promotes turbulence that tends to decrease good mixing length. It is therefore useful to be able to reduce the length by using appropriate devices.

— Substantial reduction of mixing length can be obtained by injecting the tracer through multiple orifices uniformly distributed on the pipe wall or (if possible) inside the pipe.

— Injecting the tracer counter currently at a velocity much larger than bulk flow velocity induces high mixing at the end of the jet. Reduction in good mixing length depends on the number and momentum of the jet, and of its angle with respect to the main flow direction. Little quantitative data are available on these effects. However, a simple jet arrangement can bring a 30 % reduction with respect to a single central injection point.

— Incorporating obstacles within the pipe, in the vicinity of tracer injection, produces turbulence that enhances mixing and reduces good mixing length. As an example, injecting the tracer through three triangular plates at an angle of 40 ° with main flow direction reduces mixing length by one third with respect to a central single injection point.

— If tracer is injected upstream a pump or a turbine, mixing length is considerably reduced. Available information indicates that centrifugal pumps reduce mixing length by about 100 pipe diameters.

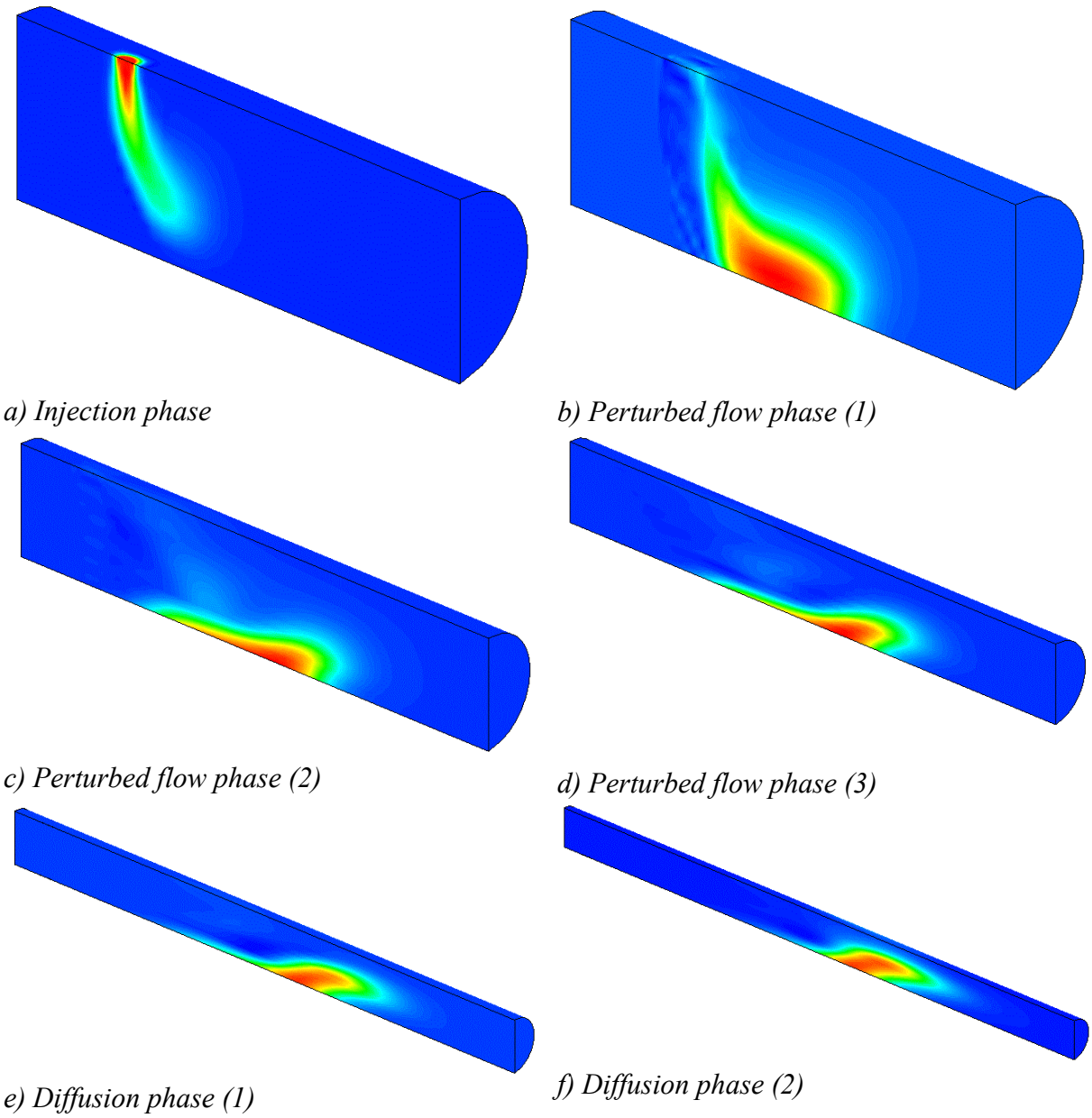

a) Injection phase

b) Perturbed flow phase (1)

c) Perturbed flow phase (2)

d) Perturbed flow phase (3)

e) Diffusion phase (1)

f) Diffusion phase (2)

FIG. 7. Simulated transient dispersion of tracer.

2.4.2. Detector response

An important point dealing with RTD formulation is "what is really seen by a detector", since a wall radiation detector does not perform local measurement but collects a certain amount of information within a solid angle called the volume of sensitivity. Since the radiotracers commonly used are gamma emitters, the photons they emit undergo multiple random interactions, i.e. with the fluid itself, walls, screens, collimator, until they reach the detection probe – NaI(T1) crystal scintillator and photomultiplier.

The importance of these interactions is a function of the energy of the emitted photons and of the nature (density and chemical composition) of the fluid and materials. The link between the tracer concentration and detector signals is therefore not direct, the problem lying mainly in the correct representation of interactions.

A relatively simple method to calculate the detection volume is the Monte Carlo method. The basic principle is to choose randomly the initial position, energy, direction and free path of a photon. Its new position is then calculated. If the photon has not left the system, it is going to interact with the surrounding matter. The major types of interactions to be considered are photoelectric effect, Raleigh effect, Compton effect and pair creation. The probability of these processes is a function of the energy of the incident photon. The type of interaction is randomly chosen and the procedure is repeated until the photon either leaves the system or is absorbed by any material in the simulated system. When a sufficiently large number of photons has been treated in this way, it is possible to build statistics in terms of detected photons energies and numbers, which in turn can be translated into count numbers. Thus, the Monte Carlo simulation provides the detector response [9].

As a validation, the Monte Carlo code calculations were tested against some of the experimental data obtained by placing a point gamma source at different locations in a Plexiglas tube fitted with a detector (Fig. 8a). Several parameters were investigated: source nature (^{137}Cs and ^{60}Co), fluid nature (air and water) and collimator geometry (see Fig. 8b). The results of comparison of detector modelling with experiments are shown in Fig. 8. They fit satisfactorily.

The distortion of real RTD for a liquid phase flowing through a porous bed due to the detection response is illustrated in Fig. 9. In some extreme cases real RTD can be different from experimental RTD. Nevertheless, simulations proved that deconvolution of raw (non-corrected) signals leads to a transfer function, which is practically not influenced by the detector response.

Experience has shown that detection geometry correction does not affect RTD results in the case where radiotracer concentration in the cross-section is uniform. This assumption is fulfilled when using simple dispersion models, series of ideally mixed regions or backmixing models. This means that, in most cases, RTD “wall correction” (or “detection response correction”) does not affect RTD troubleshooting and modelling.

2.5. INTEGRATION OF RTD TRACING WITH CFD SIMULATION FOR INDUSTRIAL PROCESS VISUALIZATION AND OPTIMIZATION

At present, two methods are used for investigation of industrial complex processes, tracer RTD experimental technique (systemic analysis), and CFD simulation [6].

RTD systemic analysis requires the choice of a model, which is quite often debatable. While the RTD method is very useful for many applications, it is limited to linear processes only. The RTD global model needs a CFD method for defining more realistic and physically sound models for different flow situations.

The numerical simulation of complex systems through CFD methods is a new approach that is more powerful for process visualization. The real time experimental RTD tracing is simple and reliable; it provides various important hydrodynamic parameters, but it is impossible to localize and visualize flow pattern inside the systems. CFD is a fine and predictive analysis, which provides nice spatial pictures of the insight of a process, such a flow patterns and velocity map. Due to lack of physical experimental data CFD calculation provides qualitative results only, especially in systems with the strong interaction

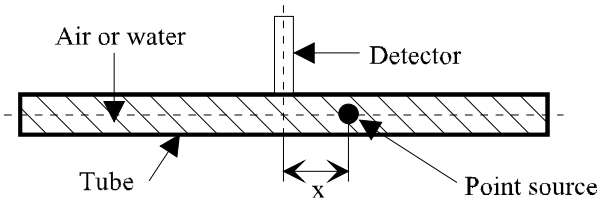

a) Experimental set-up

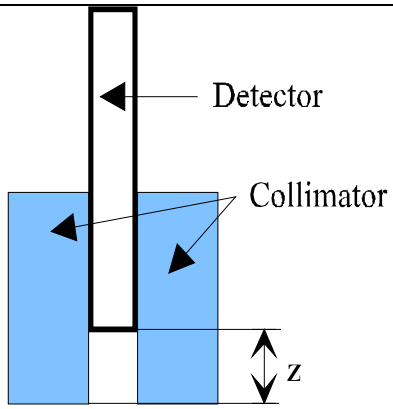

b) Detector and collimator geometry

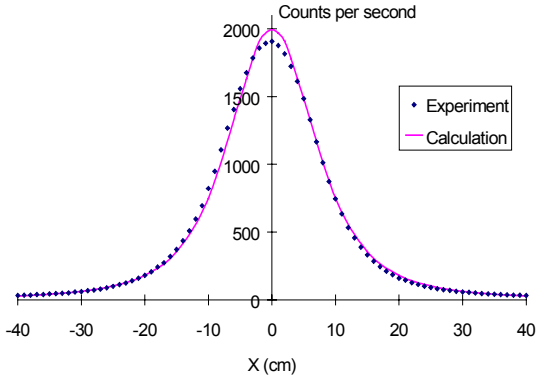

c) ^{137}Cs in air, z = 0

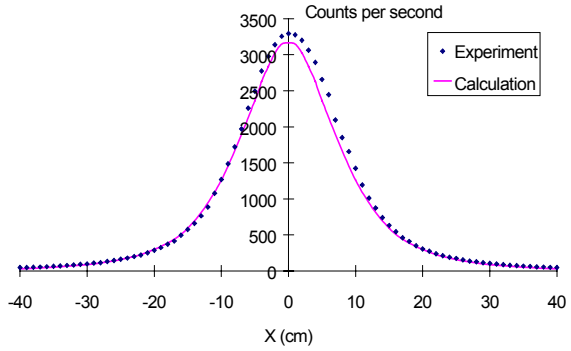

^{60}Co in water, z = 0

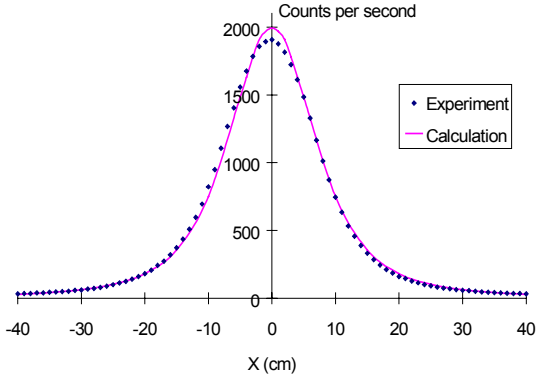

c) ^{137}Cs in air, z = 0

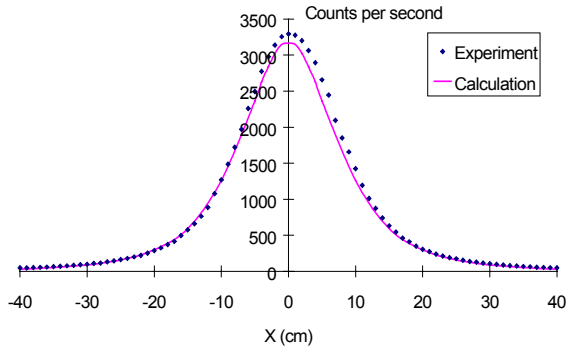

^{60}Co in water, z = 0

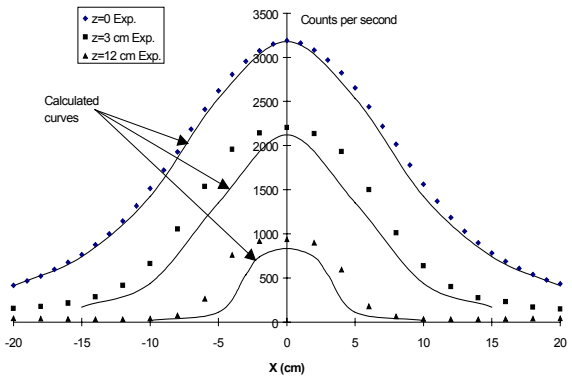

e) ^{60}Co in air, as a function of z

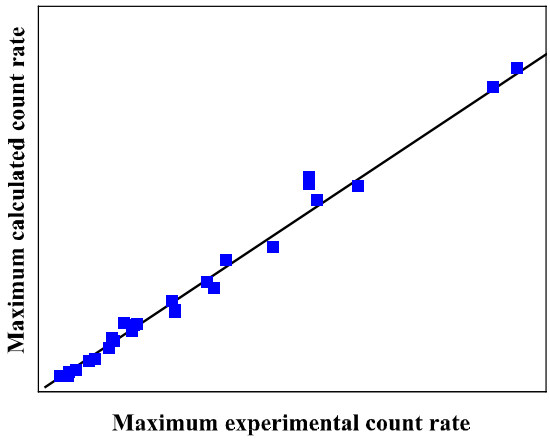

f) Comparison of experimental and calculated maximum count rates

FIG. 8. Detector modelling: comparison with experiments.

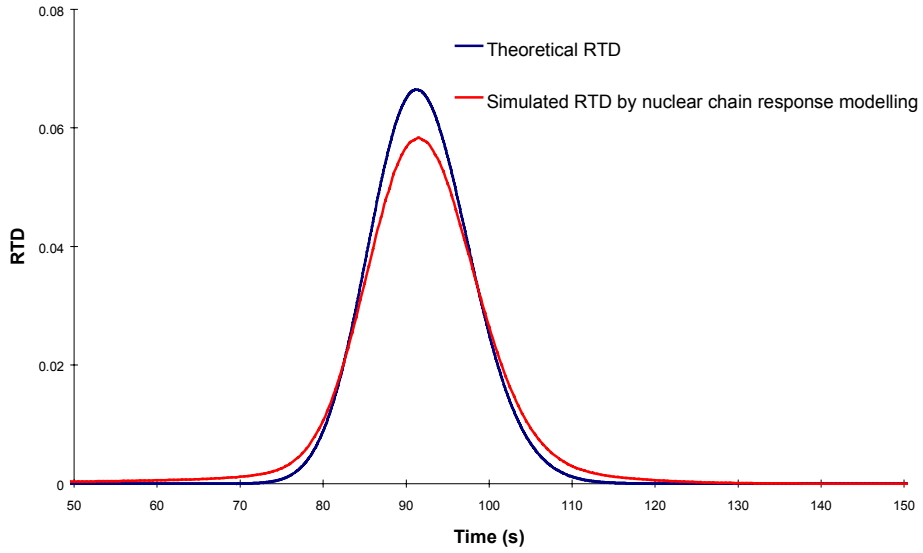

FIG. 9. Effect of the nuclear chain response on the theoretical flow.

of hydrodynamics with physicochemical reactions. This is the reason why CFD models have to be verified and validated by experimental tracer RTD results. CFD has the capacity to generate other flow conditions once it is validated.

RTD-CFD interaction involves both sides. CFD can be used also to complement information obtained from the RTD systemic approach. CFD provides data that can quantify RTD systemic model, which means that the CFD model can "degenerate" into more quantitative RTD systemic analyses, providing more comprehensive results for chemical engineers. In fact, these two approaches, experimental and numerical, are complementary to each other. The RTD systemic approach detects and characterizes the main features of the flow (mixing and recirculations) while CFD enables to locate them. The trend is to combine experimental and numerical approaches in order to obtain reliable quantitative results for industrial complex processes.

2.6. RADIATION SAFETY

Radiotracer technology is one of the many beneficial applications of ionizing radiation that is used around the world. To ensure that persons are protected from the harmful effects of radiation, such application must comply with the international Basic Safety Standards (BSS) or equivalent national regulations.

Any work with radioactive materials will normally require authorization from the relevant national regulatory authority. The authorized person or organization will have the prime responsibility to ensure that radioactive materials are used safely and in compliance with relevant regulations and standards. Guidance on occupational radiation protection, development of safety assessment plans and safe transport of radioactive materials has been published by IAEA [10–13].

3. RTD VALIDATION IN CASE STUDIES FROM CHEMICAL, PETROCHEMICAL AND MINERAL ORE PROCESSING INDUSTRIES

3.1. STUDY OF LABORATORY SCALE CONTINUOUS ORE GRINDING MILL

The main motives for the study is to minimize energy consumption of the grinding process by obtaining optimal particle size distribution. This means primarily that the amount of very fine particles in the product should be decreased.

Radiotracer tests were conducted in a laboratory nickel ore grinding mill for three slurry density 25, 35 and 45%. Water tracer was ^{137m}Ba. Results showed that fine particles tend to behave very much like water; also, that the difference in behaviour compared to larger size fractions was quite considerable. Further investigation of results shows a classification effect: relative MRT of fine particles decreased as water is added to the process. This means that increasing the amount of water in the process (decreasing slurry density) tends to improve the grinding result. This is quite opposite to industrial practice where high slurry densities are used.

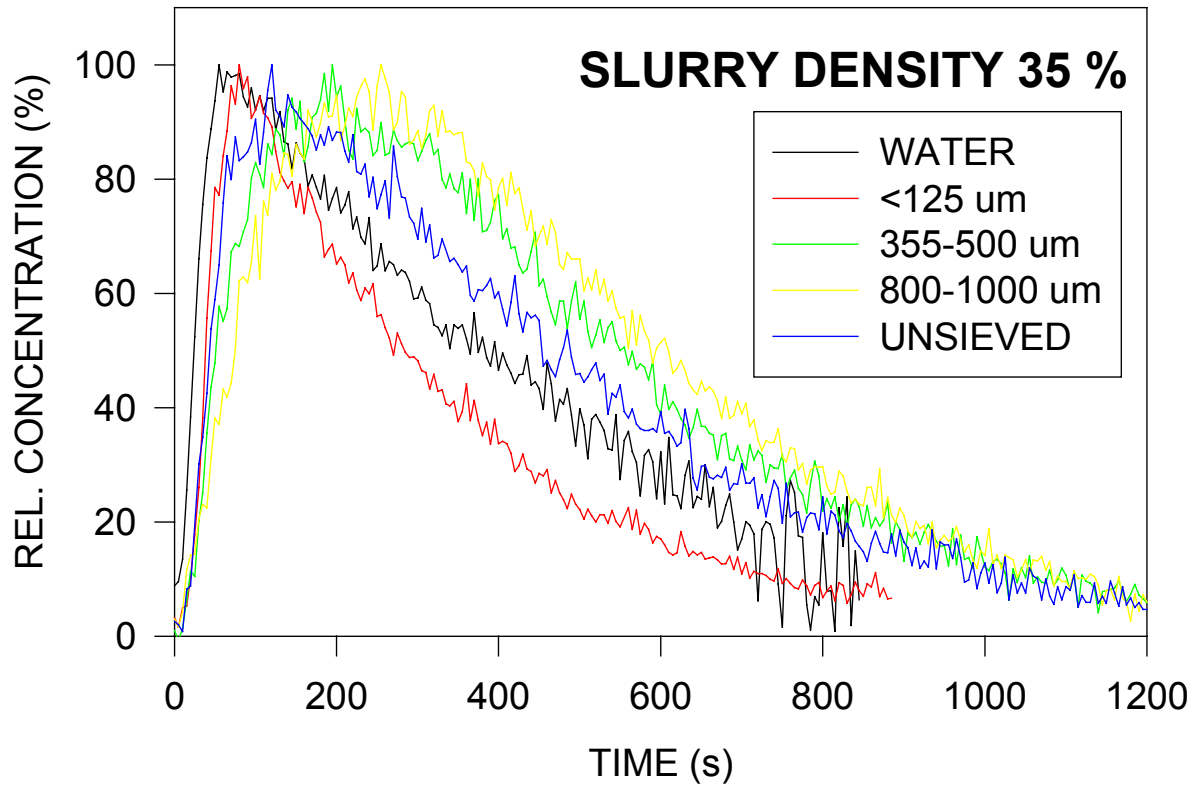

FIG. 10. RTDs for nickel ore with 35% slurry density.

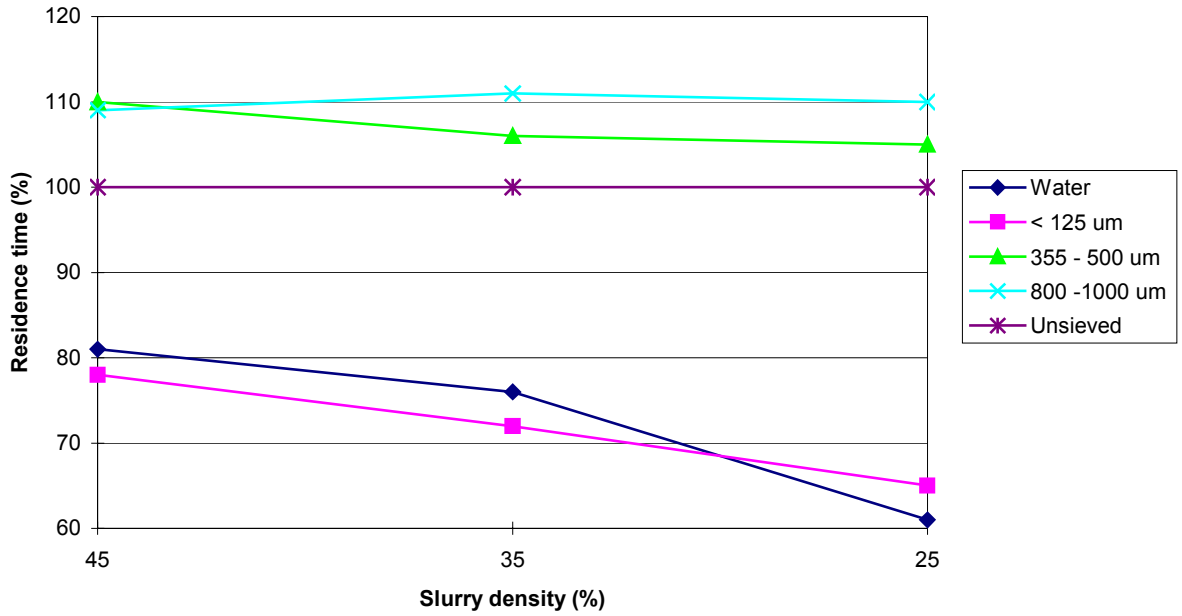

FIG. 11. MRTs of sieved fractions compared to the unsieved ore. Relative MRT of fine particles decreased as slurry density decreases (i.e. water is added).

3.2. HEAVY METAL RELEASE IN A PILOT PLANT SCALE MUNICIPAL SOLID WASTE INCINERATOR

Heavy metal release in a solid waste incinerator is an important problem in waste management. Zinc and copper are today two of the important heavy metals which cause environmental problems in the bottom ash. Both have quite different physico-chemical properties. Under the prevailing conditions zinc is volatile and copper is more or less non-volatile.

The objective of the radiotracer experiment was to verify the applicability of radiotracer method for heavy metal release and validate the technique in a municipal solid waste incinerator in a pilot scale.

The pilot plant with a thermal power of 0,4 MW consists of forward acting grate system, post combustion chamber system and flue gas purification. The main components were urban waste wood, plastics and lava as mineral component. It was expected that the result of the pilot plant be scaled up to municipal solid waste (MSW) incineration.

A tube was used to inject radiotracer materials into the combustible bed. Alongside the grate, 6 detectors were placed to measure gamma radiation. The detectors were located immediately after the injection point of the tracer at the middle and end of each grate zone. To determine the amount of evaporated radiotracer a portion of flue gas was sucked off by the post combustion chamber and washed in an absorber.

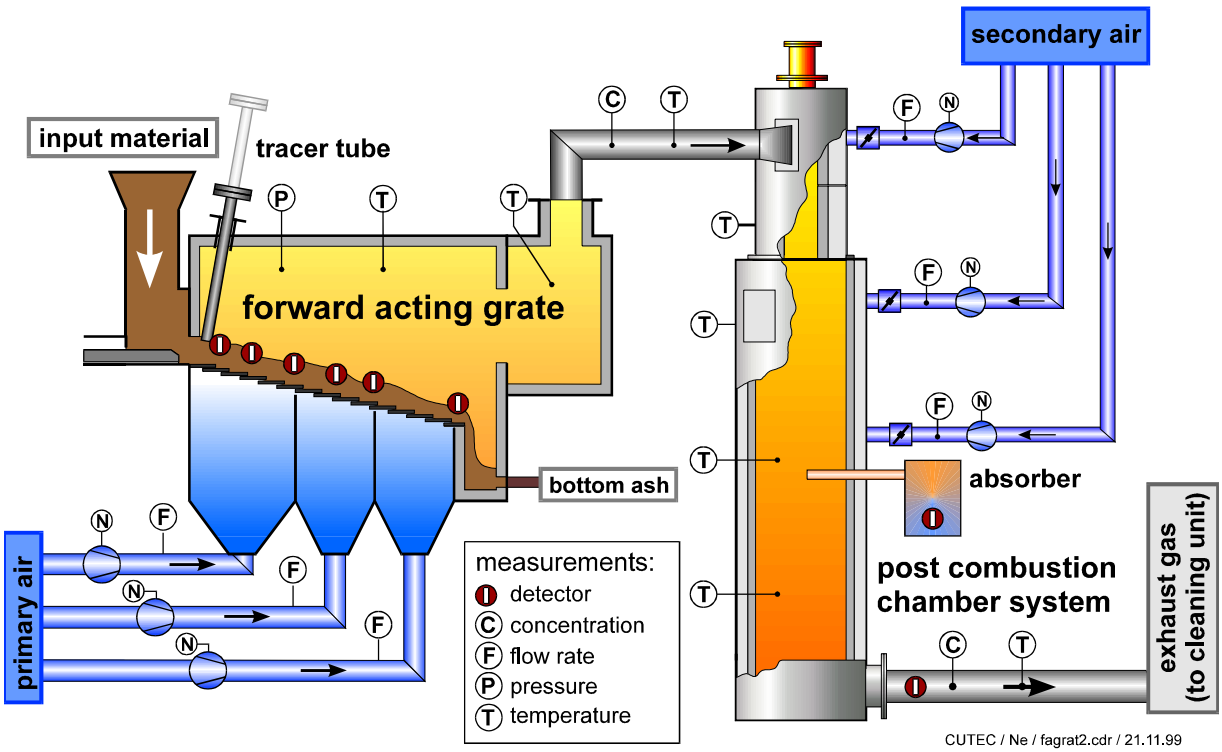

FIG. 12. Pilot plant and detector positions.

The isotopes ^{64}Cu and ^{69m}Zn were used. ^{64}Cu has a half-life of 12.7 hours and emits gamma rays with energy of 511 keV with a probability of 37 % due to positron annihilation. ^{69m}Zn has a half-life of 13.8 hours and emits gamma rays with energy of 439 keV. Both isotopes were produced in a research reactor by neutron activation. For preparation of ^{64}Cu a pure copper metal was irradiated, while of ^{69m}Zn, highly enriched target of ^{68}Zn was manufactured and irradiated into the nuclear reactor.

For each experiment 200 mCi of ^{64}Cu and ^{69m}Zn was used. The ampoule was cracked, its content was mixed with 20 grams of waste material and pressed into a pellet. This single pellet was injected instantaneously (Dirac pulse) at the entry of the grate through an injection tube.

1" NaI(Tl) scintillation detectors, collimated with tungsten alloy, were used to measure the radiotracer. 200 mCi of $^{113m}In_2O_3$ was injected to determine the solid phase RTD in the incinerator.

For determination of the quantity of copper and zinc in the flue gas, an absorber filled with diluted nitric acid was used. A partial flow of the flue gas was continuously punched from the combustion chamber and passed through the absorber. An unshielded 1,5"-NaI(Tl)-scintillation detector positioned in the centre of the absorber recorded the absorbed quantity of radioactive metal as a function of time. At the end of each experimental run the dissolved content of an irradiated ampoule containing a small quantity of the corresponding metal was applied directly into the absorber for calibration.

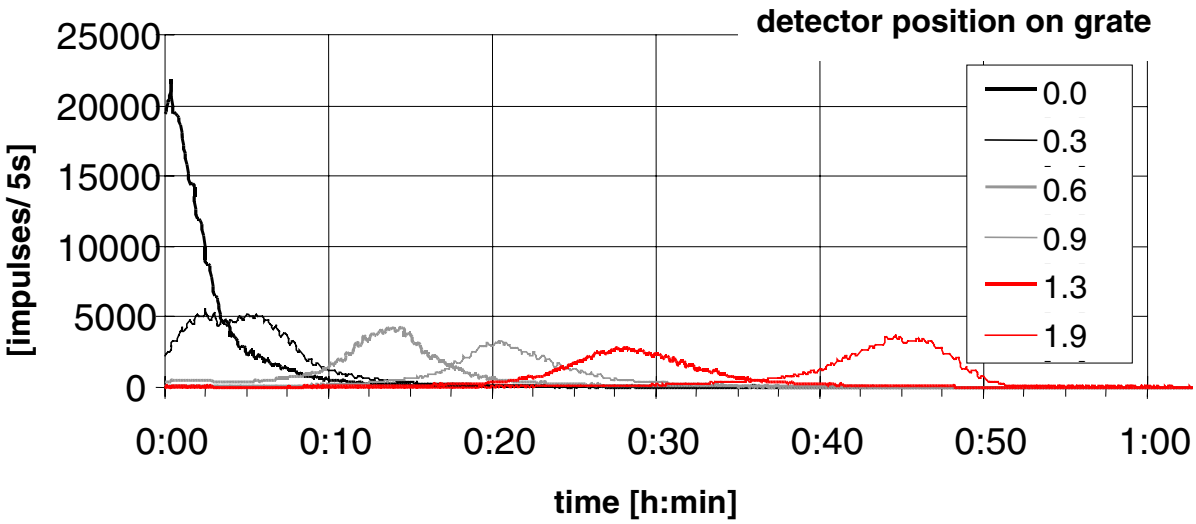

FIG. 13. RTD of waste material inside the grate measured by ^{113m}In.

RTD of waste material inside the grate

RTD information of waste material inside the grate is a prerequisite for calculating a space-dependent signal. Therefore, the RTD of waste material was measured separately using ^{113m}In. Alongside the grate the isotope radiation was measured at six different detector positions.

Waste mass flow and grate velocity of the forward acting grate were held constant for the whole measurement campaign. In Fig. 13 are shown RTDs obtained with indium adsorbed as indiumoxid/indiumhydroxid at some lava stones is shown. Because of the relatively symmetric shape of the measured curves, the residence time can be considered as the time at which each detector measures maximum impulses at first approximation. A linear correlation between detector position and residence time was determined, as expected.

Based on this indication the time-dependent evaporation signal measured in the flue gas can therefore be easily transformed into a space dependent signal. Thus, the place of zinc and copper evaporation can be localized clearly.

Heavy metal release

Fig. 14 reveals the differences between the evaporation behaviour of copper and zinc during two selected experimental runs. The diagrams on the left-hand side show the results measured with copper as tracer while the diagrams on the right hand side with zinc as tracer. The lower diagram contains the RTDs of the radioactive copper and zinc, respectively, measured by the detectors established alongside the grate. The upper diagram shows the time dependent signal measured by the detector in the absorber unit at each case.

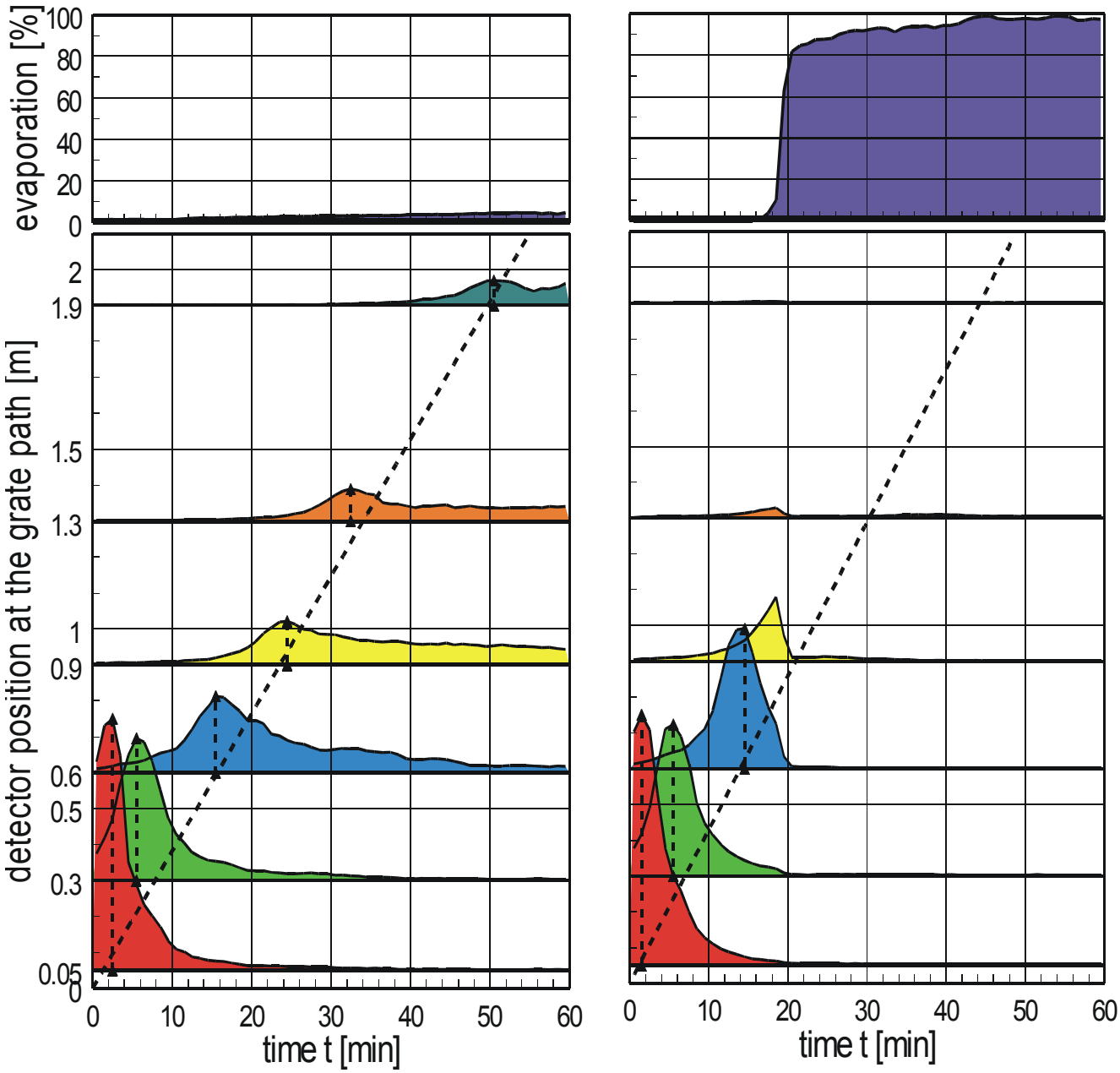

FIG. 14. Examples for the measured copper (left) and zinc (right) release on the grate (down) and in the absorber (up).

Evaporation of copper occurs alongside the whole grate and can not be allocated to a specific place. The determined 3–5 % of copper that evaporated confirms the hypotheses that even under chemically favourable conditions no substantial copper evaporation occurs.

The evaporation of zinc takes place very fast i.e. in a narrow area on the grate. The place of evaporation depends on the operating conditions. The evaporation occurs always at location with high temperatures and reducing conditions, and can reach up to 100% evaporation, as shown in the example in Fig. 14.

Conclusion

Measurements in the pilot plant confirm the hypotheses that reducing conditions in connection with high temperatures enhance the evaporation of zinc. Copper, as a non-volatile heavy metal, is not evaporated significantly from the furnace bed, as expected.

3.3. MASSECUITE FLUID FLOW IN SUGAR CRYSTALLIZATION PROCESS

The main objective of an exhaustion low grade crystallizer in a sugar factory is to reduce the loss of sucrose in the separated molasses that exit the process. Several types of crystallizers were designed in order to reach the above objective.

The greatest complication in operating this type of low-grade exhaustion crystallizer is in setting the cooling profile. At low temperature, the solubility of sucrose is lower, but the growth kinetics is much slower. There exists an optimum cooling profile which will maximize the exhaustion of massecuite for a given residence time. At the same time, with the decrease in temperature, generally an increase of massecuite viscosity is observed, becoming the major constraint to exhaustion of molasses.

As indicated previously, flow behaviour of massecuite fluid within an exhaustion continuous crystallizer follows a dispersed plug flow model with complete mixing in the radial direction, and practically no mixing in the axial direction. Little attempt was done to correlate this model with the high viscosity that normally gives the liquid a non-Newtonian pseudoplastic behaviour.

The formulation of a flow model in low-grade massecuite fluid in an exhaustion crystallizer was attempted in order to establish a proper correlation between the pattern flux in this unit and the non-Newtonian behaviour that characterizes this fluid.

3.3.1. Experiment

^{99m}Tc in the form of pertechnetate was injected at the inlet of the new Air Swept exhaustion crystallizer. For the purpose of analysis, injection was assumed to be a delta function input. The “on line” detection method was performed, employing a NaI(Tl) 1”x1” scintillation detector coupled to a Mineken ratemeter. Samples for viscosity measurements and purity analysis were drawn periodically at the outlet stream.

Two RTD softwares (DTR8, Maggio NOLDOR S.A and DTSPRO, Progepi), that were distributed by the IAEA to its Member States, and a homemade software (BEAM) were employed for processing and validation of results.

3.3.2. Results

Varying the height of the exit gate (changing the aperture of massecuite exit), three trials were performed. During the first trial, (with the gate at 400 mm height normal working conditions of the factory), parameters obtained by the RTD curve and processed by different software are presented in Table 4.

A model that includes only a simple plug flow reactor with axial dispersion was proposed but the fitting was poor. No difference between MRT of massecuite and molasses was observed. In the second trial (500 mm gate height), normalization by viscosity was performed.

TABLE 4. RTD PARAMETERS OBTAINED BY DIFFERENT SOFTWARE

Parameters	DTR8	DTSPRO	BEAM
Residence time, exp. min.	99,3	99,8	98,8
Residence time, model, min.	91,4	92,2	91,0
Variance	417,7	425	406,8
Peclet	130	130	132
% Dead time	7,9	7,7	7,9

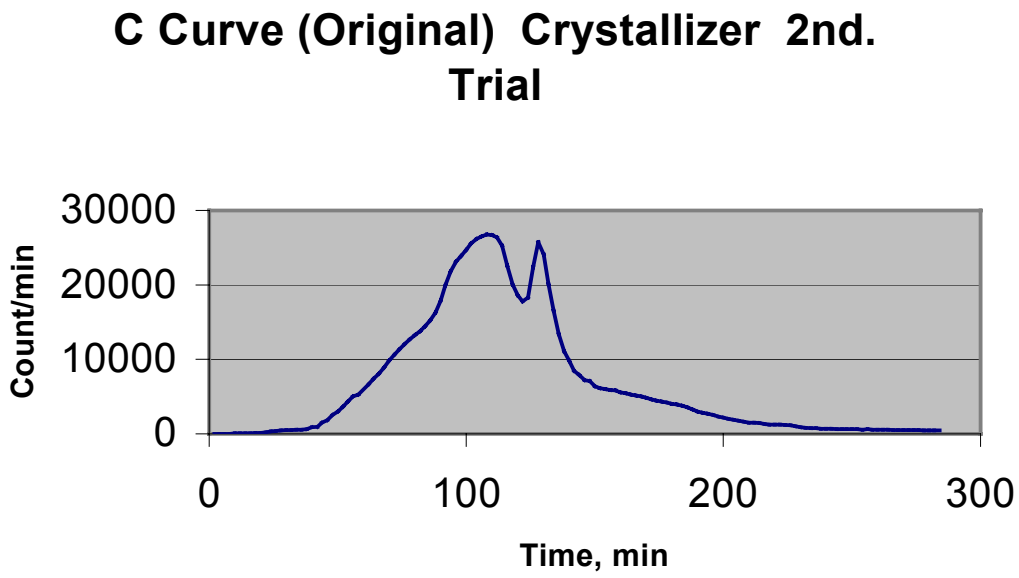

FIG. 15. Original C curve 2nd trial.

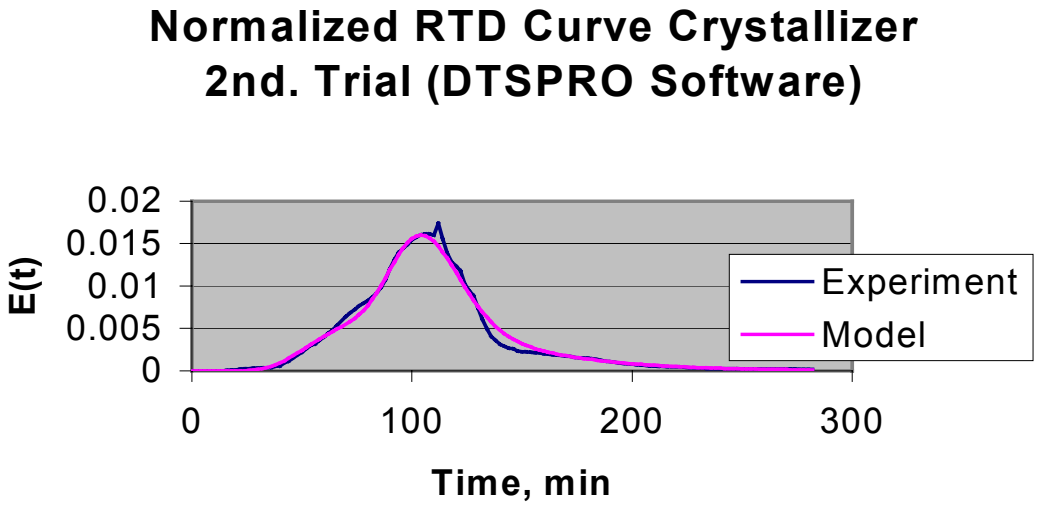

FIG. 16. Normalized RTD Curve 2nd trial by DTSPRO software.

The proposed flow model consists of two plug flow units with axial dispersion. MRT was increased to nearly 120 min and a difference of 13 min between MRT of massecuite and molasses was reached.

A third trial (600 mm gate height) was performed keeping better the steady state condition in the process. The fitting of experimental curve with RTD model was satisfied (Fig. 17). The model consisted of an initial plug flow reactor (which reflects the inlet of the pumped massecuite) followed by two parallel paths (flows), one represents a plug flow reactor connected to a perfect mixing cell with backmixing, and the other shows a plug flow reactor connected directly to the exit (Fig. 18).

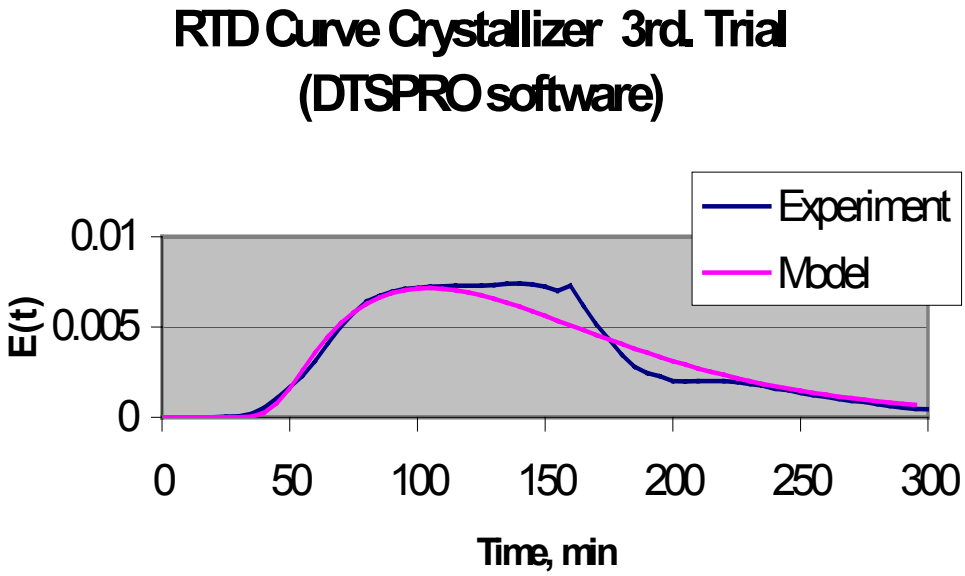

FIG. 17. Normalized RTD Curve in third trial by DTSPRO software.

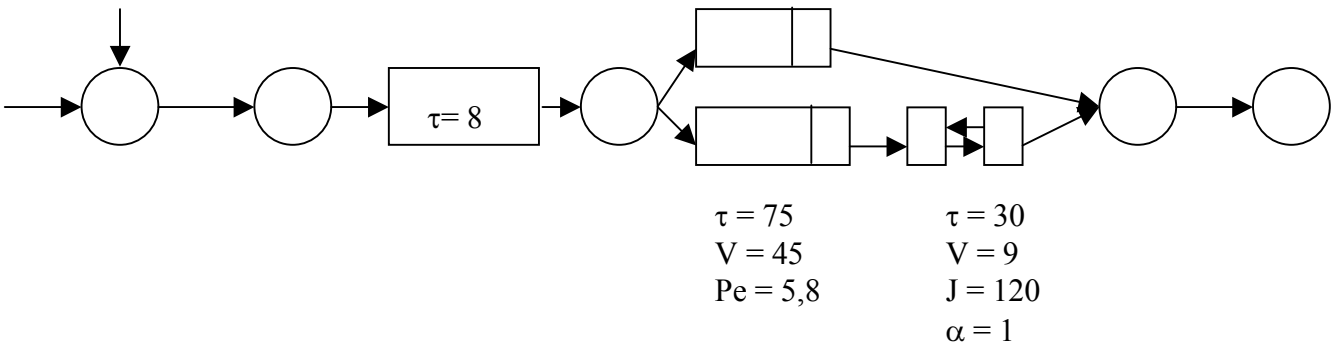

FIG. 18. Proposed model for massecuite exhaustion low grade crystallizer.

The difference between MRTs of massecuite and molasses of 20 min was achieved and the increase of purity drop in molasses (a measure of exhaustion capacity of the crystallizer) was observed.

The main conclusion was that the flow pattern in a low grade exhaustion crystallizer depends strongly on the viscosity of the massecuite fluid.

RTD normalization by viscosity can smooth fluctuations observed in experimental RTD curve of a low-grade crystallizer, allowing the possibility to find a proper model that can describe the behaviour of the non-Newtonian massecuite fluid.

An adequate purity crystallization can be achieved in low-grade crystallizer in the presence of a certain degree of mixing (axial and radial) that is achieved by at least two parallel flows helping an intermixing process.

There is a direct relation of the purity crystallization in mother liquor in a low-grade crystallizer with the difference in residence time between massecuite and molasses; the greater this difference becomes better the performance of crystallization is achieved. This fact can be used for evaluation of the exhaustion characteristics of any type of low grade crystallizer.

3.4. LIQUID FLOW IN TRICKLE BED REACTORS

Trickle bed reactor (TBR) is a reactor where liquid and gas phases flow concurrently downwards through a fixed bed of catalyst particles while the reaction takes place. In certain cases, the two phases also flow concurrently upwards. The concurrent downward flow operation is preferred because of lower axial mixing, better mechanical stability and less flooding, thus facilitating processing of higher flow rates and increasing reactor capacity.

In the last few decades the TBR has been studied extensively by chemical engineers due to its suitability for many operations in petroleum refining, chemical, petrochemical and biochemical processes. Knowledge of hydrodynamics of this reactor is important to evaluate its performance and predict its behaviour. Liquid hold-up and axial dispersion are two key parameters to describe the performance of a TBR. RTD analysis facilitates the determination of these parameters.

The main objectives of the study were:

(1) measurement of RTD and estimation of liquid hold-up from the measured MRT as a function of different process and operating conditions.

(2) mathematical modelling of RTD data, estimation of axial dispersion/backmixing and investigation of hydrodynamic behaviour of the TBRs as a function of different operating conditions.

3.4.1. Experiment

About 10–20 MBq Br-82 activity was used in each experiment. The experiments were performed at different combinations of gas and liquid flow rates. The tracer was injected instantaneously into the inlet feed line through an injection port at the top of the column using a calibrated glass syringe after the reactor achieved steady state flow condition. The movement of tracer was monitored at the inlet (D_1) and outlet (D_2) of the column using

collimated NaI(Tl) scintillation detectors separated by a distance of 125 cm. In order to investigate the radial distribution/maldistribution of liquid phase, an additional detector D_3 was also mounted diametrically opposite to detector D_2 at the outlet. The detectors were connected to a multichannel data acquisition system (DAS) through a five channel counter and a laptop computer. The tracer concentrations at the inlet and the outlet were recorded until the radiation levels reduced to the natural background level. The recorded data were transferred to the computer for subsequent analysis.

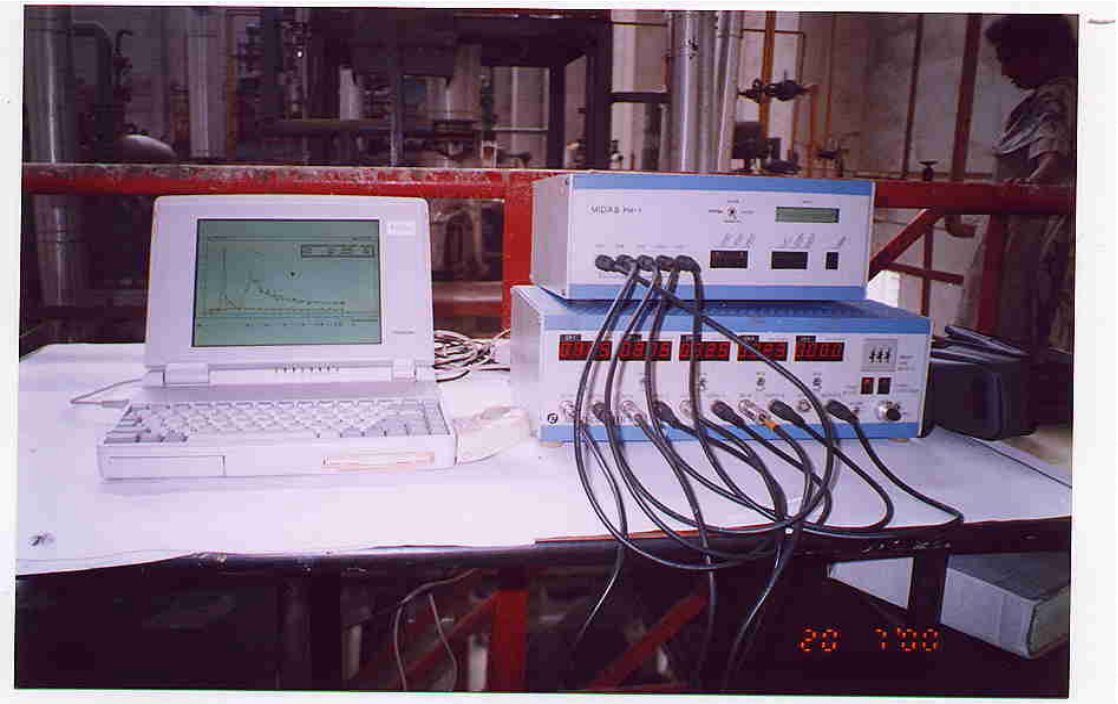

FIG. 19. Five-channel counter and data acquisition system.

FIG. 20. Trickle bed reactor (R01).

FIG. 21. Trickle bed reactor (R02).

FIG. 22. Tracer injection system used in studies at high pressure.

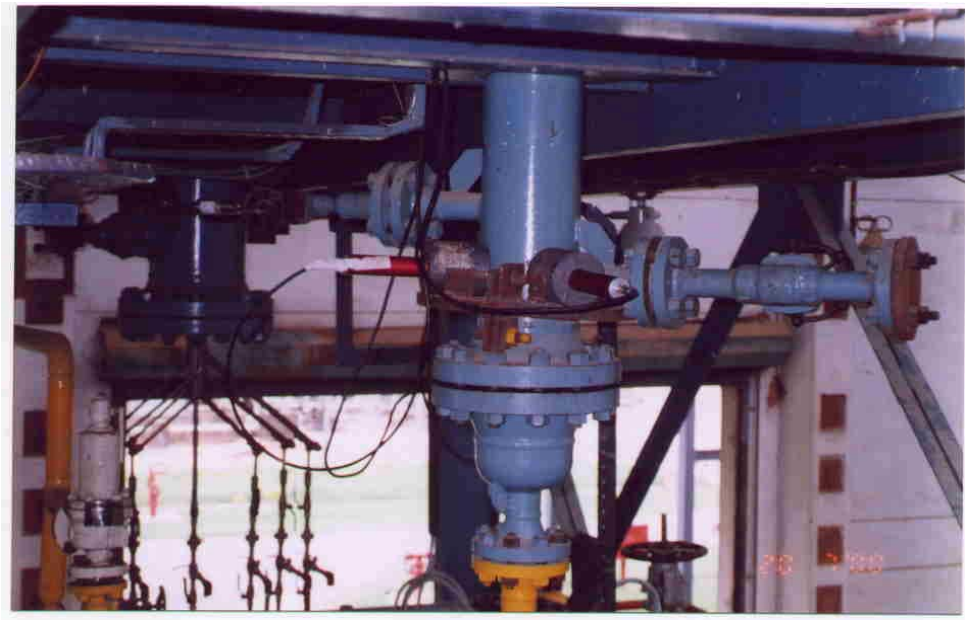

FIG. 23. Trickle bed reactor (R01) showing positions of outlet detectors.

3.4.2. Data processing

The data recorded were treated and analysed. The data treatment includes background subtraction, zero shifting, tail correction. Figs 24 and 25 show typical untreated and treated experimental RTD curves, respectively, obtained in studies at ambient conditions.

First moments (M_i) of the input and the output tracer concentration curves were determined using the following relation:

$$M_i = \frac{\int_0^t t_i C_i(t_i) dt}{\int_0^t C_i(t_i) dt}$$

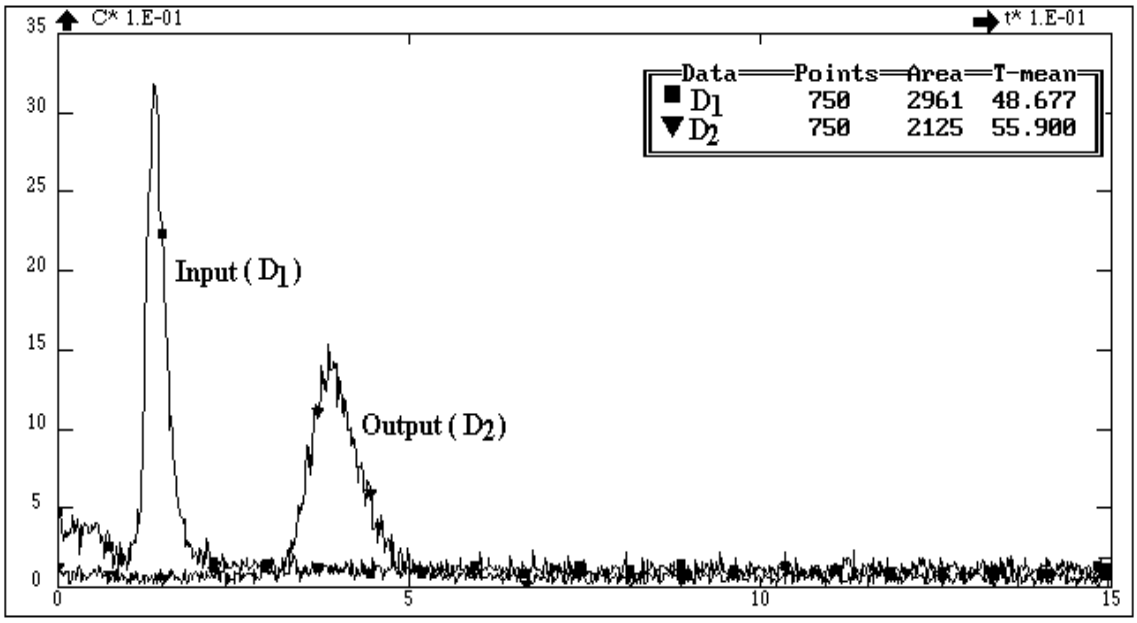

FIG. 24. Untreated RTD experimental curves.

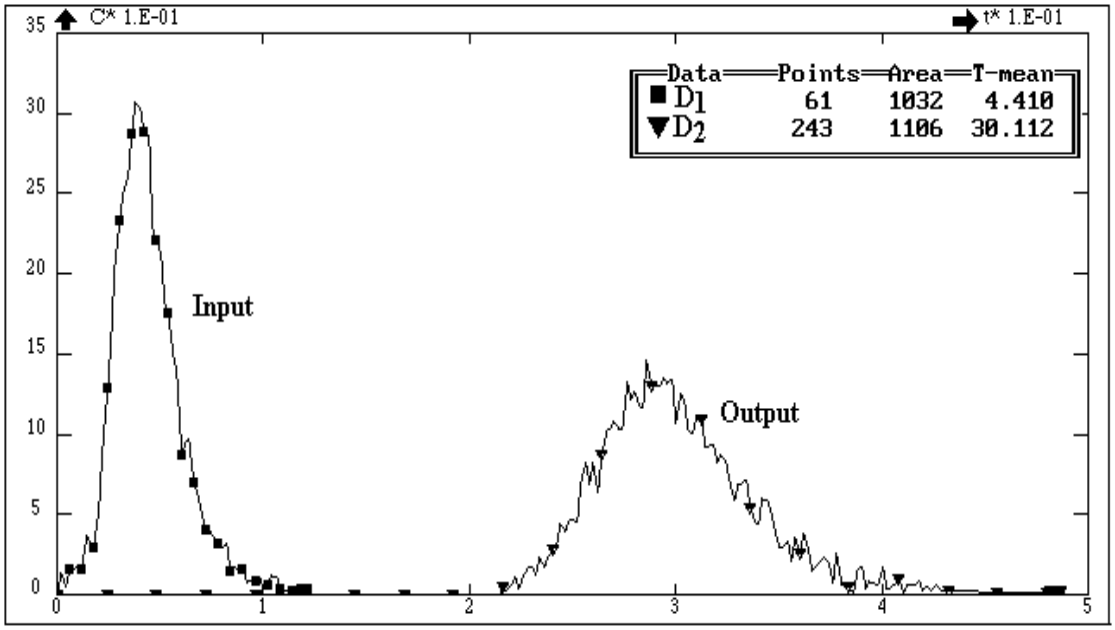

FIG. 25. Treated RTD experimental curves.

The difference of the first moments of the two curves gives MRT of the process material in the system. Thus:

$$\bar{t}\ (\text{MRT}) = M_2 - M_1 \qquad (7)$$

where

M_1 & M_2 are values of the first moments of the input and the output curves, respectively.

The theoretical MRT (τ) of the material in a closed system is given as:

$$\tau = \frac{V}{Q} \tag{8}$$

where

V is the volume,
Q is the flow rate.

For a normally operating closed system, the theoretical and experimentally measured MRT should be the same. Based on the calculated MRT, liquid hold-up was calculated using the following relation:

$$H_T = \frac{\bar{t}\ Q_L}{V_R} \tag{9}$$

where

H_T is the liquid holdup,
$\bar{t}$ is the experimentally determined MRT,
Q_L is the volumetric liquid flow rate,
V_R is the effective reactor volume.

3.4.3. Radial distribution

Radial distribution is another parameter, which determines the efficiency and product quality in industrial packed bed systems. It is of practical significance in reactors with large diameters. Ideally the flow through the packed bed should be uniformly distributed across the bed and is dependent upon the liquid distributor mounted at the top of the bed, process parameters and physical properties of the packing used. In the present study, radial distribution of the liquid phase was also investigated in glass column reactor of R-01 and R-02 by the additional detector D3 placed opposite to detect D2 – at the TBR outlet.

If D2 and D3 experimental curves superimpose each other well, radial distribution is said to be uniform. Any difference among the curves indicates non-uniform distribution of the fluid across the diameter of the reactor. Both detectors were calibrated for equal efficiencies prior to the measurements. During measurements in the glass column, for most of the studies, no radial maldistribution was observed. However, one study showed slight non-uniform radial distribution of liquid phase as can be seen in Fig. 26.

3.4.4. RTD modelling

Tracer concentration curves recorded in reactor R-01 and R-02 for cylindrical catalyst packing are shown in Figs 27 and 28.

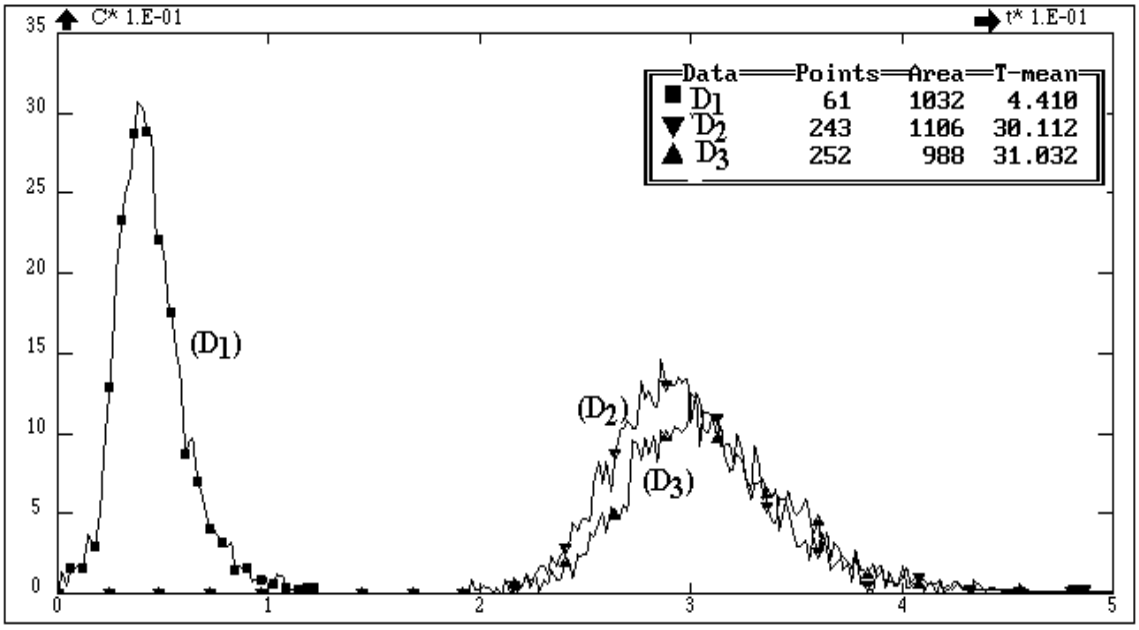

FIG. 26. Tracer concentration curves recorded by three detectors.

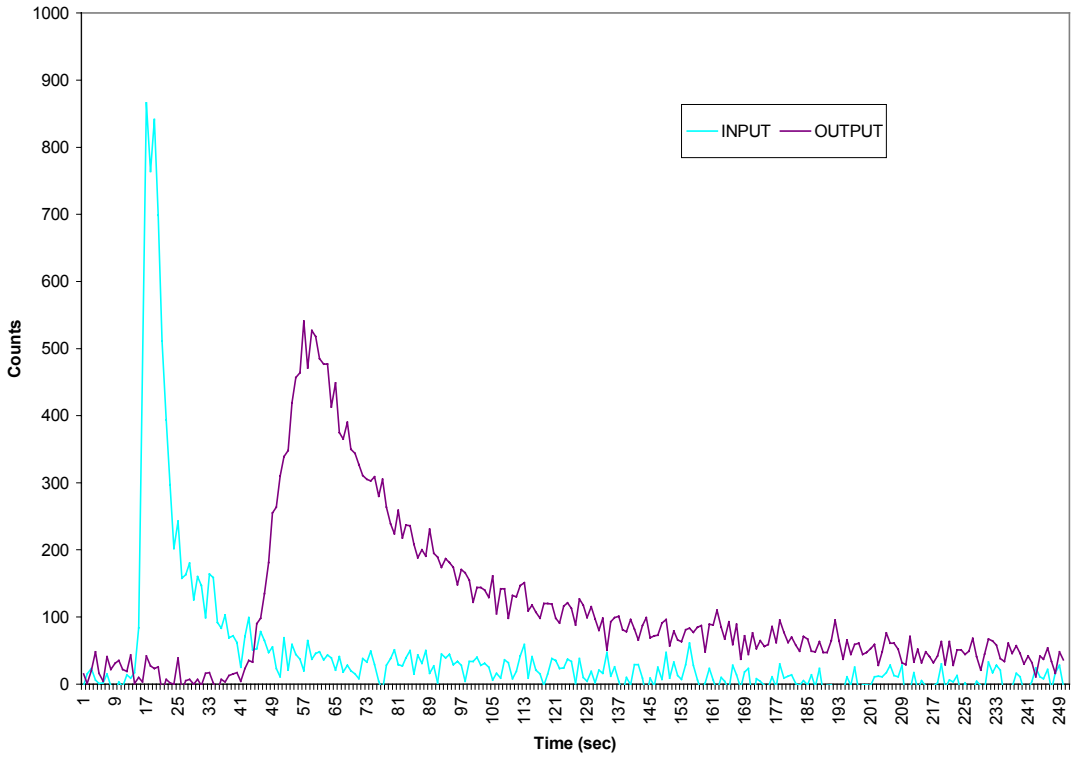

FIG. 27. RTD at outlet of R-01.
(Studies at high pressure and ambient temperature, packing: cylindrical).

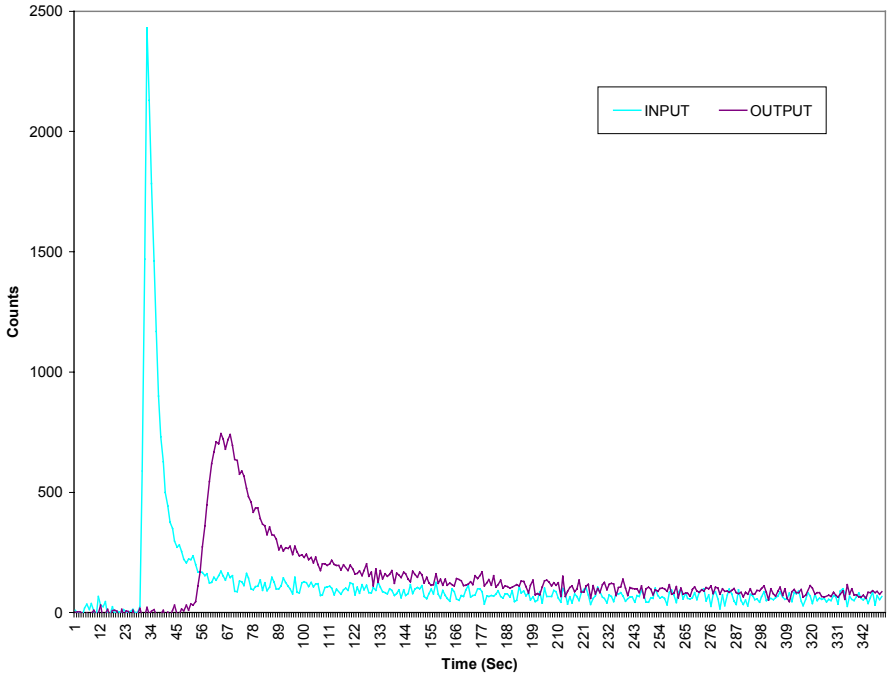

FIG. 28. RTD at the outlet of R-02.
(Studies at high pressure and ambient temperature, packing: cylindrical).

Axial dispersion model

The trickle bed reactors are designed to behave as a plug flow reactors. However, some axial intermixing is always inevitable. In many cases the deviation from plug flow is not too large and the RTD observed is highly symmetrical and approaches the normal distributions curve. This suggests that the RTD of such reactors may be considered as the result of piston flow with a superimposition of longitudinal dispersion. The latter is taken into account by means of a constant effective longitudinal dispersion coefficient D, which has the same dimension as the molecular diffusivity. The value of D is usually much larger than the molecular diffusivity because it also incorporates all other effects that cause deviation from plug flow like velocity differences, eddies and vortices. The mass balance equation for axial dispersion model in a dimensionless form is written as (Levenspiel and Smith, 1957):

$$\frac{1}{Pe}\frac{\partial^2 C_\theta}{\partial Z^2} = \frac{\partial C_\theta}{\partial Z} + \frac{\partial C_\theta}{\partial \theta} \qquad (10)$$

where

Pe is equivalent to uL/D,
u is the mean velocity of fluid,
l is the length of test section,
t is the time variable,
C_θ is dimensionless concentration,
C is tracer concentration,
C_0 is tracer concentration at time t=0,
Z is the dimensionless distance.

The Peclet number (Pe) can be considered as the ratio between the transport rate by convection and transport rate by dispersion. The physical meaning could be understood from the two extremes.

The three representative plots of model simulation of RTD data, obtained at ambient conditions, for glass beads, tablets and extrudates are shown in Figs 29, 30 and 31, respectively. The IAEA RTD Software was used for data processing and modelling.

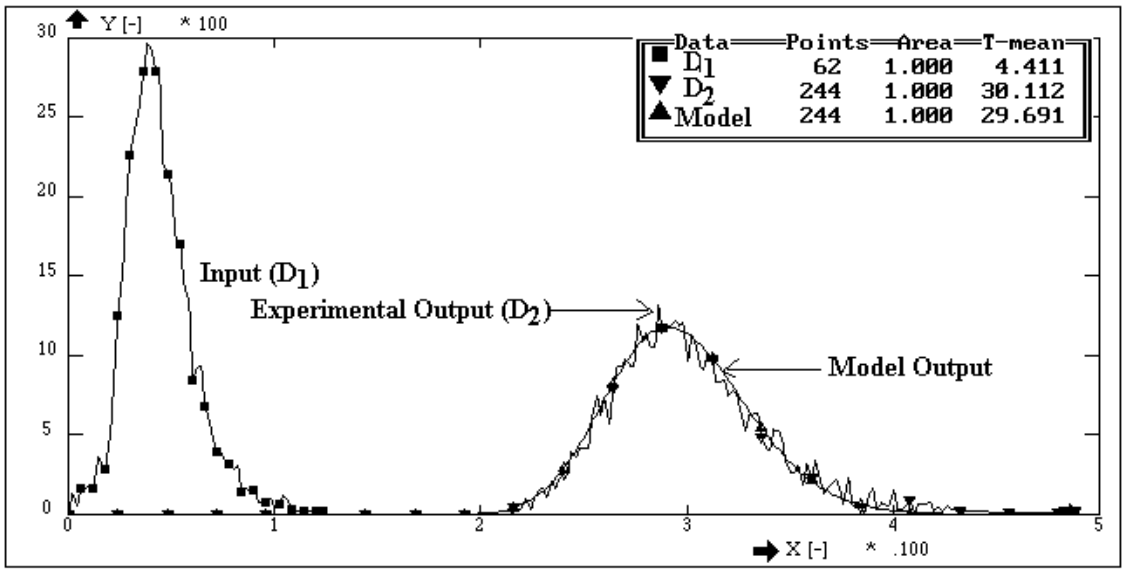

FIG. 29. Comparison of experimental and model simulated RTD curves. (Packing: Glass beads, Q_g=30 L/m, Q_l =15 L/m, P_e=150).

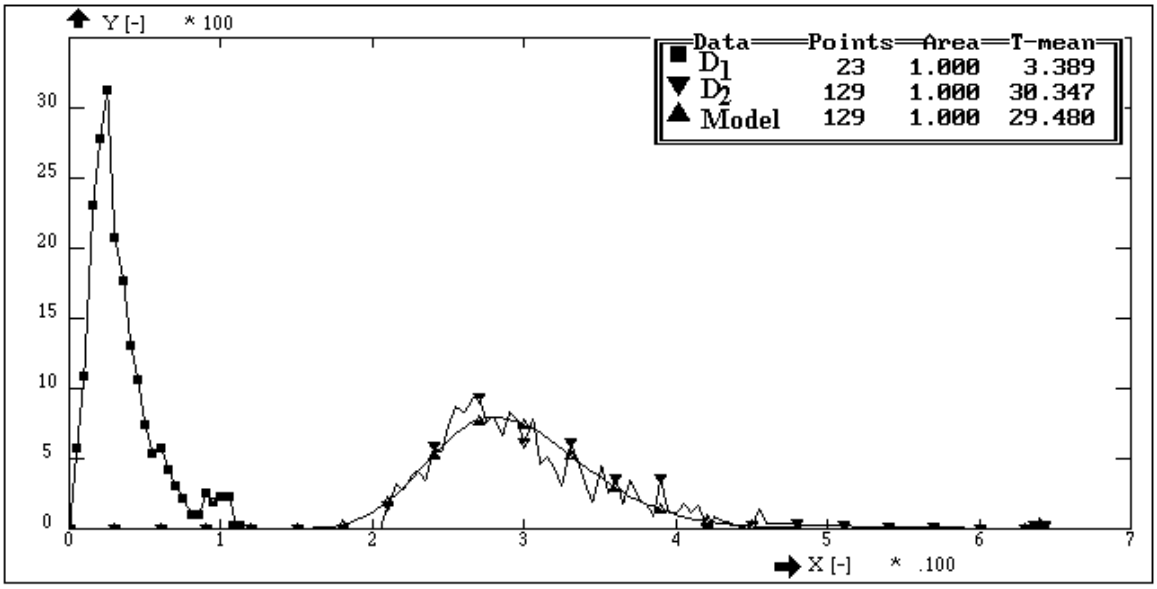

FIG. 30. Comparison of experimental and model simulated RTD curves. (Packing: Tablets, Q_g = 30 L/m, Q_l =15 L/m, P_e = 65).

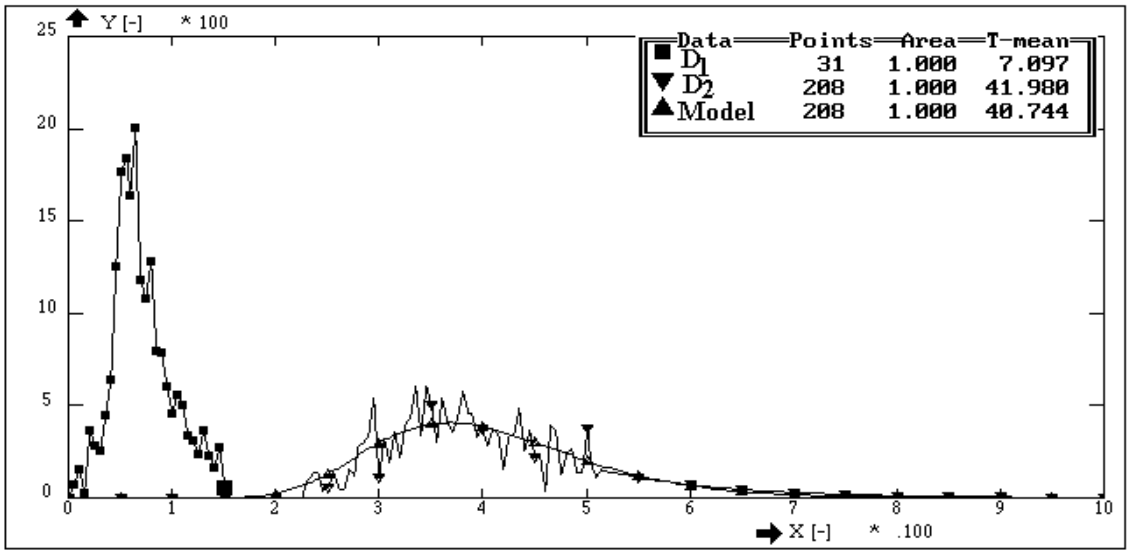

FIG. 31. Comparison of experimental and model simulated RTD curves. (Packing: Extrudates, Q_g = 0 L/m, Q_l =5 L/m, P_e = 30).

Axial dispersion plug flow with exchange (ADPE) model (exchange between dynamic and stagnant regions)

The simple axial dispersion model as discussed above is suitable to describe hydrodynamics of packed bed systems having no stagnant regions and nonporous packing. The model fails to describe the long tail present in RTD curves. The long tails in RTD experimental curves shown in Figs 27 and 28 may carry useful information about the process. To describe the RTD curves with long tail, Villermaux and Van Swaaij (1969) proposed a model based on the following considerations [2].

The liquid flow through the packed bed is divided into two parts: (a) dynamic part consisting of fluid through the bed as plug flow with axial dispersion, and (b) stagnant part consisting of perfectly mixed isolated stagnant zones exchanging mass with the dynamic part. The physical representation of the model is shown in Fig. 32.

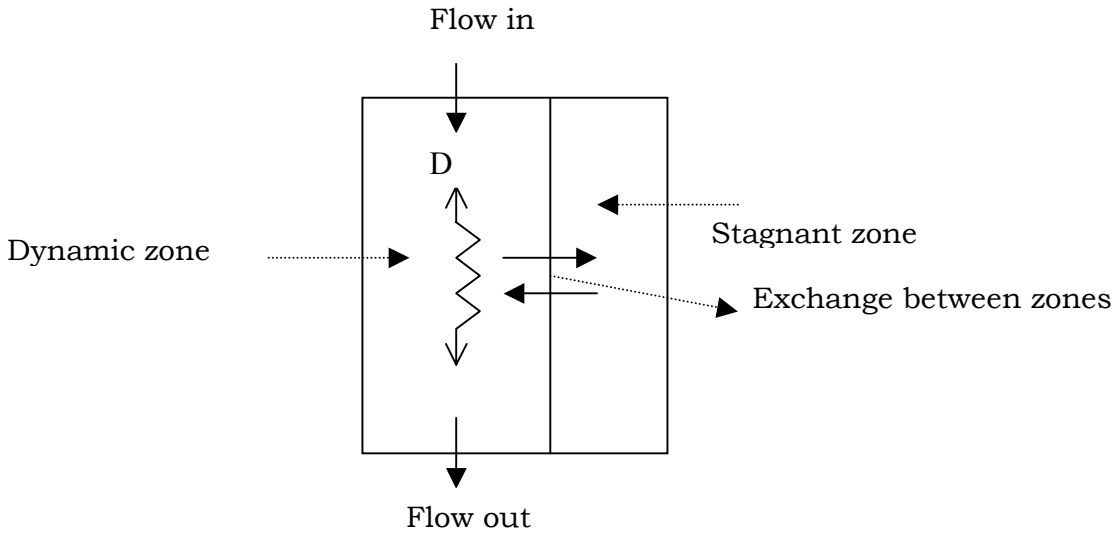

FIG. 32. Axial dispersion model with exchange between dynamic and stagnant regions.

The mass balance equations of the model for an impulse injection are given in terms of following differential equations

$$\frac{C_1}{X} + \frac{C_1}{\theta} + N(C_1 - C_2) = \frac{1}{Pe}\frac{C}{X^2}$$

$$\frac{C_2}{\theta} + \frac{N(C_2 - C_1)}{1 - \varphi} = 0$$

with initial conditions $C_1=C_2=0$ and boundary condition for an impulse injection:

$$X = 0,\ \delta(\theta) = C_1 - \frac{1}{Pe}\frac{C}{X} \qquad (11)$$

where

X is equal to x/Z,
Pe is equal to U_1Z/ D_1,
N is equal to KZ/ U_1,
φ is the volume of dynamic phase/volume of dynamic phase + stagnant phase.

The model contains four parameters: residence time, dynamic fraction of liquid, number of transfer units, and Peclet number Pe. It is clear that this model reduces to axial dispersion model for N=0.

The moments of the distribution function for C_1 at x=1 can be calculated directly by Laplace transform. MRT (first moment) and variance are calculated as:

$$M_1 = \frac{1}{Pe_1}$$

$$\sigma^2 = \frac{2}{Pe_1} + \frac{3}{Pe_1^{\ 2}} + \frac{2(1 - \ )^2}{N}\left(\frac{1}{Pe_1} + 1\right)$$

As the stagnant liquid is trapped mainly on the contact points of the packing, there will be no axial mixing within the phase.

The above described ADPE model was used to simulate RTD data obtained in reactors R01 and R02.

Experimental and model simulated RTD curves are shown in Fig. 33.

The values of model parameters τ, N, φ and P_e estimated from model simulation are given in Table 5 and 6, respectively.

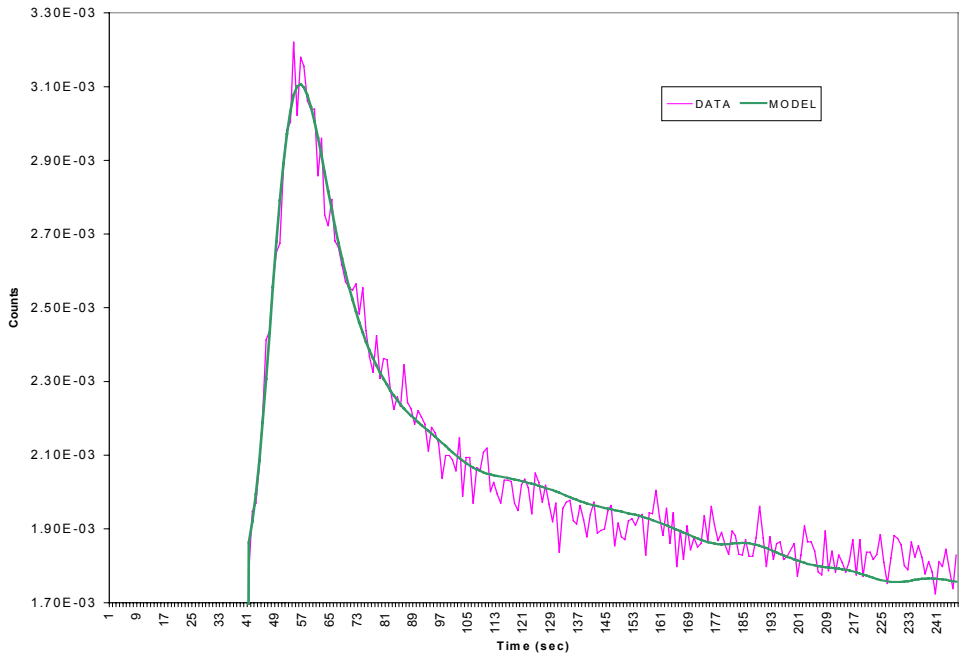

FIG. 33 a. Experimental and model RTD for R-01.
(Studies at high pressure and ambient temperature, packing: cylindrical)
P=10 Kg/cm^2, Q_l = 6 L/m, Q_g = 23 Nm^3/h.

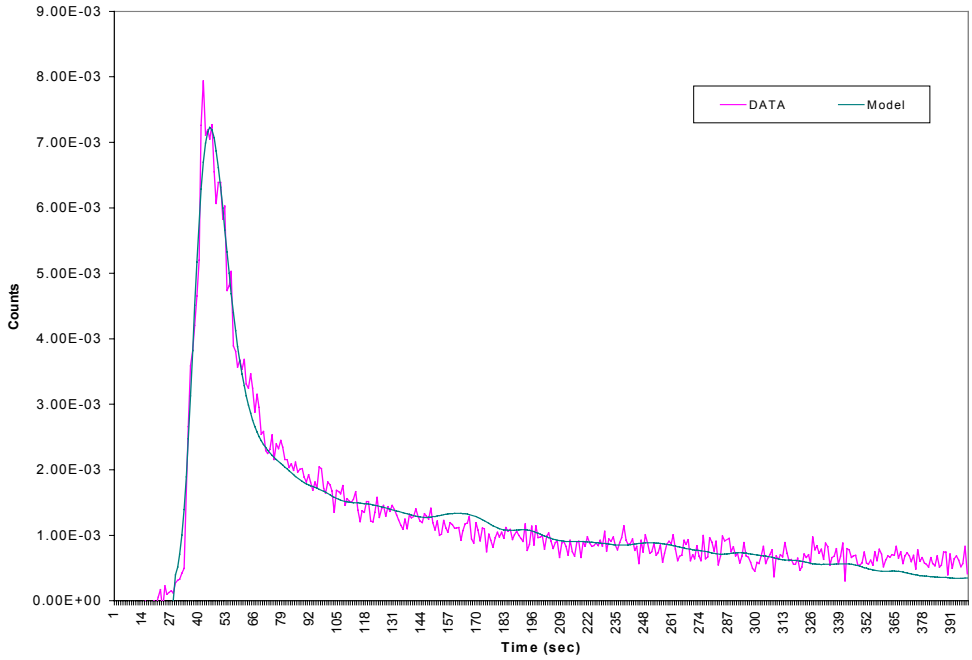

FIG. 33 b. Experimental and model RTD for R-01.
(Studies at high pressure and ambient temperature, packing: cylindrical)
P=6 Kg/cm^2, Q_l = 8 L/m, Q_g = 23 Nm^3/h.

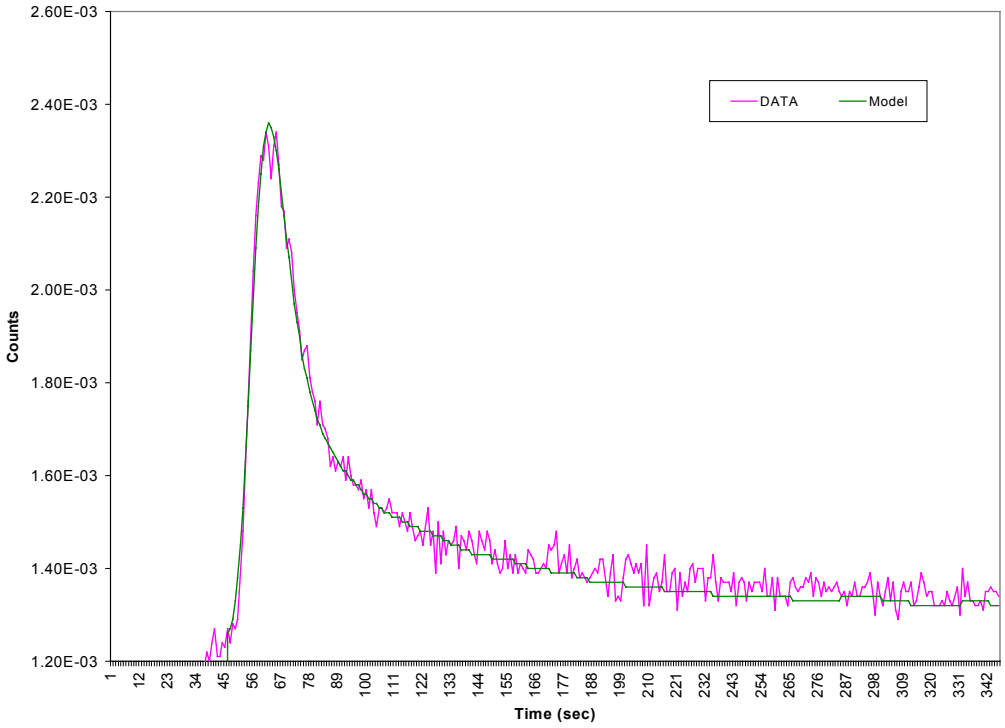

FIG. 34 a. Experimental and model RTD for R-02.
(Studies at high pressure and ambient temperature, packing: cylindrical)
P=1 Kg/cm^2, Q_l = 24 L/m, Q_g = 0 Nm^3/h.

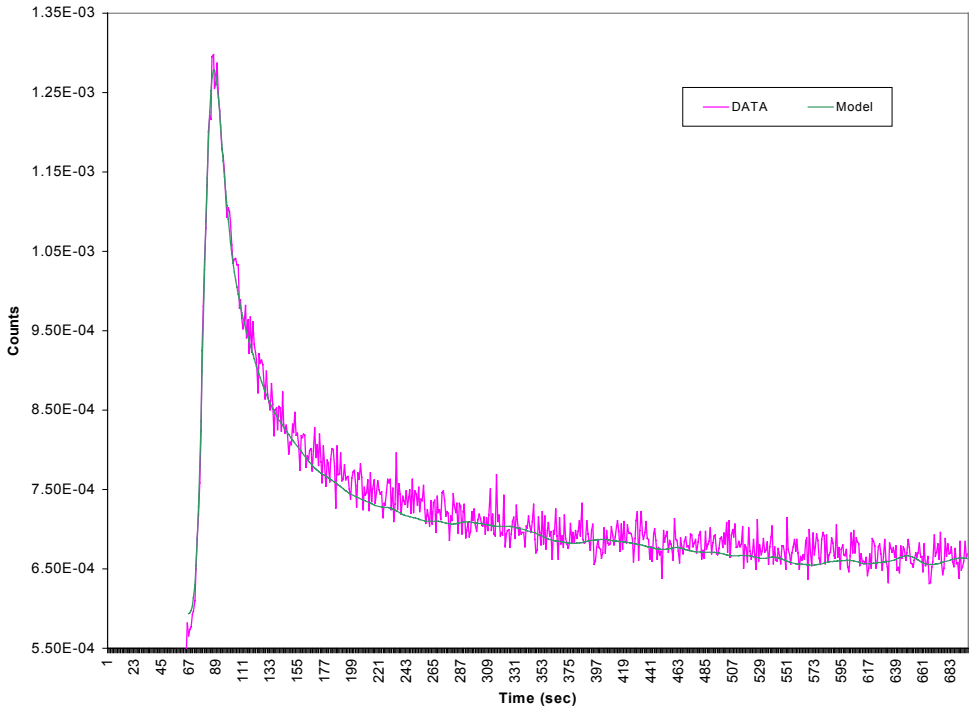

FIG. 34 b. Experimental and model RTD for R-02.
(Studies at high pressure and ambient temperature, packing: cylindrical)
P=10 Kg/cm^2, Q_l = 16 L/m, Q_g = 95 Nm^3/h.

TABLE 5. REACTOR R-01 CYLINDRICAL PACKING SYSTEM GAS-NITROGEN AND LIQUID-KEROSENE

Test no.	P (kg/cm^2)	Q_g (Nm^3/h)	Q_l (lpm)	τ (sec.)	N	φ	Pe
1	1	0	6	103	0.7	0.8	50
2	6	13	2	278	0.9	0.6	39
3	6	13	4	170	0.8	0.7	95
4	6	13	8	87	0.3	0.8	45
5	6	23	8	196	0.5	0.3	32
6	10	13	4	135	4.9	0.6	18
7	10	13	6	93	5.7	0.7	30
8	10	23	2	327	1.3	0.5	63
9	10	23	4	147	1	0.6	161
10	10	23	6	115	0.6	0.7	66

TABLE 6. REACTOR R-02 CYLINDRICAL PACKING SYSTEM GAS-NITROGEN AND LIQUID-KEROSENE

Test No.	P (kg/cm^2)	Q_g (Nm^3/h)	Q_l (lpm)	τ (sec.)	N	φ	Pe
1	1	0	24	88	0.5	0.7	53
2	6	37	24	88	1.2	0.6	117
3	6	95	16	135	0.8	0.6	47
4	6	95	24	84	1.1	0.6	99
5	10	37	16	99	0.7	0.8	11
6	10	95	8	225	0.9	0.5	28
7	10	95	16	106	0.8	0.7	70

3.4.5. Validation of radiotracer

Bromine-82 as dibromobiphenyl was used as a tracer in the experiments carried out in hydrogen-vacuum gas oil based trickle bed reactor operating at high temperature and pressure. The boiling temperature of dibromobiphenyl at atmospheric pressure is 370ºC and hence it may not be stable at higher temperature. The boiling point will increase with the increase in pressure. Since the pressure in the reactor is about 170 kg/cm^2, the tracer would not vaporize and it is supposed to remain in liquid phase at 400ºC temperature.

The results of the tracer tests carried out at a temperature of 250ºC show that the tracer did not appear at the outlet of the reactor indicating the adsorption of the tracer on the catalyst particles (Fig. 35). Test carried out at lower temperature ~150 ^{0}C showed the tracer did appear at the outlet but the intensity of tracer concentration curves was very low (Fig. 36). The area under the inlet and outlet curves was not equal and the condition of tracer balance was not satisfied. This indicates partial adsorption of the tracer. If the geometric efficiency of the inlet and the outlet detectors are the same, the area under the input and output curves should be equal in order to satisfy the condition of tracer balance. In a tracer test carried out at temperature about 100ºC the area under concentration curves recorded are almost equal and the tracer balance is achieved (Fig. 37).

The results of the study indicate that at temperature more than 100ºC, the tracer gets adsorbed on catalyst particles. The adsorption may be of chemical type with the following reaction:

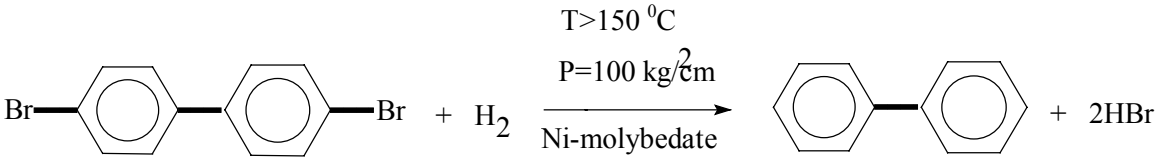

The hydrogen bromide may be getting adsorbed on the catalyst bed. However, this has to be confirmed by conducting tracer experiments in absence of hydrogen gas.

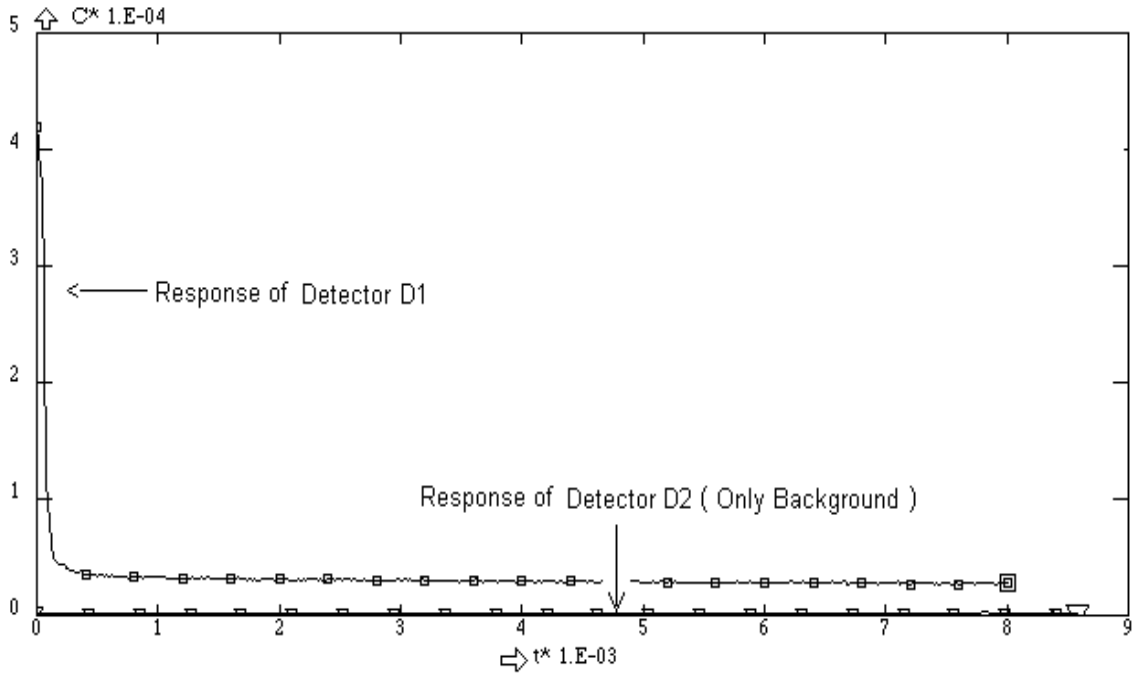

FIG. 35. Representative of tracer concentration distribution curves.

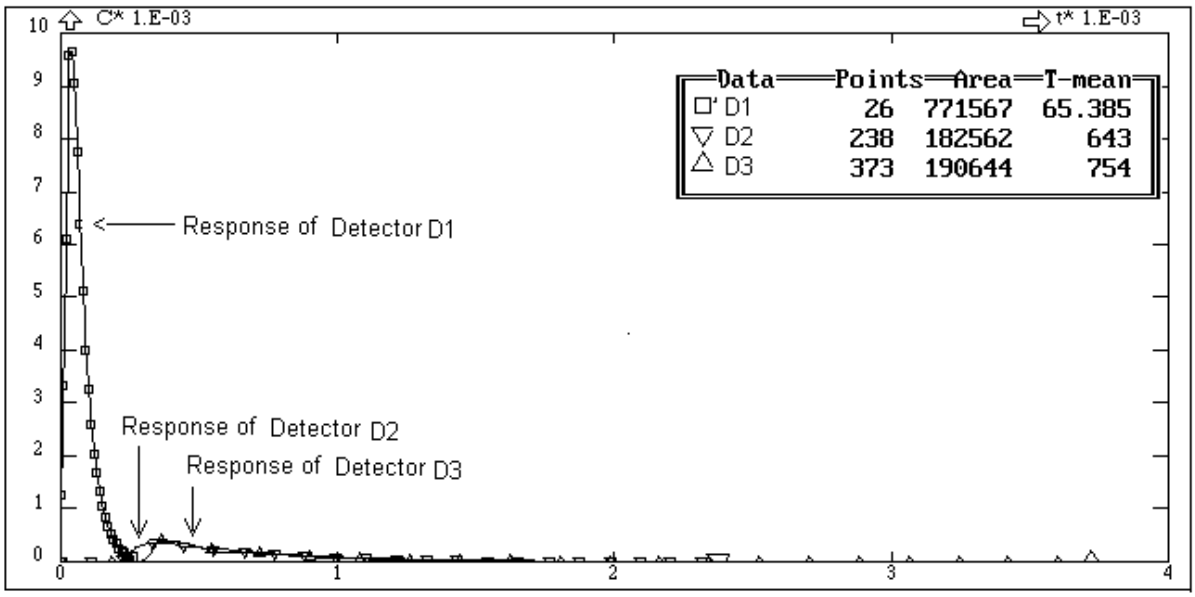

FIG. 36. Tracer concentration distribution curves.

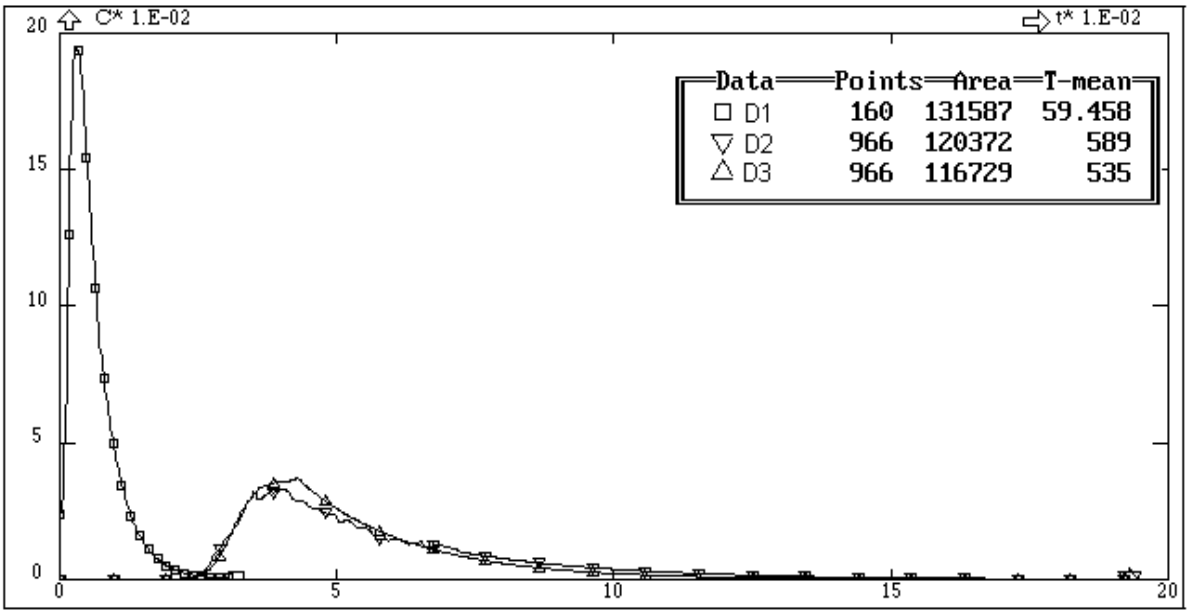

FIG. 37. Tracer concentration distribution curves.

3.4.6. Conclusions

Studies at normal temperature and pressure showed that:

— no significant radial maldistribution was observed;
— the liquid hold-up is a strong function of liquid flow rate and is almost independent of gas flow rates used in the study;
— for glass beads and tablets the degree of dispersion (*Pe*) decreases with increasing liquid flow rate and is constant for extrudates;
— no specific trend in degree of dispersion (*Pe*) is observed with respect to varying gas flow rates;
— the model estimated MRTs are in good agreement with MRTs measured experimentally; this justifies that the axial dispersion model is suitable to describe the dynamics of liquid phase in TBRs;
— the liquid hold-up and degree of axial dispersion *(Pe)* are strongly dependent upon shape and size of the catalyst used in TBRs; the degree of axial mixing is less with spherical catalyst than the catalyst of tablet and cylindrical extrudate shapes;
— the results obtained will be very useful for scale-up, design and optimize the performance of full-scale industrial TBRs.

Studies at high pressure showed that:

— no significant radial irregular distribution was observed;
— no significant effect of liquid distributor on axial mixing was observed;
— the liquid hold-up and Peclet number increases with increasing liquid flow rate;
— no definite trend in MRT and Peclet number has been observed as a function of increasing gas flow rate.

Studies at high temperature and pressure showed that:

— a high degree of backmixing was found in the reactor.

3.5. INVESTIGATIONS OF SOLID PHASE BEHAVIOUR IN A FLOTATION MACHINE

RTD data processing and modelling involves fitting of experimental data with different arrangements of plug flow and perfect mixer models using RTD software. The mathematical calculations are performed in complex Laplace transform domain. In the case of arrangement of elementary models some information carried by RTD curve may be lost. There is a possibility to use adaptive signal processing in analysis of tracer data. The mathematical model is created by adoptive algorithm using experimental data only. The continuous experimental curve is converted to discrete one by z-transform. The mathematical model in z-transform domain is suitable for computer calculations.

The z-transform software for experimental RTD data processing and modelling was used for tracer investigation of copper behaviour to flotation machine. Such parameters as MRT, mixing intensity, flow rate and separation coefficients were determined by means of a radiotracer test. The radiotracer test was carried out in a flotation machine where the enrichment of copper takes place.

Ore samples were activated in a thermal neutron flux to produce the radioactive isotope ^{64}Cu, the natural tracer for copper. The intensity of gamma was measured by scintillation probes placed at the machine's feed, where injection took place, as well as at the outlets of tailings and concentrate.

Injection was considered as an impulse function. Then, by applying moments' method basic parameters such as MRT of the concentrate were determined. RTD was modelled using RTD software and Z-Transform Adaptive Signal Processing.

In Fig. 39, the normalized tracer response curve, together with the Z model, are presented. The transfer function characterizing the concentrate's behaviour in the flotation machine may be decomposed into a product of first and second order functions.

It was concluded that the flotation machine consists of two vessels (perfect mixers) connected in parallel. The MRT for a single mixer is 7.8 min.

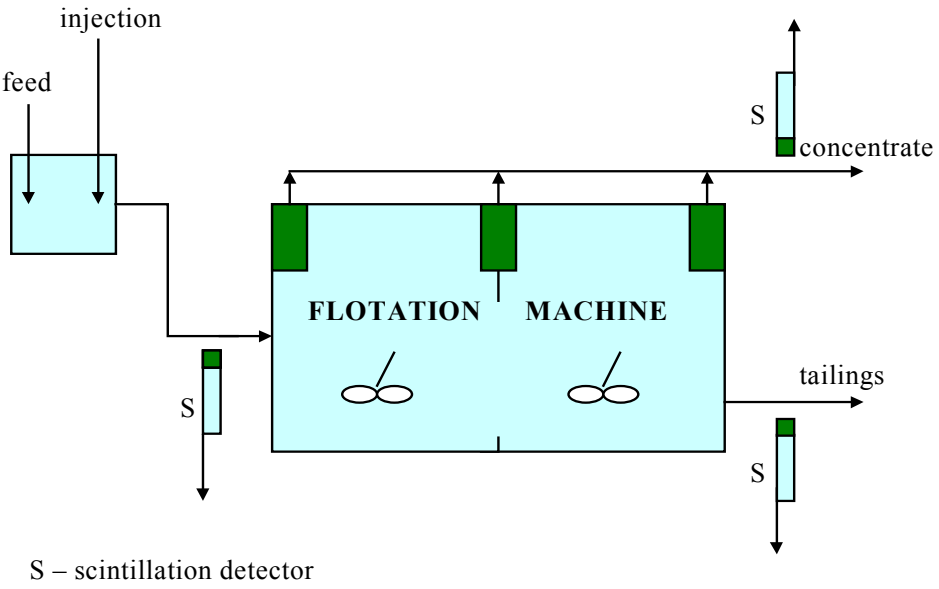

FIG. 38. Tracer experiments in the flotation process.

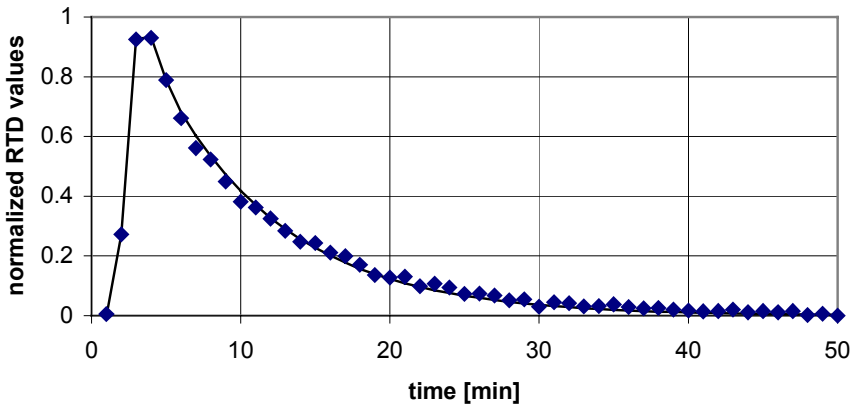

FIG. 39. RTD function derived from experimental, tracer response data for concentrate and the z-model fitted; discrete points of the z-model connected by a line. Number of data n=*50.*

4. FLOW MEASUREMENT

Flow rate measurement is a typical application of radiotracers [14].

For flow measurements, tracer data are important, rather than the RTD models. Main emphasis is given to reliability, precision, standardization, and accreditation. New areas of application and improvements of performance are, however, still important, especially in multiphase systems.

Research is going on in refining the existing methods for single phase flow measurement, and in developing new methods for multiphase flow without sampling [15].

Flow rates of liquids and gases are measured to an accuracy of 1–2% in situations where flow meters are either not installed or are unreliable due to deposits or corrosion. The installed flow meters are calibrated with 1% accuracy. The tracer techniques for single phase flow measurements are recognized as ISO standards [16].

4.1. MULTIPHASE FLOW MEASUREMENT

Flow rate measurements in two or three phase systems are very difficult due to slip velocities and very complicated flow patterns.

The spectromatic tracer technique implies injection of a mixture of three radioactive tracers each being distributed into one of the three phases. The tracers must show such differences in the emitting gamma-radiation energy spectra that they can be simultaneously detected by on line gamma spectrometry. Candidate tracers are Br-82 as bromobenzene for oil, Na-24 or La-140 for water, and Kr-85 for gas. The tracers are injected simultaneously at a constant rate into the flow in the pressurized pipe, and the concentrations are detected as a series of instantaneous measurements taken downstream using spectral gamma-detectors.

In situ measurement of the concentration of radioactive tracers in the different phases requires that the phases are separated and arranged according to density difference over the measurement cross-section in a horizontal pipe. In general, the measurements are performed with two spectral gamma radiation detectors placed on top and bottom of the pipe respectively.

In the case, where all three phases are present, the detector measurements reveal the amounts of tracers in each phase and the position of the boundaries between the phases. The cross-section area of each phase is calculated from the latter. From this the tracer concentrations and, hence, the volume flow rates of the three phases are calculated.

Experiment

Static laboratory measurements

Measurements were made in a static laboratory set-up using two sodium iodide scintillation detectors (6×3”) for gamma spectral measurements with spectral sampling time of 140 msec. A Monte Carlo simulation model for generating supplementary data was developed and verified. A statistical data treatment method was applied to estimate tracer concentration from detector measurements. Accuracy in parameter estimation in the range of 5–10% was obtained.

Dynamic test rig

After having proved the principles a dynamic test facility was built, in which it was possible to inject three tracers in a flowing liquid consisting of air, oil and water. By changing the relative amounts of the different components it was possible to explore the phase diagram and assess the limits for the measurement principle. Experiments confirmed the accuracy in parameter estimation to be below 10%, which is considered satisfactory for practical applications.

On-site test

An on-site test was performed on Danish offshore installation. The injection of ^{140}La (water tracer) and ^{82}Br (oil tracer) was made 200 m upstream of the measuring point (no gas tracer was used). The pressure involved 63 bars. Flows of individual phases were determined after passing a test separator using conventional flow meters (75 m^3/h gas, 2 m^3/h oil, 5 m^3/h water). The tracer test showed a very unexpected flow pattern with short liquid slugs separating gas with some liquid in the lower part of the pipe. Gas flow rate was determined from the slug velocity in good agreement with the test separator results. Detailed analysis of selected data showed that it was possible to distinguish between water and oil tracer concentrations and determine boundary layers between the different phases.

Conclusion

The systematic tracer method measuring only from the outside of the pipe was shown to be applicable under certain circumstances. Combination of outside measurements with liquid sampling for measuring tracer in water and oil will considerably broaden its applicability.

5. RADIOTRACER INVESTIGATIONS OF WASTEWATER TREATMENT PLANTS

Introduction

The wastewater treatment installations are composed of a multitude of elementary processes involving complex multiphase fluid flows. Behaviour of the sewage can affect either the physical process in the settling tank or biological process in aeration reactors. For the settling tank, both sedimentation curve of sludge and water flow structure are required for a proper evaluation of mass transport. For biological processes occurring in the aeration tank, determination of flow structure is helpful to improve its performance [17–18].

Under the framework of the CRP, tracer investigations were conducted in a number of wastewater plants: in Islamabad (Pakistan), Plock (Poland), Havana (Cuba) and Nancy (France).

Tracers can be used to study either the solid or liquid phase. For water labelling in-plant scale Bromine-82 in the form of Potassium Bromide aqueous solution and Pertechnetate Technetium (99m) from Mo/^{99m}Tc generator were used. For solid phase labelling, Lanthanum (La-140) was used mostly. Au-198 or Fe-59 can also label solid phase. In the settling tank and digester flow, behaviour of water is very different from the behaviour of sludge, while in aeration channels, sludge and water can be considered as a pseudo homogenous phase.

Due to relatively long MRT in wastewater treatment processes (from some hours for aeration channels up to several days for digester), pulse injection can be easily realized in a very short time.

Radiotracer can be injected in the wastewater stream simply by breaking a tracer ampoule at the site during the time of injection. A specific injection system may facilitate introduction of liquid radiotracer directly from a storage container to the stream.

The elementary processes, which take place in a wastewater treatment plant, are strongly influenced by the flow behaviour. For the settling tank an increase in flow rate results in bad decantation of the sludge. Short circuits are observed as well, which increase the solid rate in the water output. Use of tracers helps to determine material transport and hydrodynamic model of liquid and solid phases.

Stagnant volume is also present in different parts of a wastewater treatment installation. Tracer experiment can estimate the stagnant volume and consequently provides data to engineers either to better maintain it or change its configuration for improving efficiency.

Settling tank

In a settling tank the influent is flowing slowly in order that the sludge can settle at the bottom of the tank (Fig. 40). Usually, a rubber scraper in the centre pit of the tank collects the sludge. From the settling tank, sludge is transferred to a digester and the effluent goes to the aeration tank.

Interpretation of tracer experiments in the settling tank is quite complicated. Typical RTD of water phase (Fig. 41) shows that the model is composed of a main stream going from the inlet to the outlet with a recirculation on the bottom of the tank. However, the flow parameters in these two streams have been found different for different settling tanks, this means that the model is more or less the same but the model parameters are affected by the tank design.

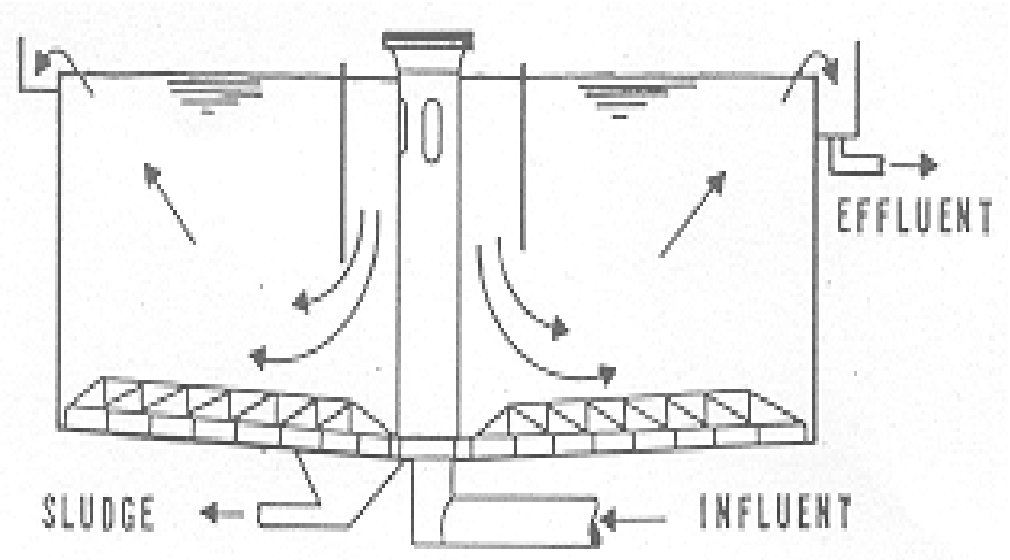

FIG. 40. Classical settling tank configuration.

Aeration tank

Due to high gas flow rate, tracer experiments conducted in an aeration tank showed that water and sludge have generally similar flow behaviour. However, stagnant volume was observed for some configurations, which results in accumulation of sludge. Tracer investigations showed that the fluid flow could be modelled either by perfect mixing cells in series or by perfect mixing cells in series with back mixing. The number of mixing cells is a function of both gas and water flow rates, and also of the geometrical configuration.

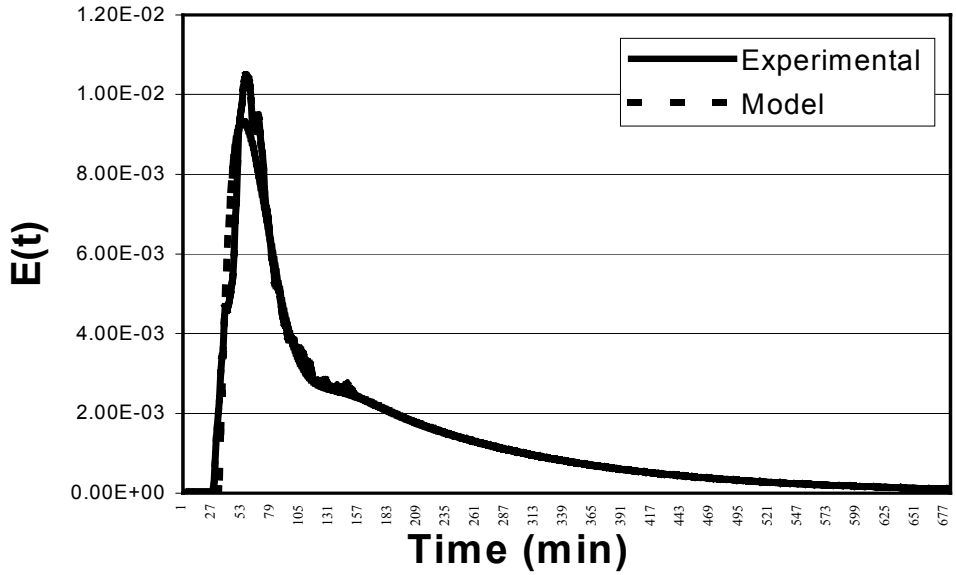

FIG. 41. Typical tracer output from settling tank.

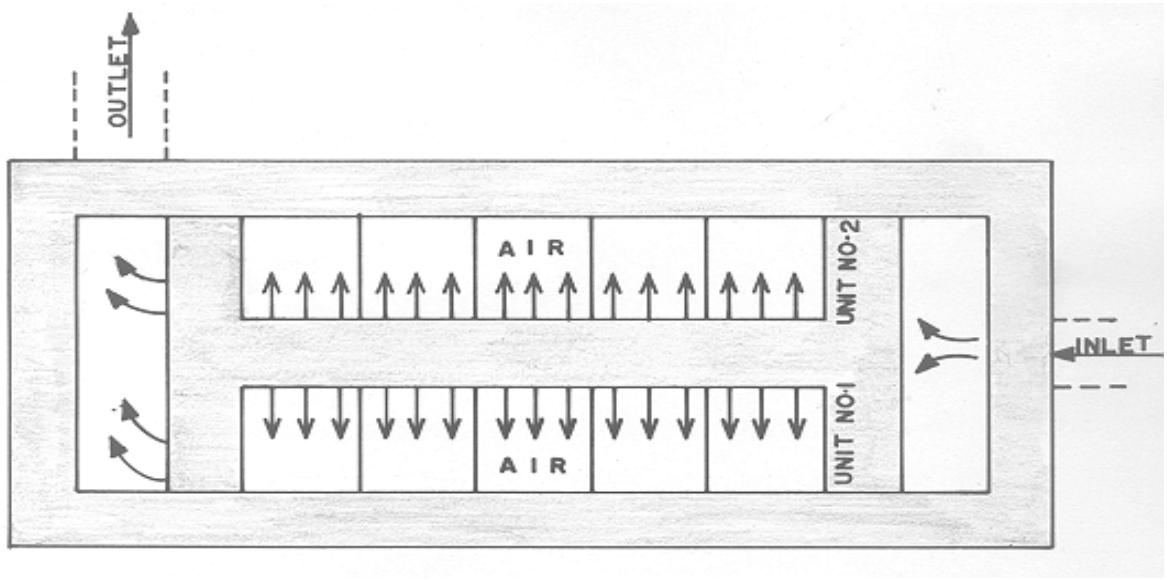

FIG. 42. Classical configuration of aeration tank.

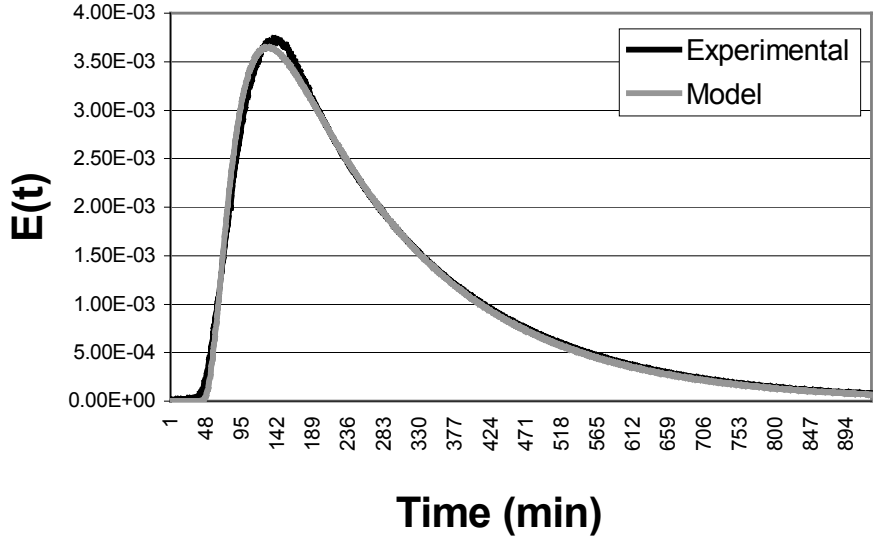

FIG. 43. Typical tracer output for aeration tank.

5.1. RADIOTRACER TESTS IN WASTEWATER INSTALLATION — CASE STUDIES

5.1.1. Investigation of clarifiers and aeration tank

Hydrodynamic behaviour of primary and secondary clarifiers and the aeration tank was investigated by determining RTD using radiotracer.

Radioactive tracer ^{82}Br in the form of water soluble potassium bromide (KBr) was used to investigate different units of a wastewater treatment in Islamabad, Pakistan.

The activity of ^{82}Br injected in the primary clarifier, aeration tank and secondary clarifier included 1.296 GBq (35 mCi) , 1.11 GBq (30 mCi), and 1.48 GBq (40 mCi), respectively. The tracer was detected at different points with submersible scintillation detectors (including injection-inlet, outlet and two internal points). On-line data acquisition was used to collect the experimental data.

The theoretical MRT of the primary clarifier was calculated at 287 min, while the experimental MRT was found to be 164 min. Therefore, 43% dead volume was estimated in the primary clarifier. The theoretical MRT of the aeration tank was calculated at 272 min, while its experimental MRT was found to be 271 min. Therefore, almost a negligible amount of dead volume was estimated in the aeration tank. This is due to the vigorous mixing process inside the aeration tank.

Theoretical MRT of the secondary clarifier was calculated at 669.6 min, while its experimental MRT was found to be 284.7 min. Therefore, 57.4% dead volume was estimated in the secondary clarifier.

Progepi RTD software was used for preliminary treatment of the experimental data and modelling of these systems. The following figure, as an example, shows the experimental RTD curve and its model for the secondary clarifier.

The model is reproduced in Fig. 45.

All final results are summarized in Table 7.

The experimental conclusions are:

— The hydrodynamic behaviour of the aeration tank is according to expectation. The model, consisting of five perfectly mixing cells in series, fits well with the design.

— Some abnormal behaviour of primary and secondary clarifiers were found, that is why large dead volume was observed. Necessary remedial action was required to be taken in order to improve and enhance efficiency of the clarifiers.

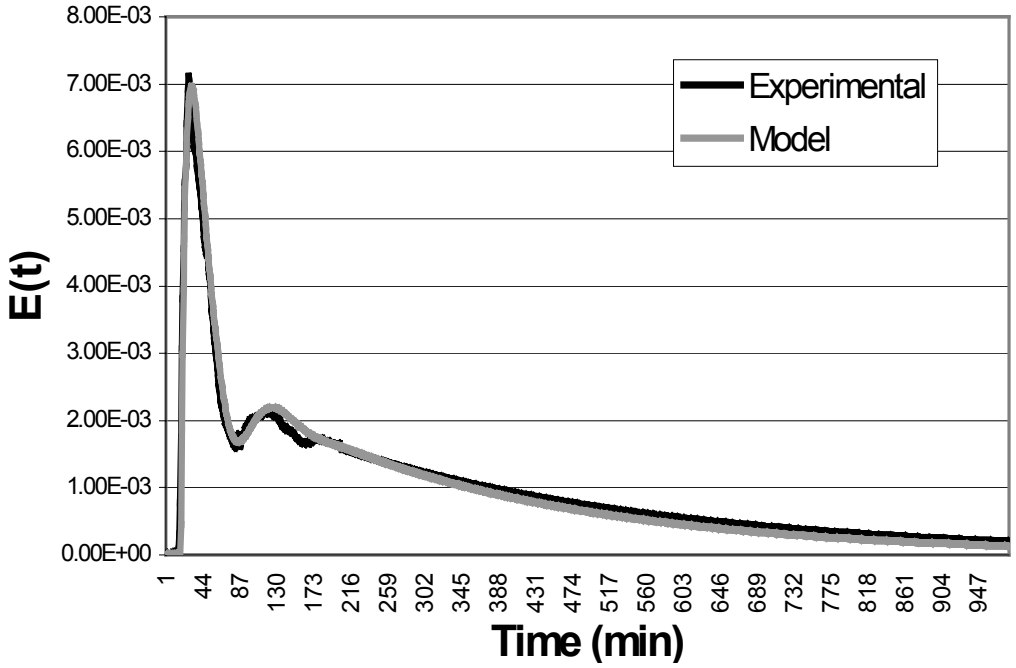

FIG. 44. Experimental RTD curve and its model for secondary clarifier.

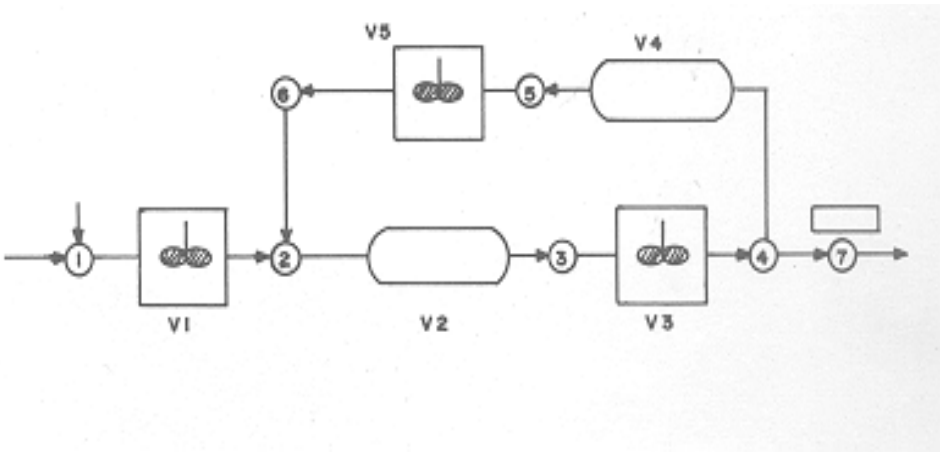

FIG. 45. V1, V3, V5 represent perfect mixing modules, while V2 and V4, plug flow modules.

TABLE 7. SUMMARY OF RESULTS OBTAINED BY RADIOTRACERS

System under investigation	Volume (m^3)	Flow rate (m^3/min)	Theoretical MRT (min)	Exp. MRT (min)	Model MRT (min)	Dead Vol. (%)
Primary clarifier	1387	4.83	287	164	166	43
Aeration tank	567.5	2.08	272	271	269	0.2
Secondary clarifier	2790	4.17	670	285	260	57

5.1.2. Investigation of channel bioreactor

In Poland and France, investigations were made of the petrochemical wastewater treatment stations during 1998–2000. Three major units involved in wastewater treatment process in the Polish petrochemical industry are equalizer-clarifier, biological aeration chamber with settler and final sedimentation basin.

Effectiveness of the purification process carried out in such an installation strongly depends on flow pattern of wastewater and sediment. From the process-engineering point of view these tanks represent continuous multiphase flow systems. In equalizer and settlers the concurrent flow of water and sediment occurs. In biological reactor there are three phases, water, sediment and air. Their good contacts create conditions for interphase oxygen exchange.

The best radiotracer for a liquid phase is Br-82 in form of aqueous KBr solution; the sediment was labelled with La-140 in $La(NO_3)_3$ form, which is firmly absorbed on sediment surface. A data acquisition system connected to 16 NaI (Tl) detectors was used. The simultaneous determination of RTD for both phases (water and sediment), of sediment deposition map on tank bottom and of oxygen concentration distribution were performed.

The results of tracer experiments carried out in different technological conditions (flow rate, sediment contents) gave possibility to propose the model of liquid and sediment flow patterns and to estimate the efficiency of purification. As the result of tracer studies the design was improved and the efficiency of purification was increased considerably.

Equalization clarifier tank

A new equalizer-clarifier constructed at a big Polish petrochemical plant was investigated by radiotracer. Using Br-82 in the form of KBr aqueous solution with total activity 3.7 GBq, the parameters of water flow in a new equalization tank of 5000 m^3 volume and 230 m^3/h flow rate were determined.

The principal scheme of a new circle shaped equalizer-clarifier is presented in Fig. 46.

A simple model of wastewater flow consisting of delay To, two perfect mixing units in series with time constant T1, T2 and dead volume Vd was proposed. The optimal values of model parameters were T0 =0.2 h, T1=15.4 h, T2=0.2 h, Vd=1218 m3.

Radiotracer investigations resulted in a better design of the equalizer-clarifier tank, bringing considerable improvement in purification efficiency of the new system in comparison with the old. Technological observation proved the tracer results. It was observed that stagnation volume zones were well located at the tank bottom. The scraper efficiency in these stagnant zones where the sedimentation takes place is very high.

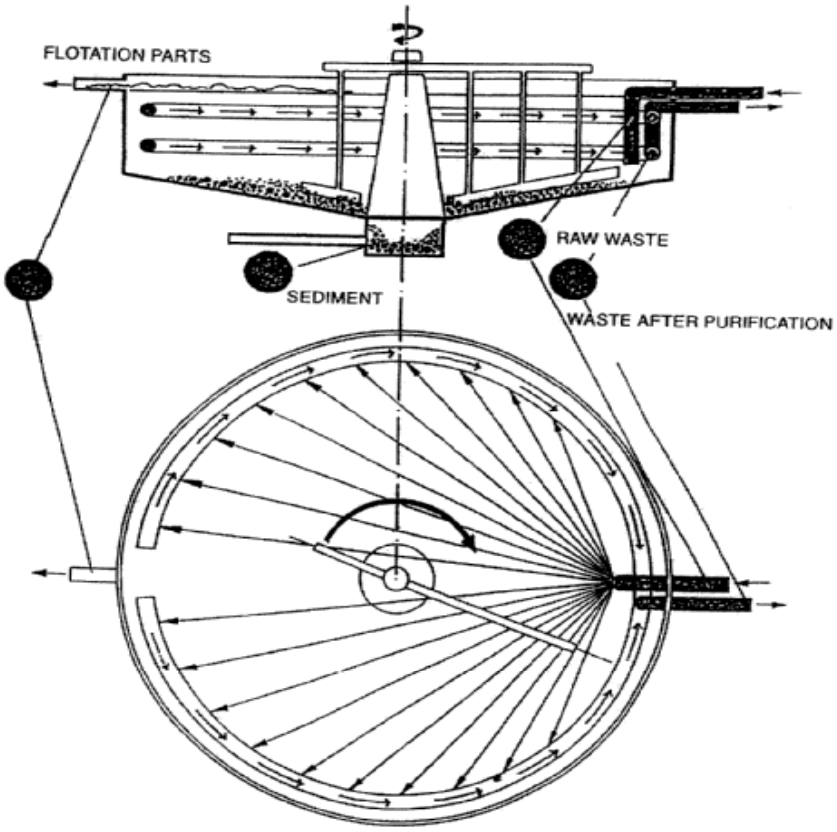

FIG. 46. Principal scheme of a new circle shaped equalizer-clarifier.

Aeration tank

In a biological aeration chamber organic compounds are removed from wastewater by microorganisms in the presence of oxygen. The influence of water and sediment flow conditions on the process efficiency was studied. Fluorescine was used as a water tracer and radiotracer La-140 with activity of 1 GBq was applied for tracing solid phase. The solid transport parameters and location of sediment deposition in the bottom zone of the biological chamber were determined in an industrial installation. The scheme of the chamber is presented in Fig. 47.

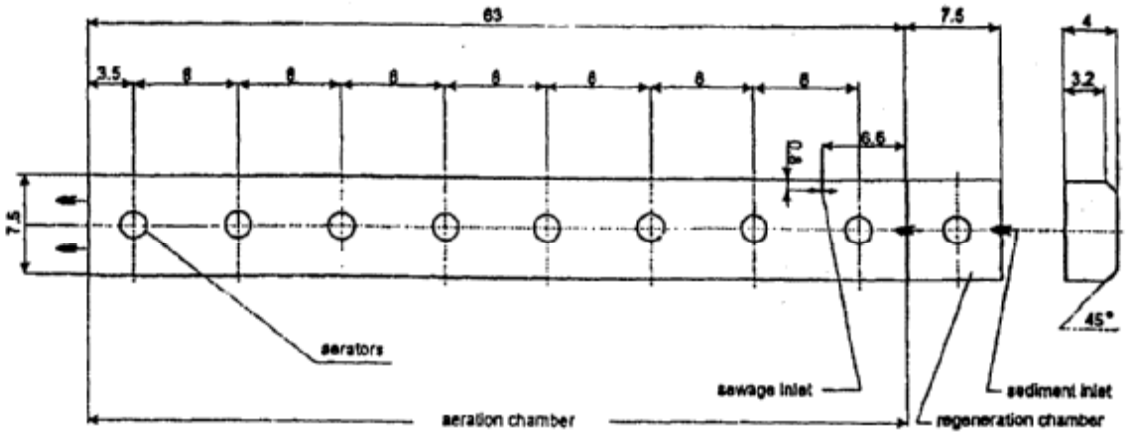

FIG. 47. Scheme of the biological aeration chamber.

Simultaneously, distribution of oxygen in the cross-section of the chamber was measured. Volume of aeration tank was V=1800 m3, flow rate q=180 m3/h, recirculation of sludge r=0.3 and the number of aerators n=9.

The MRT for water and sediment were practically the same, about 570 min. The dead volume was estimated at about 10%.

Results showed that efficient separation of water and sediment was not achieved. The location of dead volume was dependent on sediment concentration. For high sediment concentration (about 8 g/dm3) sediment accumulations between aerators were observed, while for small concentrations sediment deposits were located near the chamber walls.

The fluid flow model (unified for water and sediment) that better fitted better the experimental data consisted of two perfect mixing units in a series, with time constants of T1=504 min, T2=60 min., and dead volume d=0.1.

Radiotracer investigation showed serious irregularities of sludge distribution in biological tanks with aerators, in particular relatively high sediment accumulation for high solid concentration. It was decided to change the aeration system. Bubbling system was implemented for better fluid homogenization. It was found efficient by a radiotracer test.

Hydrodynamics of activated sludge channel reactor

In wastewater treatment plants, performance of the biological reactor is related to its hydrodynamics. This is particularly important in the case of channel type reactors where longitudinal concentration gradients are found. A complete model of such bioreactors should take into account the hydrodynamics and bioreactions. The tracer test was conducted to characterize the hydrodynamics of such bioreactor and propose a systemic model of reasonable complexity.

Experimental study on ful scale plant

The channel type reactor, aerated by porous diffusers, has a volume of 3300 m^3, is 102 m long, 9 m wide and 3.6 m deep. After settling the sludge is recycled at the inlet of the channel. Tracing experiments on the liquid phase were carried out with lithium chloride (chemical tracer), which is adsorbed weakly on sludge flocs, is easily detected by atomic absorption and is non-toxic for the quantities used here (10 kg LiCL/experiment). The injection mode can be considered as a Dirac pulse.

A first experiment was carried out for a total liquid flow rate Q of 2200 m^3/h (0.61 m^3/s) (incoming wastewater + sludge recycle). Under these conditions the reactor can be considered as a series of 12 perfectly mixed cells (J=12 PMC). No gradient is observed across the width of the channel. It has been verified that one third (respectively $^2/_3$) of the reactor can be considered as a series of 4 (respectively 8) PMC.

Two other experiments were subsequently carried out at Q = 1650 m^3/h (0.46 m^3/s) and Q = 1280 m^3/h (0.36 m^3/s), under similar aeration conditions: the corresponding values of J were 9 and 6, showing the effect of the flow rate on the hydrodynamic regime. This result confirmed the observation that an increase of the liquid flow induces an easier breakage of the swirls due to aeration in a channel-type reactor.

Experimental study on pilot plant

To widen the range of operation conditions an aerated channel type pilot-scale reactor (volume 0.03 m^3) was built (Fig. 48). It is divided into several compartments by baffles. Its dimensions are 0.5 m long, 0.3 m large and 0.205 m high. Aeration is done uniformly, over the entire length, by tubes of stainless steel pierced with small holes.

The tracing experiments are carried out with sodium chloride, the concentration of which is monitored with a conductimetric probe. A series of experiments was carried out for different flow rates, i.e. residence time $\tau = V/Q$. As shown in Fig. 49, the hydrodynamic regime varies largely with the flow rate. The reactor can always be modelled as a series of perfect mixers (PMC) but with J varying from 18 to 5 when τ varies from 56 min (3360 s) 327 min (16620 s).

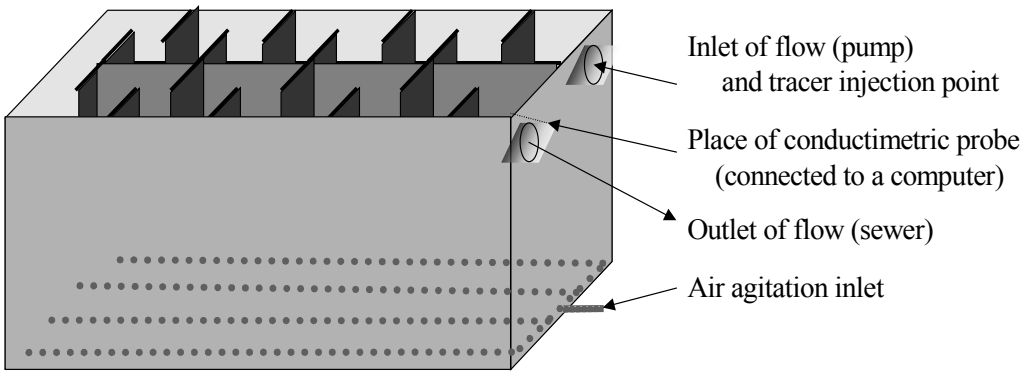

FIG. 48. Aerated channel type pilot scale.

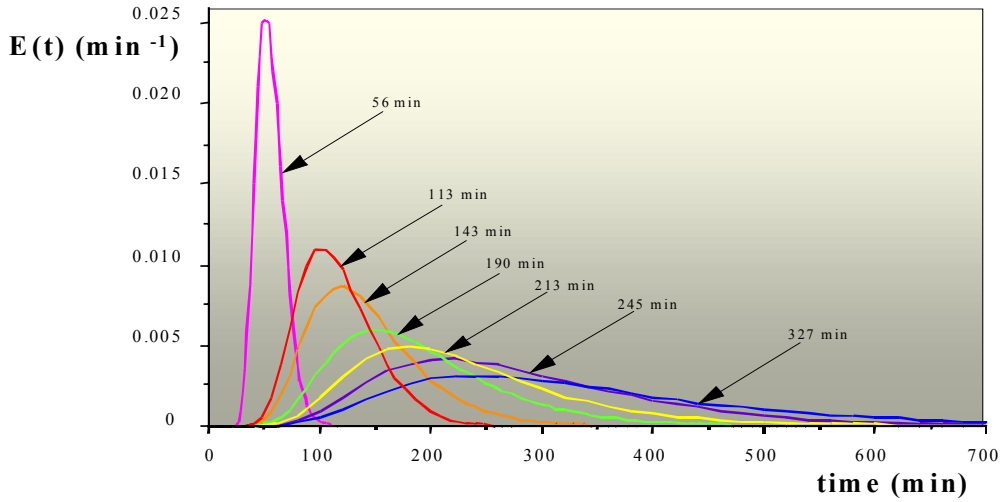

FIG. 49. Influence of the MRT (i.e. inlet flow rate) on the RTD curve in an aerated sludge channel reactor.

Model

Instead of representing the channel by a series of PMC, a model that considers a plug flow with axial dispersion can be applied. A dimensional number P can quantify the relative importance of the convective flow with respect to dispersion, which is similar to the Peclet number.

$$P = \frac{u \cdot L}{D} = \frac{L^2}{D\tau} \tag{12}$$

where

$u = L/\tau$ is the average velocity of the liquid,
L is the length of the reactor,
D is an axial dispersion coefficient.

However, P can be related to J: $P \cong 2(J-1)$, which finally gives:

$$J \cong \frac{L^2}{2D\tau} + 1$$

As the aeration conditions do not change, D can be considered as constant.

$$J = 1 + \frac{K}{\tau} \text{ with } K = \frac{L^2}{2D}$$

In Fig. 50, an excellent agreement was observed between the experimental data obtained on the pilot reactor and theoretical curve. A similar agreement was observed for the experimental data obtained on a full scale reactor. The largest residence time was obtained when the flow-rate was the lowest (early morning in a dry summer day). The shortest residence time was observed at mid-day, under rainy conditions. These two residence times were the limits of what was observed on the full-scale-plant under study.

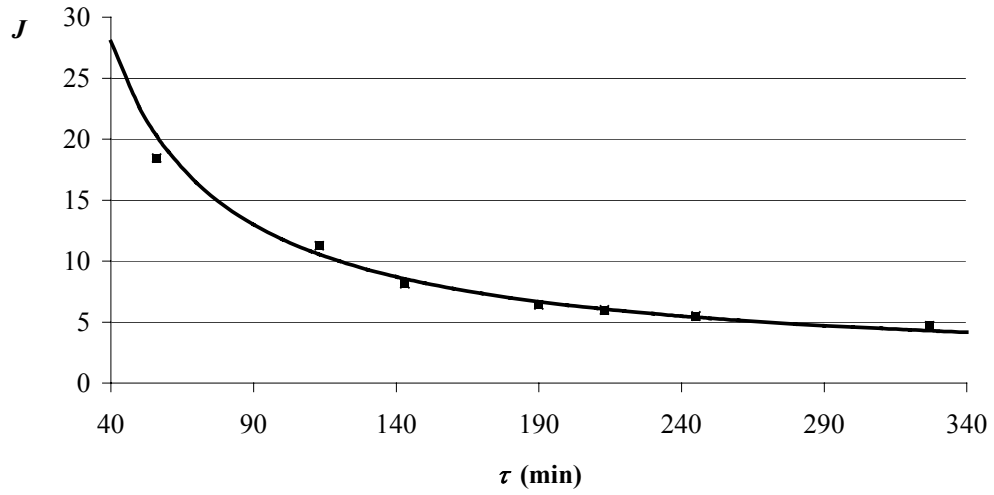

FIG. 50. J = f(τ) comparison theory and experiment, channel reactor pilot.

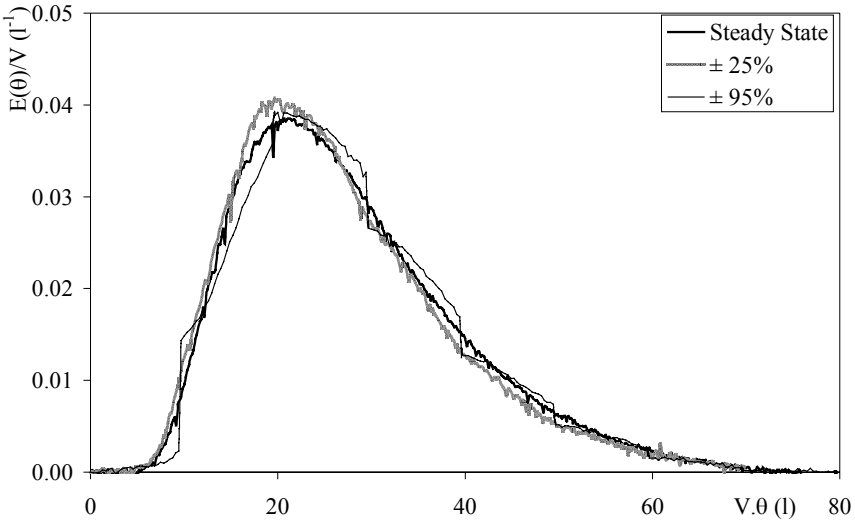

FIG. 51. RTD under transient and steady state in the aeration sludge reactor. The period of fluctuation (10 min) is lower than the MRT.

The RTD distribution for steady state conditions can be directly derived from a pulse injection of tracer in the studied process. However, for wastewater treatment plant the inlet flow rate may change from 1 to 3 during the day and from 1 to 7 for a longer period depending on the climate.

The method proposed by Niemi was used in the pilot to check if it is possible to derive RTD under transient state conditions [19]. At steady state, perfect mixing cells in series can model the flow pattern. As it has been shown before, J is a strong function of the flow rates: J=4.6 for 1 L/min; J=3.9 for 0.58 L/min and J=7.5 for 1.88 L/min. Fig. 60 shows results for the steady state at flow-rate Q=1L/min and for transient state with a change of flow rate every 10 min between two values of the amplitudes ±25% around the mean flow rate Q_{mean} (dotted line), and ±95% around the mean flow rate Q_{mean} (thin solid line).

Using the transfer function defined by Niemi and the number of cells corresponding to the average flow-rate (N=4.6), the obtained RTD curves are similar in transient and steady states despite the important influence of the flow rate on the number of cells.

Conclusion

A significant variation of the hydrodynamics of a channel type bioreactor was observed when the liquid flow rate varied. A simple model based on a series of perfectly mixed cells is proposed. The number of mixing cells is a function of the flow rate. The method proposed by Niemi to estimate RTD under transient state was used and validated in order to determine an average value of the number of mixing cells.

5.1.3. ^{99m}Tc as a radiotracer for determination of hydrodynamic characteristics of anaerobic digester reactors

Investigation was made of the behaviour of $^{99m}TcO_4^-$ as a radiotracer for the hydrodynamic analysis of anaerobic digesters in a sugar wastewater treatment plant. Although laboratory assay showed the redox potential of the medium was not enough for the chemical

reduction of the species TcO_4^- to $TcO(OH)_2$, sorption rate between 0.045 to 0.083 h^{-1} was observed, probably associated with its retention by the biomass as a result of the metabolization and catalytic reduction due to microbiological activity.

RTD curves for the three digesters of the wastewater treatment pilot plant at a Sugar factory were obtained. In order to improve the design of future wastewater treatment plants for the sugar industry, the hydrodynamic characteristics of the first digester were found and a complex model that includes four parallel dispersed plug flows shifted by a plug flow was proposed. Recommendations to the end-users were likewise proposed.

The digester (aerobic or anaerobic) is almost the heart of any wastewater treatment plant; complex microbial processes consisting of several interdependent consecutive and parallel reactions take place in this unit. An early digester design was of continuous stirred tank type, in which effective contact between the waste requiring treatment and the active microbial flora was achieved by a lengthy retention time within the digester.

Application of tracers for such kind of installations gives possibilities to check and verify the flow models used for the design of different types of reactors for these purposes. Therefore, due the complexity of the system, when attempting to model hydraulics reactors, extreme care must be exercized in the choice of a tracer compound and in the ultimate interpretation of RTD functions obtained.

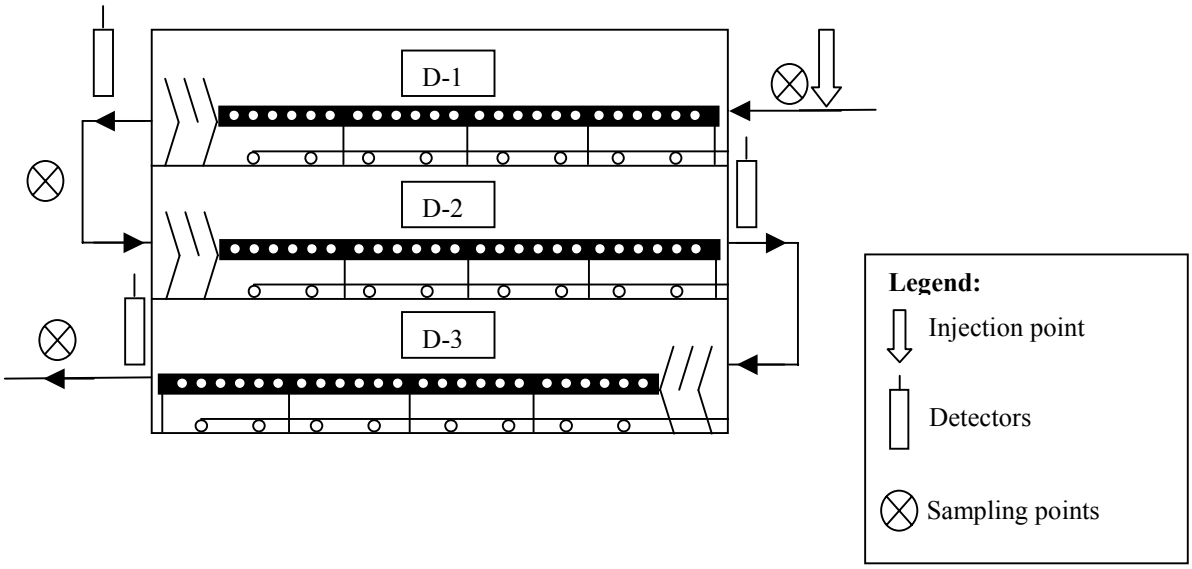

FIG. 52. Sampling scheme, injection and detection points in digestion system.

Radiotracer experiment

A tracer experiment was performed by injecting instantaneously 37 GBq (1 Ci) of ^{99m}Tc in the form of pertechnetate, in the first digester (all three digester was connected in series). The injection device was attached to the inlet pipe of D-1 and a glass tube was coupled at the outlet of D-1 in order to control fluid level into the vessel.

Three scintillation probe with 1×1 NaI (Tl) crystal, each one coupled to a Minekin rate meter were attached to each digester. The count rate was registered continuously each 120 s during 14 h. Time and count rates from each detector were transferred to a personal computer through an RS-232C interface port.

During the assay, consumption of the system, temperature and pH of sewage at the Settling gas meter exit were controlled. Flow rate was maintained at 4L/s, pH values between 6.4–6.7 and temperature ≈ 37°C.

RTD curves at the outlet of the three digesters are shown in Fig. 53. The estimated parameters for each distribution are presented in Table 8.

TABLE 8. RTD PARAMETERS AT THE OUTLET OF THE DIGESTERS

Parámeters	RTD 1	RTD 2	RTD 3
Hydraulic retention time (h)	9.3	12.6	12.2
Variance	72.70	129.28	86.02
Time of maximum concentration (h)	2.07	2.53	3.47
Time of appearance (h)	0.17	0.20	0.30

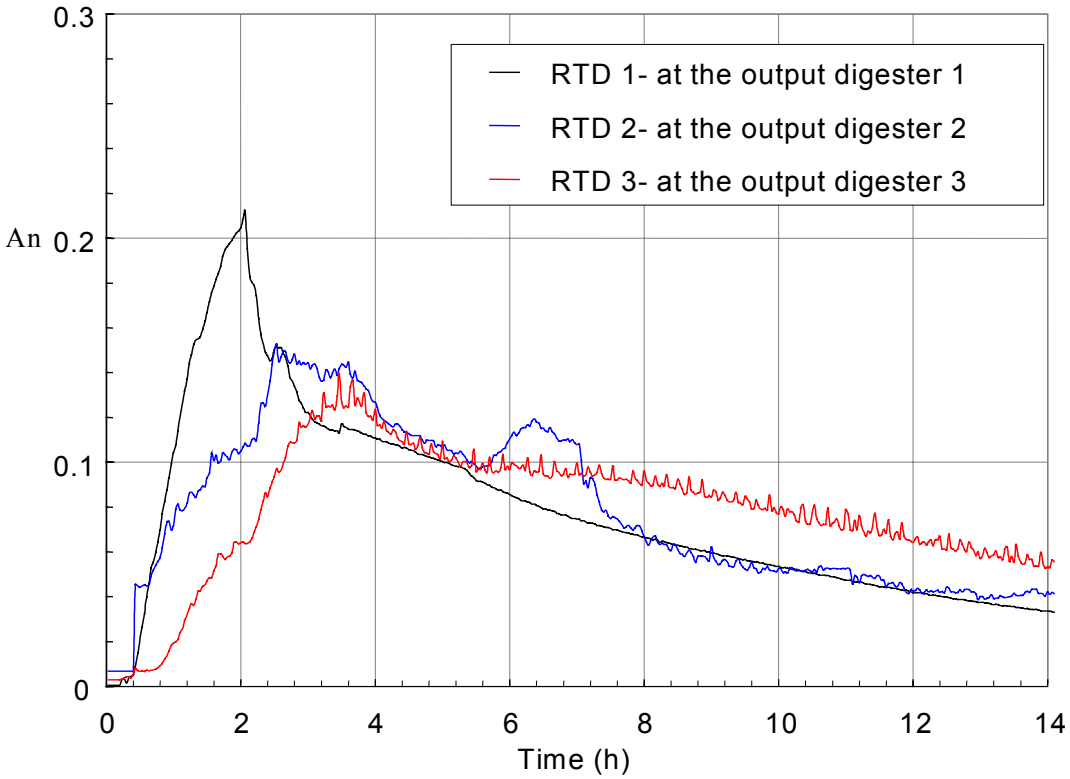

FIG.53. RTD curves at the outlet of the three digesters.

The presence of several peaks in the RTD curves indicates that a complex model is being dealt with, probably with several paths in parallel. This hypothesis was corroborated when none of the distribution curve could be adjusted to a basic simple model.

Attention was focused in analysis of the RTD function for digester 1 in which really a response curve from a Dirac impulse was achieved.

For the simulation four possible paths were evaluated, all shifted by a plug flow with a residence time of 0,43 h. For the model optimization based onn Progepi RTD software, 100 iterations and a precision of 0,01 were selected. Results of the parametric analysis of each path are presented in Table 9. Shown in Fig. 54 are the experimental and the theoretical response curves for the digester.

TABLE 9. PARAMETERS OF THE OPTIMIZED MODELS

Parameters	Path 1	Path 2	Path 3	Path 4
% Flow	12.80	20.70	14.50	52.00
Flow (m^3d^{-1})	46.08	74.52	52.20	187.20
τ (h)	0.97	1.51	2.15	3.89
Peclet number	35	105	120	18
% volume	4.49	11.29	11.27	72.95
Volume (m^3)	2.91	7.31	7.30	47.26

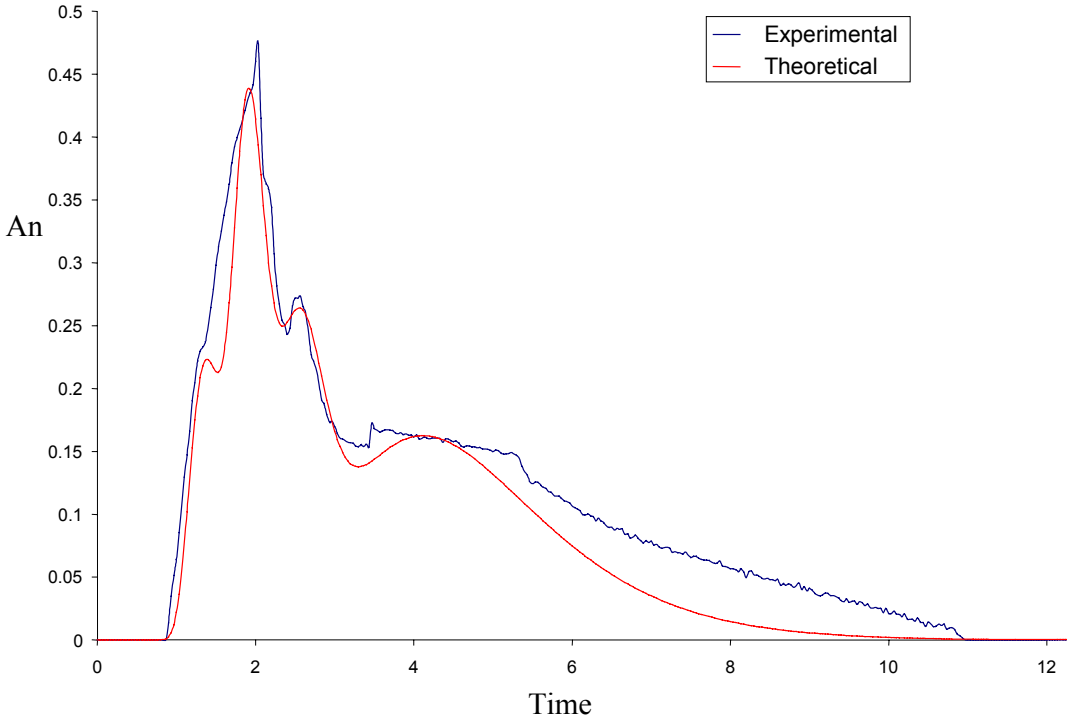

FIG. 54. Experimental and theoretical responses, DTR digester D-1.

The parallel flow model (four parallel path model) was found as the best model to describe the RTD of digester 1. The observed tail in the curve was related with the existence of a dead zone within the digester. This phenomenon could be associated with an incomplete utilization of the useful volume of the reactor, probably due to different densities of the sewage stream or that the sewage is pumped non-continuously, working sometimes as a "batch" system, that could lead to the formation of stagnancy zones. A dead volume of 17.2 m^3 was estimated, meanwhile that the useful volume, by difference, was 82 m^3.

There are four zones in the D1 digester separated by baffles to avoid backmixing of sewage. It can be supposed that the fluid at the inlet is forced to flow throughout the reactor in four parallel zones with different volume, residence time and dispersion coefficients. Each of these zones may be considered as a dispersed plug reactor, shifted by the impulse that the sewage pump provokes. A scheme that resumes this process is shown in Fig. 55.

Conclusions

Technetium can be used as a tracer for RTD analysis in anaerobic digester reactors.

The model that best describes the fluid hydrodynamic in digester D-1 is composed of four parallel dispersed plug flows shifted by a plug flow. The dead volume of digester D-1 was 17,2 m^3 that represent nearly 20% of the total volume.

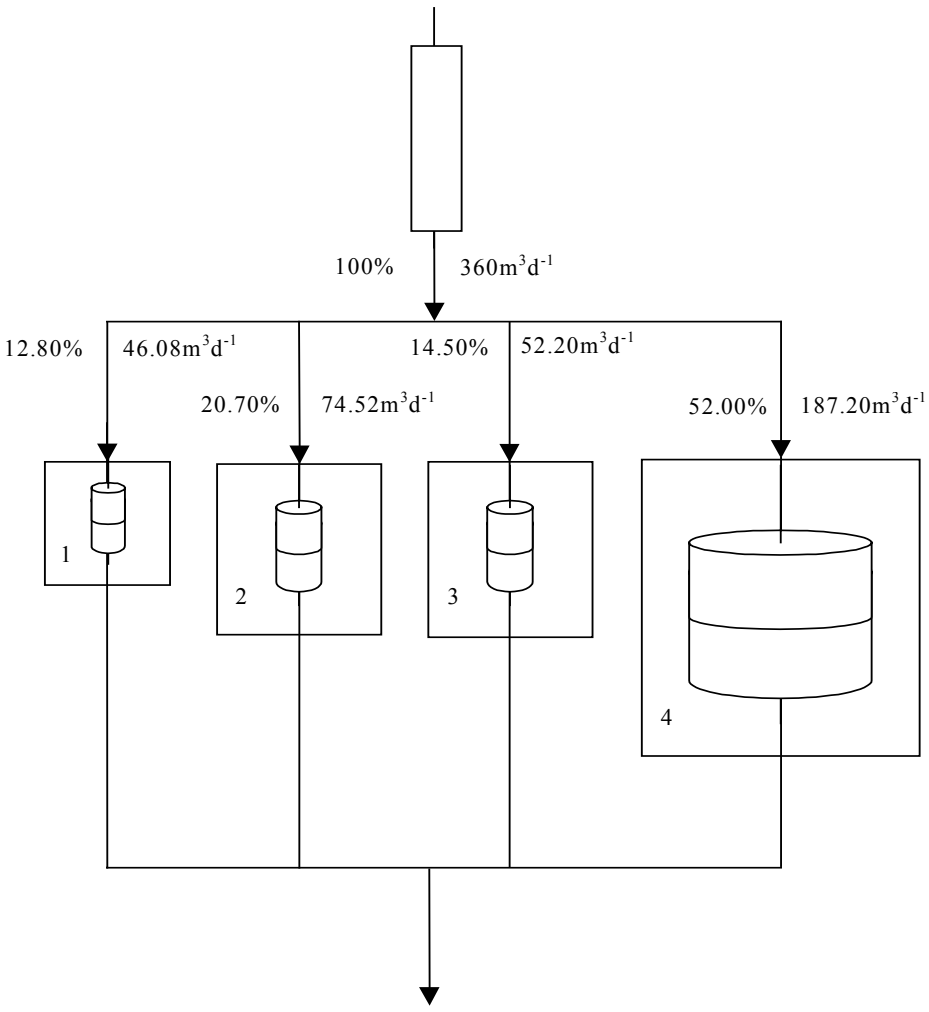

FIG.55. Scheme of the model proposed for digester D-1.

5.1.4. Conclusions relating to tracer applications in wastewater treatment plants

During the last three years about 12 wide range industrial scale radiotracer experiments were carried out under different technological conditions. The following are the major conclusions coming up from this CRP:

For the aeration tank similar results were obtained for different configurations. Aeration channel can be modelled by perfect mixing cell in series. In this case, the number of the mixing cells should be adjusted according to the flow rates and geometrical configuration. An equivalent possibility is to use the perfect mixing cell in series with back mixing.

Due to the decantation effect, it is difficult to determine a reliable model for the settling tank.

The RTD of separate phases in the aeration tank, clarifiers, equalizers and digesters gives good results about working conditions of the system.

Utilization of computer data acquisition systems perfoming *in situ* multipoint measurements is recommended to obtain larger information about the flow pattern map inside the wastewater installation. The experimental data from measuring points located inside the installation can be used for verification of the proposed model.

During industrial scale tracer experiments continuous measurement and control of flow rate is strongly recommended. Uncertainties and fluctuations of flow rate during the whole tracer experiment duration may cause serious mistakes in process parameter evaluation and validity of proposed models. Simultaneous with radiotracer experiments, it is recommended to perform conventional measurements of chemical oxygen demand (COD), total sediment content, oxygen distribution and pH to facilitate interpretation.

The tracer technique is very competitive and sometimes unique in troubleshooting diagnosis of wastewater treatment installations. It helps end-users improve the performance and efficiency of existing installations and design better new water purification systems.

6. RADIOTRACERS IN PETROLEUM RESERVOIRS — THE CASE OF INTERWELL EXAMINATION

Introduction

Use of radiotracers in oil reservoirs includes methods for [20]:

A. reservoir evaluation, and
B. well operation monitoring purposes.

Class A includes:

— interwell fluid tracing
— single-well push-and-pull techniques for near-well investigation of heterogeneity's, cross-flow and fluid saturation
— reservoir fluid drift examination

— fluid injectivity (and productivity) profiling
— well inflow monitoring (water, oil, gas)
— well fracture detection and characterization
— mud filtrate invasion monitoring for near-well formation damage and extracted core integrity studies.

Class B includes:

— cementing operation
— leak detection behind casing
— well completion and proppant positioning
— perforation efficiency (zone production)
— produced fluid transport rate distribution (RTD) for individual fluids
— mud circulation monitoring
— well workover monitoring (scale, wax and asfalthene removal)
— well stimulation monitoring (i.e. acidizing)
— tertiary recovery efficiency monitoring high-permeability zone plugging).

The CRP was exclusively focused on interwell fluid tracing technique.

6.1. INTERWELL TRACER OPERATIONS

When primary oil production decreases in a field because of reduction in original pressure, water is usually injected to increase oil production. Injected water in special wells (injection wells) forces the oil remaining in certain layers to emerge from other wells (production wells) surrounding the injector. This technique, commonly called *secondary recovery*, contributes in extracting up to 50% of the original oil in place.

Although this technique was first used in old reservoirs where oil production had decreased, it is today a common practise to begin the exploitation of new wells with fluid injection as a way to optimize oil recovery. For this reason, the name secondary recovery is being replaced by the more general term *waterflooding*.

Efficiency of the waterflooding process is highly dependent on the rock and fluid characteristics. In general, it will be less efficient if heterogeneity is present in the reservoir, such as permeability barriers or high permeability channels that impede a good oil displacement by the injected water.

Fluid flow in most petroleum reservoirs is anisotropic. The reservoir structures are usually layered and frequently contain significant heterogeneity leading to directional variations in the extent of flow. Information on flow dynamics is important in order to estimate reservoir volumetric sweep and allow for an optimal production strategy.

Interwell tracer tests give quantitative information on the fluid dynamics in a reservoir. One obtains unambiguous identification of directional flow paths between wells [21].

A carefully designed and executed interwell tracer test makes it also possible to:

— detect heterogeneity like permeability stratification
— delineate faults, highly conducting fractures and flow barriers
— evaluate volumetric sweep efficiency

— quantify the causes of early water breakthrough (problem injectors)
— measure the relative in-situ velocities of injected fluids
— obtain information on production mechanisms.

Complementary dynamic information from a reservoir may be obtained by three other methods: Logging of production rates (profiles) of reservoir fluids, pressure testing and time-lapse seismic examinations (4D seismic). A full reservoir evaluation should preferably merge information from all these techniques.

A field radiotracer investigation consists, in brief, of the following main steps [22]:

— Design of tracer strategy together with reservoir engineers that works on the actual field
— Selection of applicable tracers
— Application to the relevant authorities based on a safety report
— Tracer mixture preparation, calibration and quality assurance
— Selection/design of tracer injection and sampling procedures
— Tracer transportation to injection site
— Tracer injection
— Tracer sampling and sample transportation to analytical laboratory
— Tracer analysis
— Data evaluation and simulation
— Reporting of results.

Some of these points are further discussed below.

6.2. RADIOTRACERS AND INTERWELL INVESTIGATIONS

The principal requirements for a tracer are [23]:

— it should behave in the same way as the material under investigation;
— it should be easily and unambiguously detected;
— injection and detection should be made without disturbing the system;
— the residual tracer concentration in the system should be minimal.

As in many other industrial applications, radiotracers have important advantages compared with chemical ones. Perhaps the most relevant characteristic of radiotracers is the small amount of mass required to label huge volumes of the substance under study. Normally the underground reservoir volume the liquid tracer is supposed to penetrate is in several million cubic meters.

Interwell comunication investigations deal mostly with water tracing; therefore, the ideal tracer is tritium, as tritiated water. Other suitable beta tracers are ^{14}C and ^{35}S. Additionally, a few gamma radiotracers have been tested. Among them ^{57}Co and ^{60}Co as hexacyanocobaltate and ^{51}Cr as EDTA complex can be mentioned.

Chemical tracers, thiocyanate, nitrate and water soluble alcohol could be used. In this case several thousand kilograms have to be injected in order to obtain a concentration – time curve compatible with radiotracer.

Tritium was the largely used tracer for interwell comunication. The main reasons are [24]:

— behaviour of tritiated water which is like natural injected water
— good safety record and very low environmental impact
— high measurement sensitivity
— availability and low cost price and handling.

However, the need for alternative tracers is evident for multiwell and multilayer situations. Gamma ray tracers were used in some applications as well.

Radioisotope tagged compounds could generate new tracer with ideal properties. S-35 tagged SCN^- was developed as new radiotracer for waterflood. S-35 is a beta emitter with half-live of 87 days. S-35 tagged SCN^- can be used in reservoir with relatively quick breakthrough of water, such as reservoir of long waterflooding history. Co-58 tagged $Co(CN)^-_6$ as waterflood tracer was tested as well.

Nuclear reaction ^{35}Cl (n,p) ^{35}S is used for ^{35}S production. Target material, KCl can be irradiated in the nuclear reactor (several MW) to produce up to 3Ci ^{35}S-SCN^- .

Synthesis of ^{35}S-KSCN is completed in four steps:

(1) preparation of carrier free ^{35}S-sulphate from irradiated KCL
(2) reduction of ^{35}S-sulphate into sulphide in solution
(3) preparation of elementary S-35
(4) synthesis of ^{35}S-KSCN by the reaction of elementary sulphur with sodium cyanide.

Co-60 tagged $K_3[Co(CN)_6]$ is a good water tracer for IWTT studies. But, radiation hazard of Co-60 limits its use and, in fact, Co-60 tagged $K_3[Co(CN)_6]$ is going to be replaced by Co-58, which has a half-life of 67.8 days only. It can be produced by $^{58}Ni(n,p)^{58}Co$ reaction.

Preparation of Co-58 tagged $K_3[Co(CN)_6]$ in curie scale was completed. Natural Ni metal was used as target material for reactor neutron irradiation. The target can be irradiated in few MW nuclear reactors. Synthesis of Co-58 tagged $K_3[Co(CN)_6]$ can be realized into three steps, i.e. target dissolution, Ni/Co separation and forming Co-58 tagged $K_3[Co(CN)_6]$.

6.3. INJECTION AND SAMPLING

A typical tracer interwell study has four stages: tracer injection and sampling, sample measurement and data interpretation.

Injection techniques

In most industrial applications the tracer can be injected into the system either instantaneously or continuously, but in an oil field only the former is used. Pulse injection consists in introducing the tracer over a time interval that is very short compared with the time it is staying in the system. This condition is easily accomplished because of long transit time involved in the system (several months).

Two different situations can take place concerning the pressure in the injection well. In some cases pressure in surface equals atmospheric pressure and consequently tracer can be poured directly into the well without any special device. However, a more general situation implies to work with pressures of around 150 p.s.i., where direct injection is not possible. The bypass injection technique is appropriate in this case. Using bypass technique contamination risk and mechanical failures are avoided.

In both cases, direct or bypass injection, a very simple pneumatic device operated by hand is employed. In the former case it is used to pour the tracer into the well and in the latter situation to store it in the injection receptacle through which injection water will be derived to push the tracer. The mentioned pneumatic device is coupled directly in the tracer bottle container without further manipulation of radioactivity.

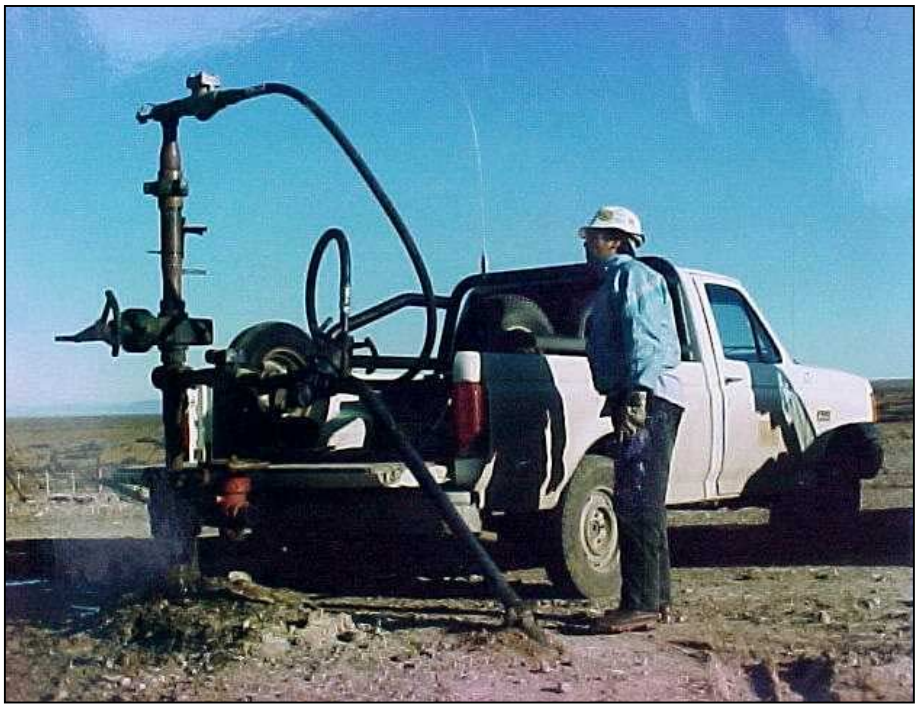

FIG. 56. Tritium injection using bypass technique.

In both cases, direct or bypass injection, a very simple pneumatic device operated by hand is employed. In the former case it is used to pour the tracer into the well and, in the latter, to store it in the injection receptacle through which injection water will be derived to push the tracer. The mentioned pneumatic device is coupled directly in the tracer bottle container without further manipulation of radioactivity.

Sampling

The sampling schedule includes a relatively higher sampling rate during the first days after the injection. A few months after the injection taking two samples a month is enough. Samples should be collected till the end of tracer cloud, that means for a period of 3–4 folds the peak concentration time. Depending of the distance from injection to production wells and and oil reservoir structure the total sampling period can go from several months to few years.

There are theoretical and practical considerations to optimize sampling schedule. The main consideration is to collect enough information to obtain entire reliable response curve with a minimum of samples.

6.4. RADIOTRACER MEASUREMENTS

Measuring techniques depend on which kind of tracers (beta, gamma or chemical) are used. In general, all of them include sample treatment prior to detection.

When counting a radioactive sample it is well known that instrument reading is a measure of sample activity plus background. The latter must be subtracted in order to evaluate the net sample activity. The background is usually measured by using samples taken before the injection (blank sample).

Generally, the following criteria are used to calculate minimum detectable concentration (MDC) of radiotracer, taking account its background:

$$n > 2\,\sigma(n)$$

That means that the sample count rate should be at least two times its own standard deviation in order to be distinguished from the background. The standard deviation is given by the following expression:

$$\sigma(n) = \sqrt{\frac{n_g}{t} + \frac{n_b}{t}} \tag{13}$$

where

®(n)	is standard deviation for the net count rate (c/s),
n_g	is gross count rate (c/s),
t	is measuring time (s),
n_b	is background count rate (c/s).

After some operations and approximations the following expression is obtained for MDC.

$$MDC = \frac{2.8}{e\,V_m}\sqrt{\frac{n_b}{t}} \tag{14}$$

where

MDC	minimum detectable concentration (Bq/L),
n_b	background count rate (c/s),
t	measuring time (s),
e	efficiency (counts/disintegration),
V_m	volume of the sample (L).

As a consequence of statistic fluctuations pre-processing of experimental data is usually needed in addition to background subtraction in order to filter noise and smooth the response curves.

Finally, radioactive decay correction is needed. Although in the case of tritium its half-life is long enough to avoid this kind of correction when the sampling periods last only a few months, in a general situation, an interwell study implies more than a year of sampling and tritium decays at a rate of 0.45% per month.

Beta-radioactive tracers

The most common beta-radioactive tracers for interwell studies are labelled with tritium (^{3}H), carbon-14 (^{14}C) or sulfur-35 (^{35}S). All of them are usually measured by means of liquid scintillation technique.

A small volume of a liquid sample is mixed with a special solution known as scintillation cocktail, commonly in a 20 mL light transparent (glass, polypropylene, teflon) vial. Beta particles cause emission of light when passing through and slowing down in the scintillation cocktail. This light pulses are registered by photo-multipliers (PMT) suitable for that particular photon wavelength.

The light output in a pulse (light intensity) is proportional to the energy of the beta particle. This process is called scintillation, and since it happens in liquid media, it is known as liquid scintillation.

The vial is placed inside an instrument, a liquid scintillation counter (LSC), which has normally two PMTs operated in co-incidence to reduce background. The LSC analyses the pulses from the PMTs and provides information about the energy of the beta particles and the rate of beta emission (activity) in the sample.

Pulses are sent to an analogue-to-digital converter (ADC) where they are digitized and stored in an address memory according to their amplitudes that are proportional to their beta energies (energy spectrum in a multi-channel analyser).

In order to further reduce the background coming from natural radiation, a lead shield usually surrounds the PMTs and the vial while the sample is in the measuring position. Modern low background detection equipment also has a so-called active shield. In most cases it consists of a liquid scintillation detector surrounding the PMTs and the counting sample. This shield detector is operated in anti coincidence with the PMTs, i.e. any event, which is registered both in the two PMTs and in the shield (cosmic rays, environmental radiation) detector simultaneously, is rejected. In case of simple non-spectrometric detection equipment (single channel analyser), contribution of the background to the sample count rate can be further reduced by setting a counting window only over the interesting energy portion of the energy distribution by selecting narrow upper and lower limits. In case of tritium the upper gate should, for instance, be set at 19 keV.

Various processes may perturb the beta spectrum obtained in a liquid scintillation process. Here, we will only mention briefly the most important:

Chemiluminescence: When different chemicals are mixed in the sample vial together with the scintillation cocktail, chemical processes may start; they have relatively slow kinetics and which result in emission of low-energy photons. These photons may contribute to the very low-energy end of the beta spectrum. Chemiluminescence may be reduced or completely

removed by gentle heating of the vial to 50–60 °C for some minutes before counting to speed up the chemical process.

Phospholuminescence: When a sample vial with the scintillation cocktail is exposed to white light (daylight or lamplight) the light energy may be temporarily "stored" and slowly given off during sample counting (phosphorescence). Also this light will contribute to the far low energy end of the beta spectrum. Therefore, counting samples should always be stored in the dark a few hours before start counting.

Colour quenching: Coloured sample liquid may absorb some of the light emitted by the scintillator. Yellow or brown are the heaviest colour quenchers. Hence, one should try to remove such colours during the sample preparation process and before counting.

Chemical quenching: Some components in the sample may kill the energy transfer process that takes place in the scintillation cocktail; they eventually results in light emission. Such chemicals absorb the energy and release it in the form of heat. Heavy chemical quenchers are for instance organic compounds containing oxygen and in particular chlorine.

Physical quenching: Solid particles or non-transparent emulsions in the sample may prevent light from being detected by the PMTs.

All these forms of quenching result in a shift of the energy spectrum towards lower channel numbers because the number of photons detected by the PMTs per beta decay is reduced.

Quenching may change from one sample to another. Evaluation of quenching effect is necessary in order to calculate counting efficiency.

Conclusion

Liquid scintillation counting requires careful sample preparation. Most often, chemical separations are involved. When these procedures are optimized, very low detection limits may be obtained ranging from 2 Bq/L for HTO to <0.02 Bq/L for $S^{14}CN^-$.

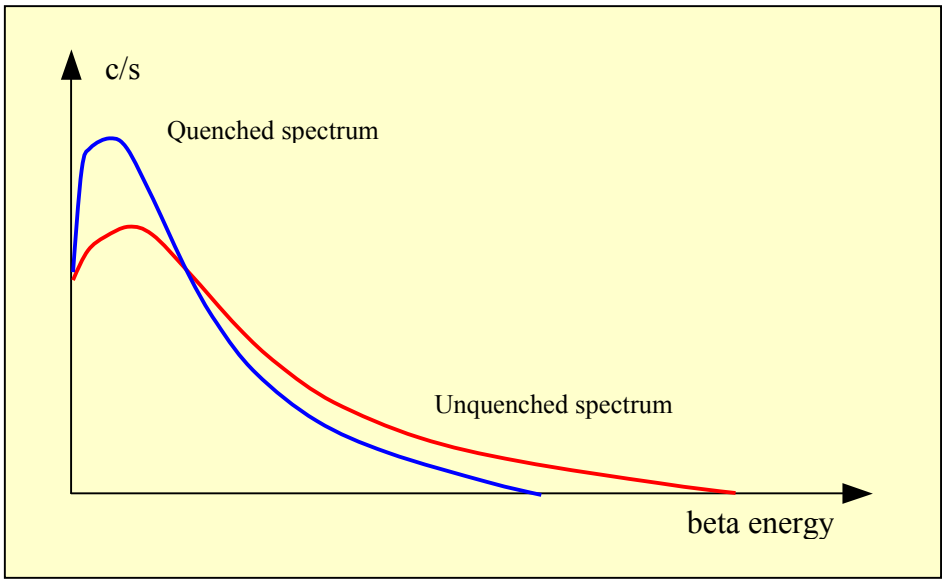

FIG.57. Principle sketch on the effect of quenching on a liquid scintillation beta spectrum.

Gamma tracers

Gamma tracers are commonly measured using either solid scintillation detectors or semiconductor detectors.

Solid scintillation detectors: These are of different types, but the most generally applicable is the detector based on a single crystal of sodium iodide doped with traces of thallium, the so-called NaI(Tl)-detector. The crystal is optically coupled to a PMT. Interaction of a gamma photon with the scintillation crystal results in emission of light, which is detected by the PMT. The light output is proportional to the gamma energy. The electronic system associated to the PMT analyses the pulses according to pulse amplitude (energy) and stores the results in a multichannel analyser (MCA). Thus, energy and intensity are recorded, and the result is the gamma energy spectrum of the radiation source.

The NaI(Tl)-detector has a high intrinsic efficiency but a limited energy resolution. The scintillation crystals are provided in different sizes. The efficiency for high gamma energies increases with detector volume. Common counting equipment has cylindrical crystal sizes of 2" × 2" to 5" × 5" (height × diameter). The larger the crystal the higher the price. The detectors can be made quite rugged, and are suitable in field instrumentation.

Semiconductor detectors: Today, these are mainly based on high purity germanium crystals, so-called HPGE-detectors, where a semiconductor junction is created by suitable elemental dopants on the crystal surface. A gamma ray interacting with the detector will result in an excitation of electrons from the valence band to the conduction band in the crystal, and a small electric pulse is created in a high-voltage field. The pulse height is proportional to the gamma energy. The pulses are sorted and stored in an MCA.

The intrinsic efficiency of semiconductor detectors has, for many years, been lower than for NaI(Tl)-detectors. Today, it is however possible to purchase detectors with efficiencies 100% relative to that of a 3"x3" NaI(Tl)-detector, but prices are very high. The main advantage with an HPGE-detector is, however, its excellent energy resolution. This property may be indispensable for analysis of complex radiation sources. HPGE-detectors need cooling to liquid N_2 temperature during operation. They are not generally applicable as field instrumentation.

In general, gamma tracer detection requires little sample preparation except for the extreme low-energy emitters' (i.e. ^{125}I).

There are several ways to reduce the minimum detectable concentration in gamma detection:

— Increase the detector intrinsic efficiency. This is a matter of cost.
— Increase counting sample volume (constant activity concentration in the sample leads to higher total activity in the sample.). There is a practical limit to the sample size.
— Optimize the counting geometry by shaping the counting sample. For a given radionuclide, a selected detection set-up and a certain sample volume there is an optimum shape of the sample volumes. For practical reasons these are most often cylindrical-like shapes.

— Enrich the tracer from a large into a smaller sample volume (increased total activity for a better sample counting geometry). This requires sample treatment either by liquid evaporation or by chemical separation. Sample treatment time and cost increase.
— Reduce the background level (equation T11) by effective detector shielding. This is most often done by passive shielding with lead walls (5–10 cm thickness) around the detector and sample.

A typical counting set-up for a NaI(Tl)-detector and a liquid sample in a Marinelli beaker is shown in Fig. 58.

For HPGE-detectors the corresponding detection limits are <0.1 Bq/L.

Several sample pre-treatments and scintillation cocktails were tested in order to get the best efficiency and eliminate eventual discrepancies between samples of different origins.

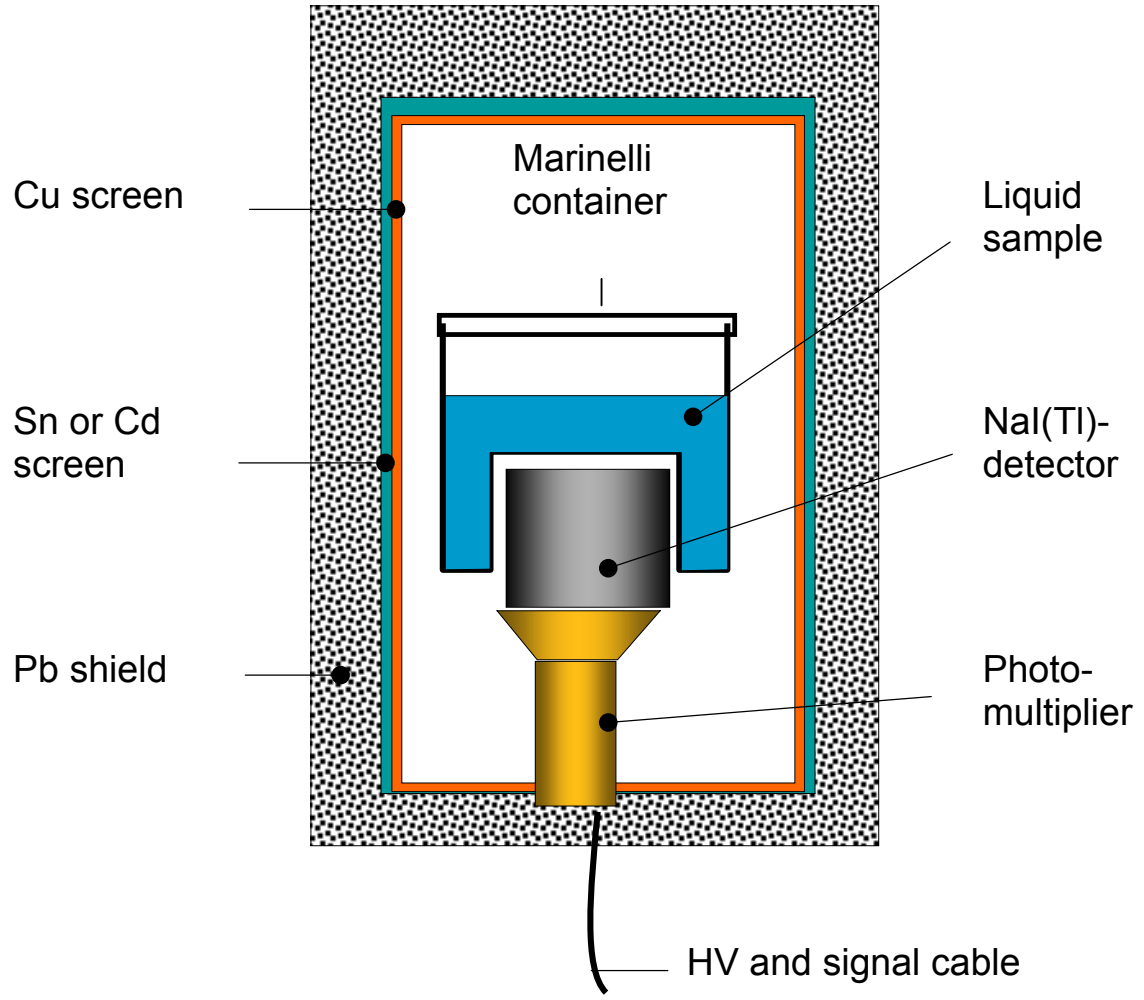

Fig. 58. Sketch of a common set-up for counting of gamma active liquid samples: 1000 ml Marinelli sample container, 3"x3" NaI(Tl)-detector, Pb-shield (5-10 cm), a Sn (or Cd) screen to filter away Pb x rays generated by the sample activity in the Pb-shield, Cu filter screen to filter away Sn (or Cd) x rays generated by the Pb x rays in the Sn (or Cd) screen.

More than three thousand samples coming from five different oil fields were measured; some of them were selected to test the pre-treatment effect and need. The data were analysed by statistic tests, such as student's and variance analysis.

In one case, several samples were filtered using a standard filter paper with and without activated carbon. Each sample was measured ten times under the same conditions. Applying the student's test a value of 0.425 for the t-statistic was obtained while the critic value taken from tables for a standard signification level of five percent is 2.262. Therefore, the different ways of filtering have no effect in detection.

In another case, groups of four samples, each one cleaned with a different reactive and four scintillation cocktails, were used. In this case two-way analysis of variance was used. The calculated values for the F-test were 5.292 for the reactive and 0.855 for the scintillation cocktails while the critical values taken from tables for a standard signification level of five percent are 4.149 and 2.901, respectively. This means that no modification in the results can be expected in working with different cocktails, but a slight change was observed when using different chemical agents. In practice, however, the effect of sample treatment prior to detection is too small to take into account.

6.5. DATA PROCESSING AND INTERPRETATION

Two levels of interpretation of the tracer data were developed. The first level is oriented to the practical operation of the field and the second one is aimed to the measurement of parameters needed for numerical simulations.

First level or direct interpretation

Tracer concentration versus time curves were analysed to measure the main characteristics of flow in the group of wells under study (Figs 59, 60).

From these curves it is possible to compare transit times and quantify the amount of injected water produced in different directions. The relative flow performance in each flow directions is analysed using the following definitions and measurements from the concentration curves:

Mean residence time:

$$\bar{t} = \frac{\int_0^\infty t\, C(t)\, dt}{\int_0^\infty C(t)\, dt}$$

Percentage of the recovered tracer activity:

$$R(t_i) = \frac{100}{A_{TI}} \int_0^{t_i} q(t)\, C(t)\, dt \qquad (15)$$

where

t_I is the early time when the tracer concentration reaches a 1% of the maximum measured concentration,

A_{TI} is the total injected activity in the injection well.

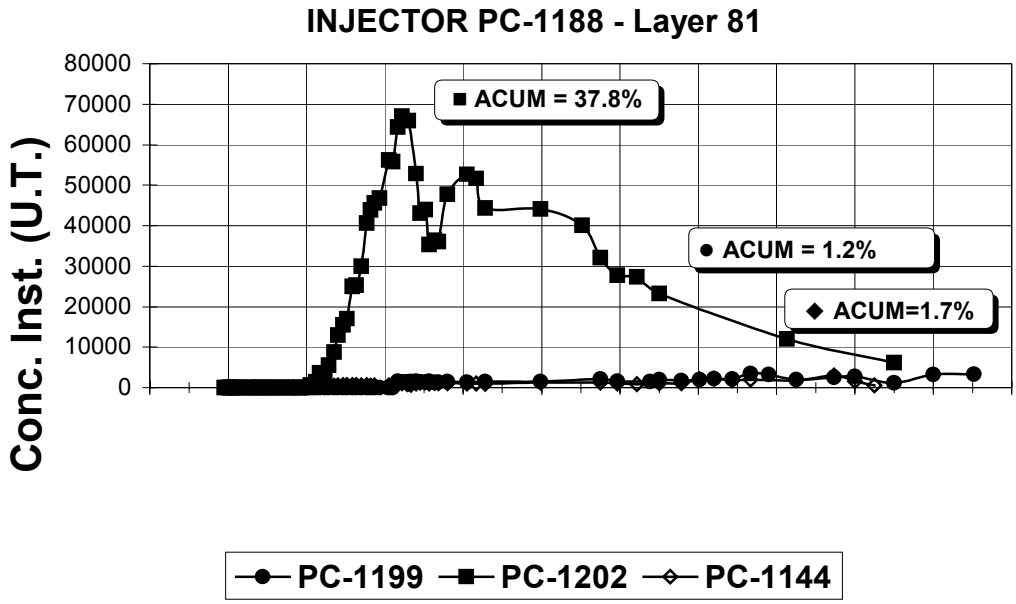

FIG. 59. Tracer concentration in the producing wells from the injector PC-188, layer 81.

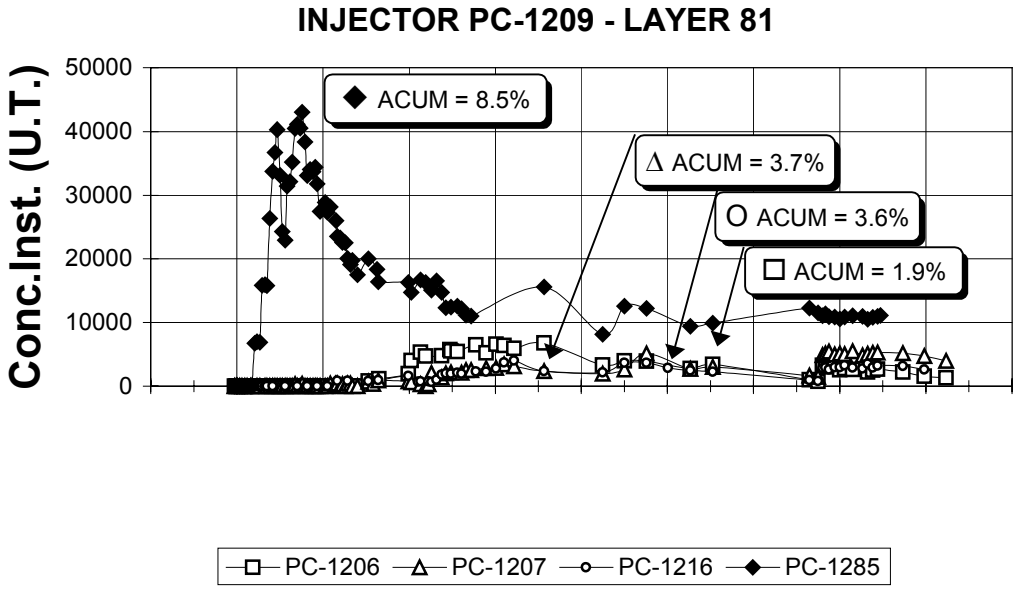

FIG. 60. Tracer concentration in the producing wells from the injector PC-1209, layer 81.

Cut off final time:

t_f is the late time when the tracer concentration reaches a 1% of the maximum measured concentration.

The final time is usually too large. It is extrapolated using an exponential decay trend in the final values of the measured concentration curve. Some authors prefer a double exponential approach.

This type of data presentation helps the reservoir engineer and geologist to relate the measured tracer data with the available geological data of the producing layer under study.

In the plot of maps like the one presented in Fig. 61, arrival time and relative amount of produced tritiated water in the injection pattern is plotted on a map of the net pay distribution of the layer and the estimated existing geological faults. The areas of the circles surrounding the producing wells are proportional to the recovered tritiated water. Usually the geological maps have some degree of uncertainty, due to the fact that they are obtained from extrapolated logging measurements made at the wells or inferred from seismic measurements made at the surface. The flow behaviour of the injected water provides, instead, a direct knowledge on the hydrodynamic characteristics of the layer. It gives a direct information of the degree of seal of the faults and the role they play in the flow paths. Some faults provide a sealant effect in the flow acting like impermeable barriers. In other geological formations the faults can be high permeability zones giving preferential flow directions.

From this analysis it is possible to have enough information to make improvements in the operation, such as to reduce injection rates, to decide a polymer injection to reduce water relative permeability (conformance treatment) or to decide the shutoff of the water invaded zones.

Second level interpretation

A second level of interpretation is based on the use of analytical or numerical models of the flow of tracers in porous media. By matching the observed data with the models it is possible to measure the parameters of the model such as dispersion coefficients or permeability. However, due to the high complexity of the flow of fluids in the reservoirs the use of these models must be done with caution. Oil reservoirs are very complex systems where at least two phases (oil and water) flow in a heterogeneous three dimensional porous media of not well known shape and dimensions.

Analytical models

The usual procedure is to simplify assumptions to describe the real system with simplified differential equations. The differential equations are solved using the appropriate initial and boundary conditions, and the resulting analytical solutions are used to describe the model behaviour.

The simplest analytical models assume the flow of a single phase in a homogeneous, constant thickness, infinite system, and can be used to estimate flow velocity and dispersion coefficients. These models can be used when mobility of the water and oil phases are similar (mobility is the ratio of the relative permeability to the viscosity of the phase). Also, we are using them when the mobility of the oil is much lower than the water mobility, in such a way that the flow of oil can be neglected. This is usually the case when there are a strong channelling of water in viscous oil and the producing well have close 100% of water-oil ratio.

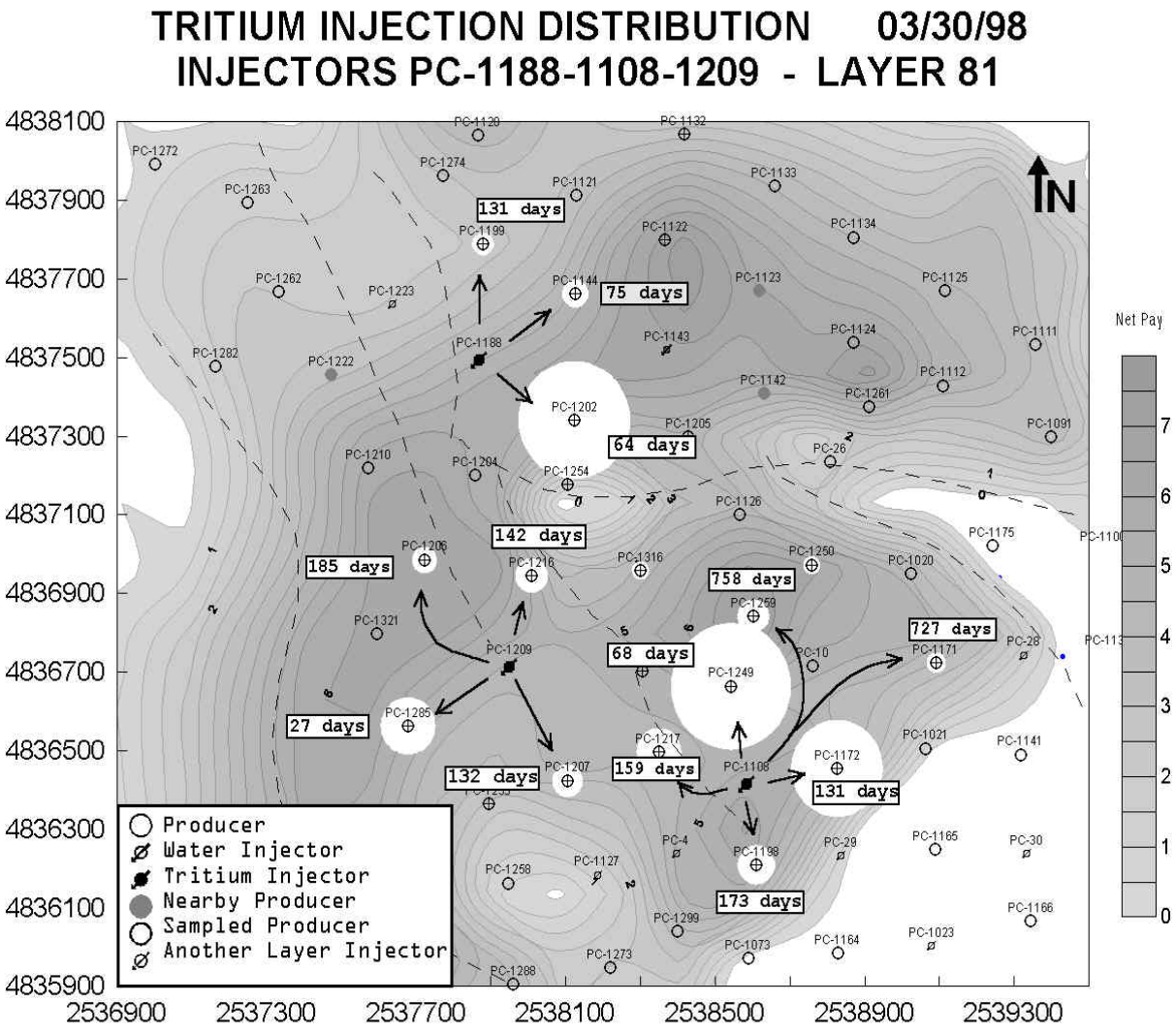

FIG. 61. Map of central zone of the field showing transit times and circles proportional to the accumulated tritiated water.

A pattern of oil secondary recovery in which water is pumped into an injection well surrounded by several production wells can be modelled as a system ruled by radial flow. In such a case, the tracer concentration as a function of time and space can be analysed by means of the classical dispersion equation for unidimensional flow.

$$D\frac{\partial^2 C}{\partial x^2} - v\frac{\partial C}{\partial x} = \frac{\partial C}{\partial t}$$

Lenda and Zuber proposed the following solution (model) where concentration is described in terms of space and time.

$$C(x,t) = C_{REF}\frac{1}{\sqrt{4\pi\frac{D_l}{v}\frac{}{x}t_N^3}}e^{-\frac{(1-t_N)^2}{4\frac{D_l}{vx}t_N}} \qquad (16)$$

where

$C(x,t)$	is the tracer concentration as a function of distance and time (Bq/m^3),
t_N	is normalized time (adim.),
D_l	is the coefficient of dispersion (m^2/day),
v	is tracer velocity (m/day),
x	is distance from the injection point (m),
C_{REF} :	reference tracer concentration (Bq/m^3).

Matching of the above equation to experimental data is shown in Fig. 62 for a complex response with four picks. The complex response of this well was approached using four simple functions based on the axial dispersed plug flow model. A possible explanation of the tracer behaviour could be that it reached the production well following four paths of different permeability belonging to a unique layer. The complex response curve was decomposed in four elementary functions that represent four parallel flows (Fig. 63).

The total amount of tracer recovered in this well was 46%, in relation to the injected activity. The parameter f_i is the contribution of each path expressed as a fraction of this percentage and was evaluated from the area under each curve. The parameters of each function are exposed in the following Table 10.

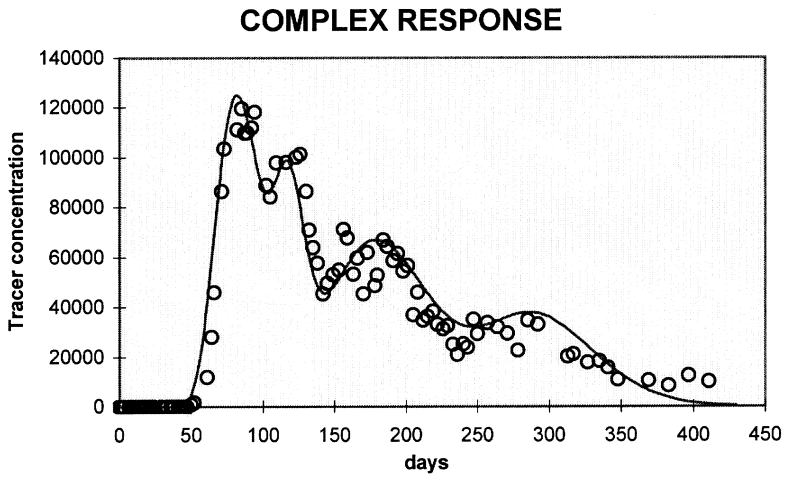

FIG. 62. Matching of experimental data with analytical model of Lenda and Zuber.

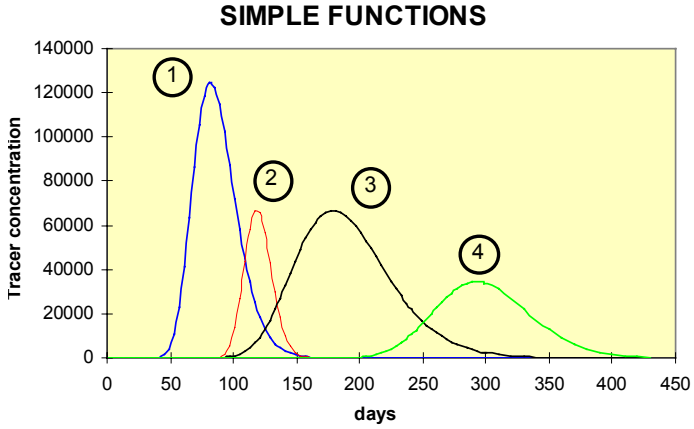

FIG. 63. Individual theoretical functions.

TABLE 10. FUNCTION PARAMETERS

Curve	D_l/vx	t_{mean} (days)	f_I
Curve 1	0,020	87	0,292
Curve 2	0,004	120	0,105
Curve 3	0,020	190	0,384
Curve 4	0,008	300	0,219

6.6. CASE STUDY 1: TRITIUM TRACER DISTRIBUTION AROUND INJECTION WELL

Fig. 64 shows a pattern belonging to an oil reservoir sited in Southern Argentina where an interwell study by means of radiotracers was performed. K-22 is the injection well where tritium tracer was injected.

Since tritium was the selected tracer, liquid scintillation technique was used for measurement. The detection limit was calculated using the parameters in the following Table 12. Because of operative limitations in the measurement laboratory, samples were not distilled before counting and, in addition, a short counting time was used. For that reason the detection limit was much higher than usual.

From the detection limit the mean output concentration was fixed as ten times this value (295 Bq/L), which leads to an activity of 167 GBq (4.5 Ci). In fact, 10 Ci of tritiated water was injected in well K-22 using the bypass injection device.

Fig. 65 shows an example of tracer concentration and cumulative response curves for well K-329 whose output was followed during a full year. according to K-22 pattern.

Information in Table 13 is extracted from a quick analysis of the graph.

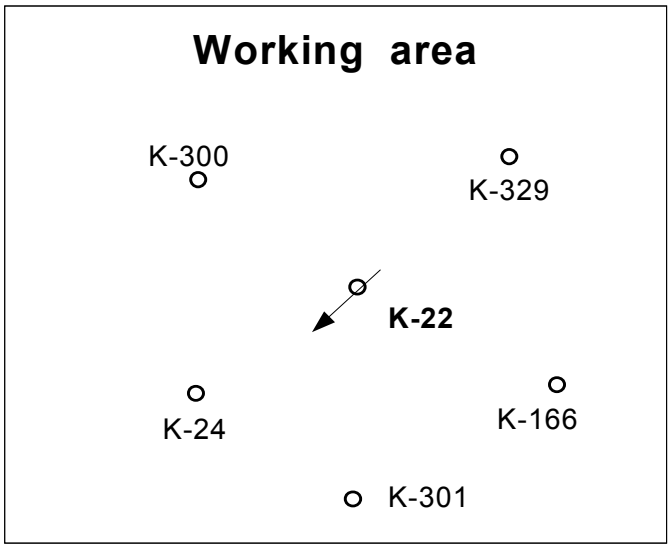

FIG. 64. Reservoir pattern.

TABLE 11. K-22 PATTERN RESERVOIR PARAMETER VALUES

Parameter (K-22 pattern)	Value
Maximum injector-producer distance	284 m
Mean layer porosity	0.32
Water saturation	0.5
Mean layer thickness	14 m
Volume	567 590 m^3

TABLE 12. DETECTION SET-UP PARAMETERS FOR HTO ANALYSIS OF SAMPLES FROM K-22 PATTERN

Parameter (K-22 pattern)	**Value**
Background	20 cpm
Efficiency	0.28 (counts/disintegration)
Measurement time	10 min.
Volume of the sample	8 mL
Detection limit	29.5 Bq/L

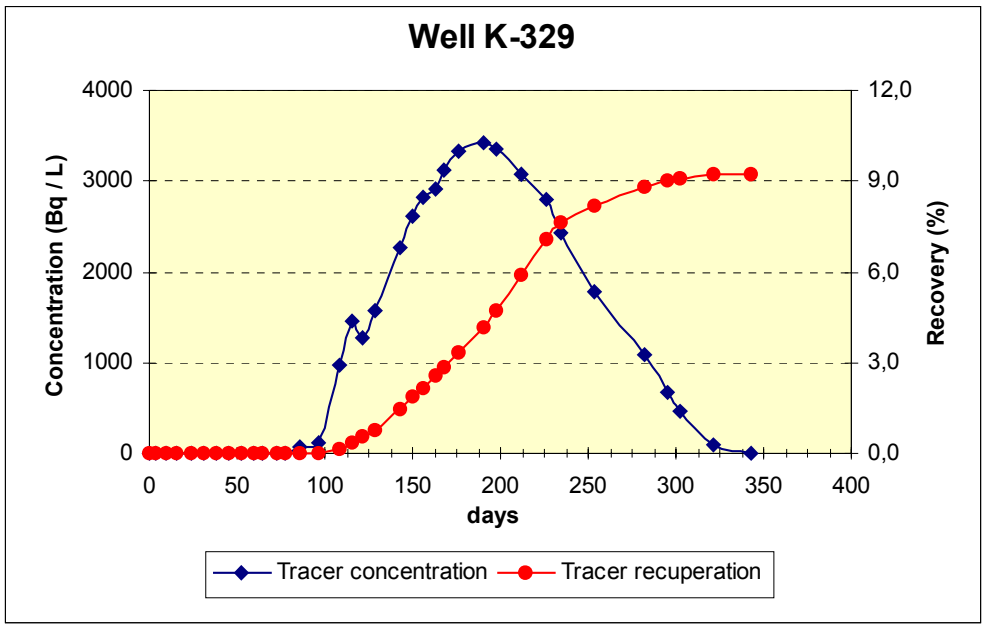

FIG. 65. Tracer concentration and cumulative response cures for well K-329.

TABLE 13. INFORMATION DERIVED FROM THE TRACER RESPONSE CURVE FOR WELL K-329

Parameter (well K-329)	Value
Breakthrough	86 days
MRT	193 days
Final time	321 days
Tracer recuperation	9.2%

The distance between K-22 and K-329 wells is 251 m. Minimum, medium and maximum water velocities were 0.78 m/day, 1.3 m/day and 2.9 m/day, respectively.

Permeability was also evaluated using the simplified expression. A value of 282 mD was obtained, which was deemed to be reasonable by reservoir engineers.

An approach by means a radial dispersion model was made by use of a simple software for the basic processing of the response curves coming from interwell studies. MRT of 210 days and a dispersivity factor of 0.04 were used. Fig. 66 shows the result.

From this theoretical approach some basic parameters were calculated again. Table 16 shows a comparison between both sets of data.

The volumetric response for well K-329 appears in Fig. 67 in terms of cumulative injected volume.

In this case, information in Table 14 is extracted from a quick analysis of the graph.

The last value is the pore volume swept from the injector to the production well (K-329). It is equal to the mean volume multiplied by the recuperation factor (0.092 or 9.2%).

From the same pattern, well K-301 is another good example because the sampling was interrupted before the output concentration reached the background level, Fig. 68.

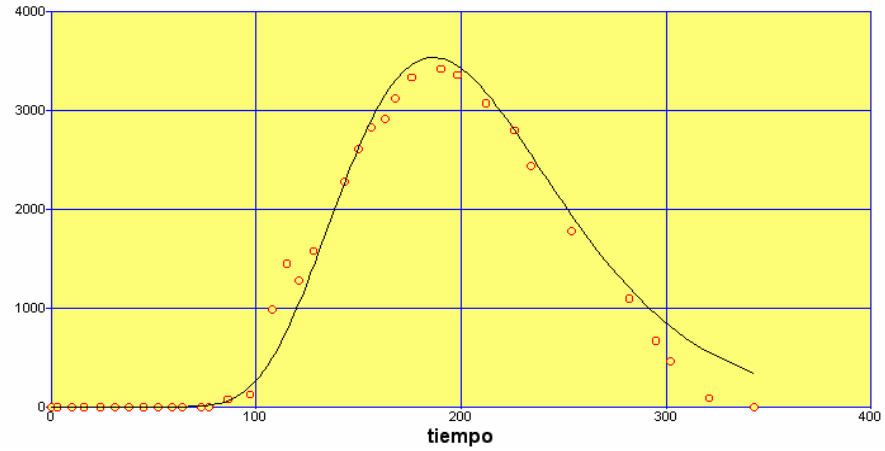

FIG. 66. Results of an approach by means of a radial dispersion model.

TABLE 14. COMPARISON BETWEEN EXPERIMENTAL AND THEORETICALLY DERIVED TRACER RESPONSE CURVE PARAMETERS FOR WELL K-329

Parameter (well K-329)	Unit	Experimental	Model
Breakthrough	days	86	75
MRT	days	193	210
Final time	days	312	410
Tracer recuperation	%	9.2	9.1

TABLE 15. RESERVOIR INFORMATION EXTRACTED FROM THE TRACER RESPONSE CURVE IN WELL K-329

Parameter (well K-329)	Value
Breakthrough	86 days
Mean volume	19.073 m^3
Swept volume	1.775 m^3

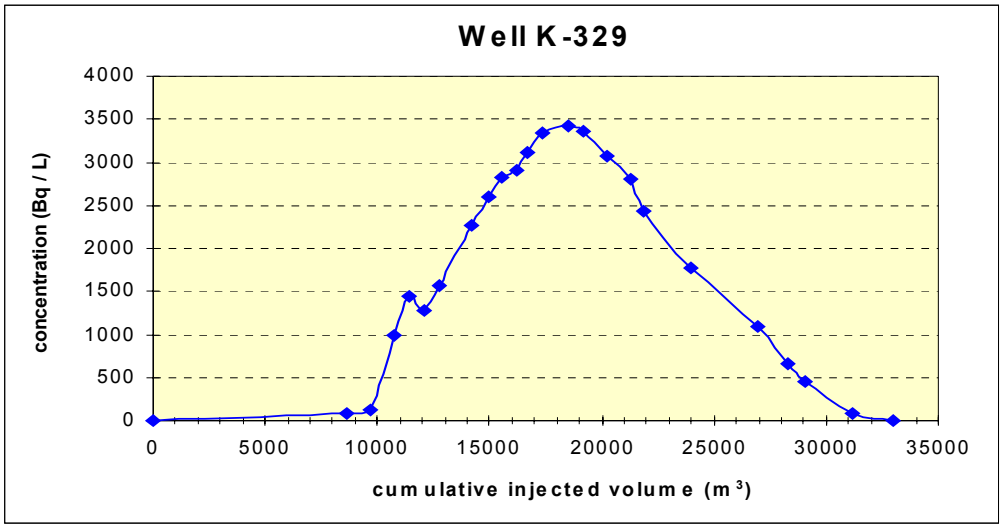

FIG. 67. Volumetric response for well K-329.

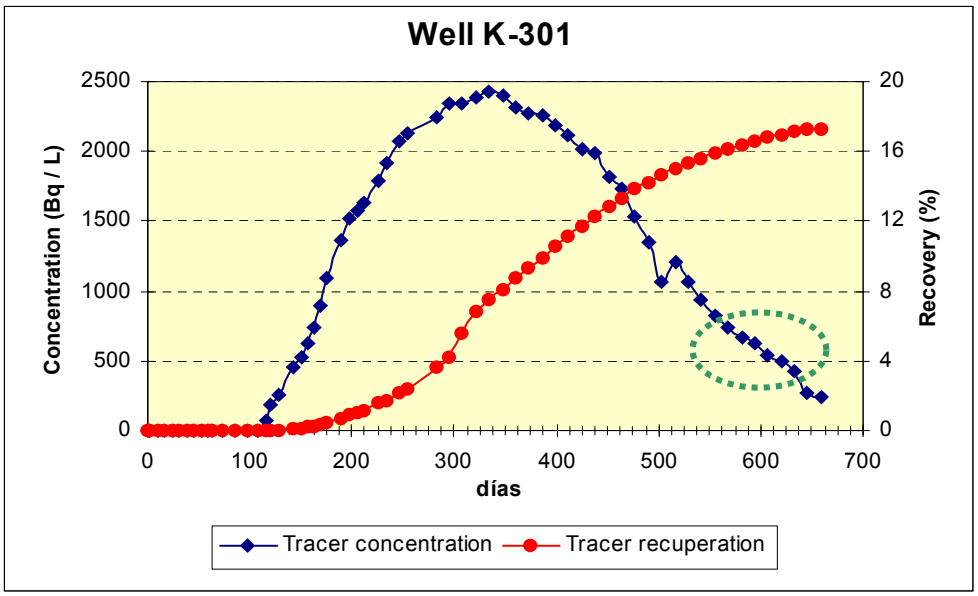

FIG. 68. Instantaneous and cumulative response curves (well K-301).

The concentration curve tail was extrapolated on the basis of points surrounded by the ellipse arriving at results shown in Fig. 69.

The following exponential function was used for extrapolation purposes:

$$C(t) = 932\, e^{-0{,}0083\,(t-542)}$$

A better evaluation of the basic parameters was obtained from the complete curve (the experimental data plus the extrapolated tail). A comparison is presented in Table 16.

The tracer distribution among the wells belonging to the K-22 pattern is shown in Fig. 70. The total tracer recuperation was 62.8%.

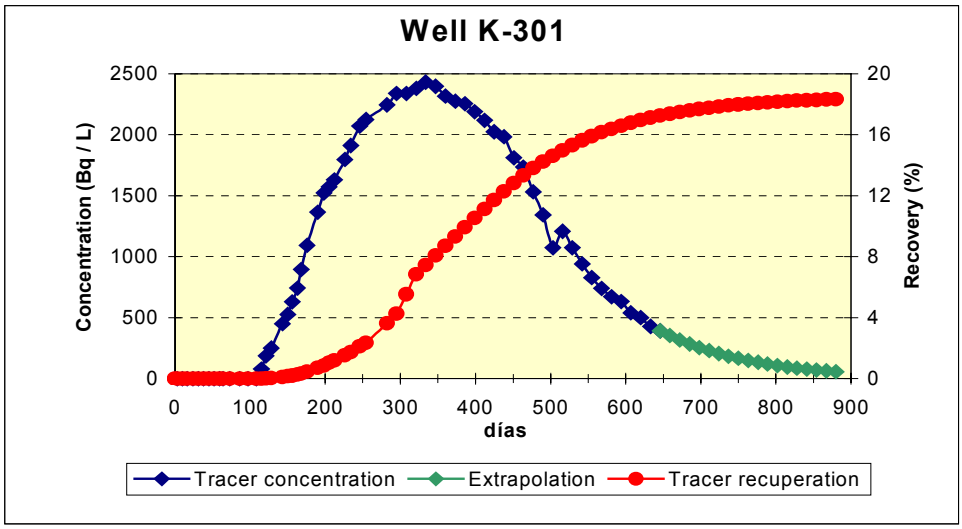

FIG. 69. Concentration curve with extrapolated tail (well K-301).

TABLE 16. COMPARISON OF BASIC PARAMETERS

Parameter (well K-301)	Unit	Experimental data	Experimental data + extrapolated tail
Breakthrough	Days	115	115
MRT	Days	363	380
Final time	Days	659	880
Tracer recuperation	%	17.3	18.3

6.7. CASE STUDY 2: ^{35}S-SCN$^-$ RADIOTRACER IN INTERWELL WATERFLOOD

The tracer investigation was conducted in the ShengLi Oil field, China. It lasted for 120 days.

The purpose of this test was to validate the $^{35}SCN^-$ as the tracer and verify possible connections between wells throughout the fault.

The well group consisted of injector well, namely: M4-3-30 and six producers wells around it, namely M4-3-28, M4-3-31, M4-4-29, M4-5-30, M12-8-1 and M12-10-1.

The rate of water injection in well M4-3-30 was 72m^3/day at 10 mpa.

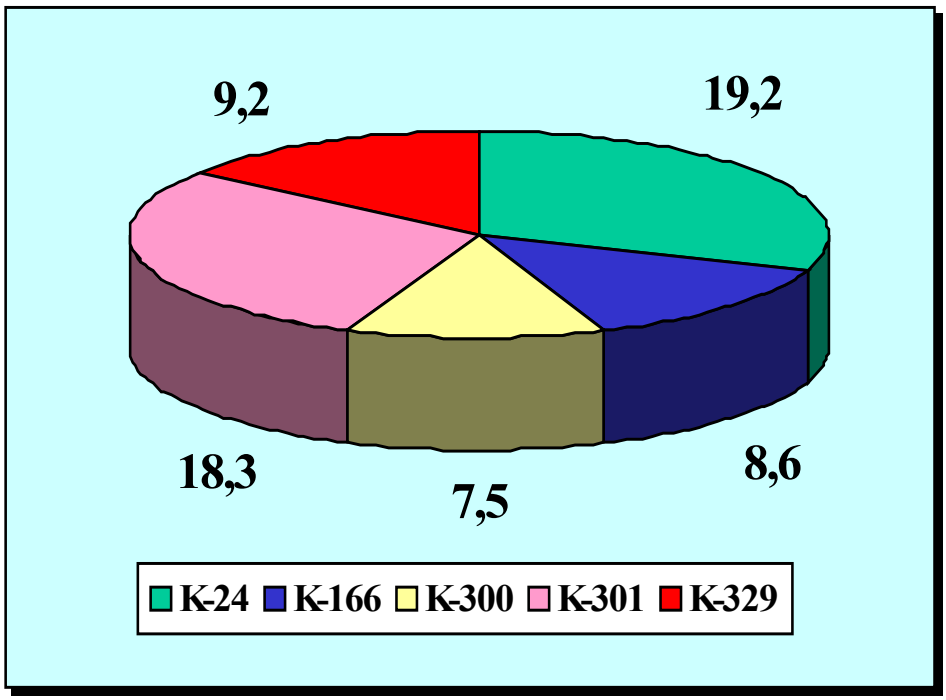

FIG. 70. Tracer distribution in the pattern.

3 mCi of ^{35}S-KSCN was injected as the tracer. Tracer was found in all of the six producers successively well. Tracer response curves are shown in Figs 71–76. Fig. 77 shows the pattern of target wells and the movement of tracer from injector to producers. It was found that the fault was not completely enclosed, there were connections between injector and producers located beside it.

6.8. CASE STUDY 3: TRITIUM AND ^{35}S-SCN AS RADIOTRACERS IN INTERWELL WATERFLOOD

The tracer experiment was carried out in the ShengLi Oil field, China for 74 days.

The purposes of this test were to evaluate waterflooding performance and compare the behaviour of $^{35}SCN^-$ with tritium.

The well group: one injector namely, CN8-10 and 8 producers, namely: CN6-8, CN6-10, CN6-12, CN8-8, CN8-12, CN10-8, CN10-10, CN10-12.

10Ci of THO and 10 mCi of ^{35}S-KSCN was injected as the tracers simultaneously in the same injection well. Tracers were found in 4 of the 8 producer wells successively. The response to THO and ^{35}S-KSCN was quite identical from detection sensitivity and flow behaviour point of views.

Tracer response curves are shown in Figs 78 and 79. They were almost the same for both tracers. Fig. 80 shows the pattern of target wells and the movement of tracer from injector to producers.

Text cont. on page 84.

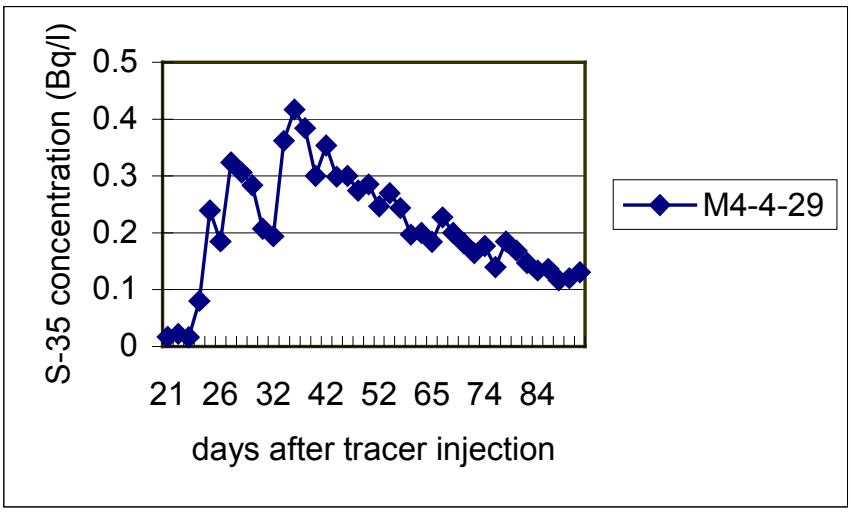

FIG. 71. Tracer response curve.

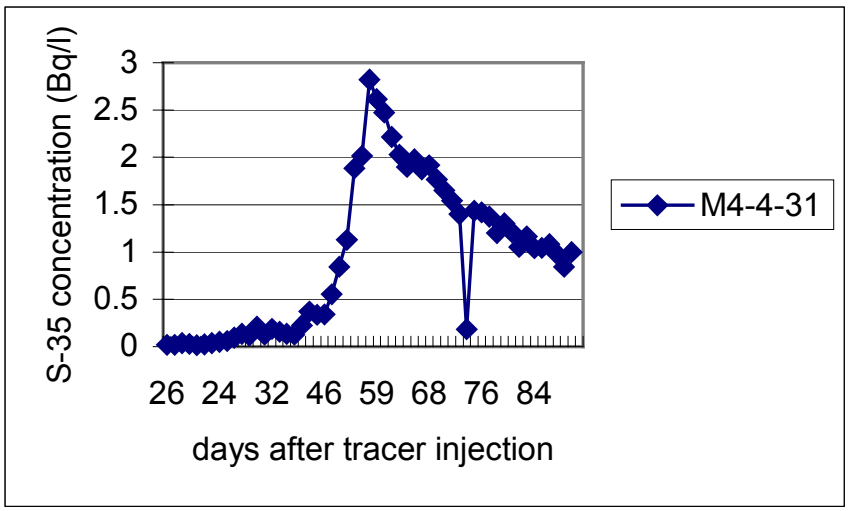

FIG. 72. Tracer response curve.

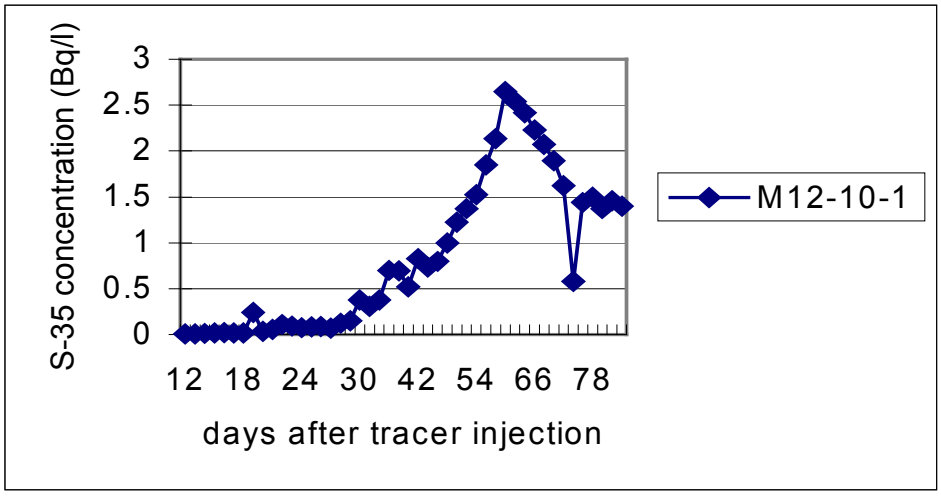

FIG. 73. Tracer response curve.

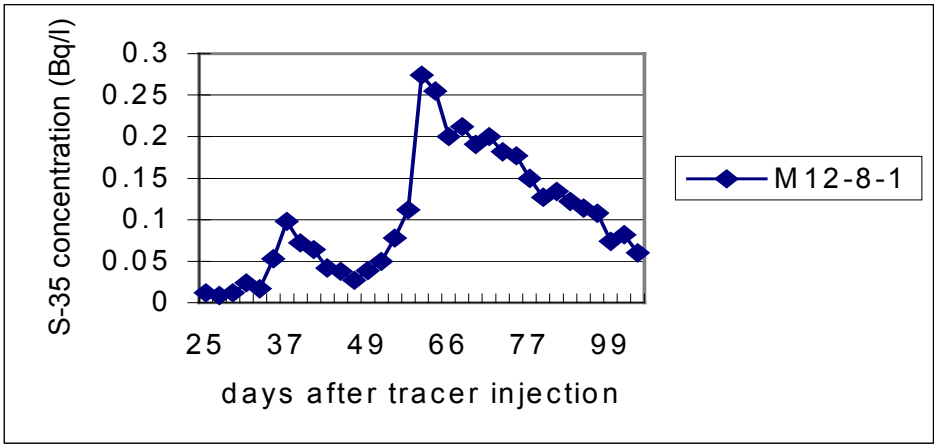

FIG. 74. Tracer response curve.

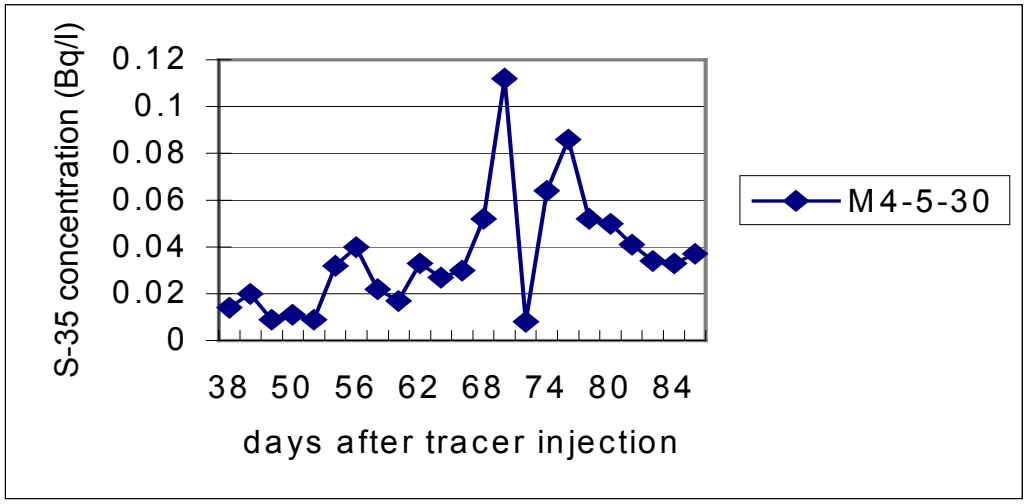

FIG. 75. Tracer response curve.

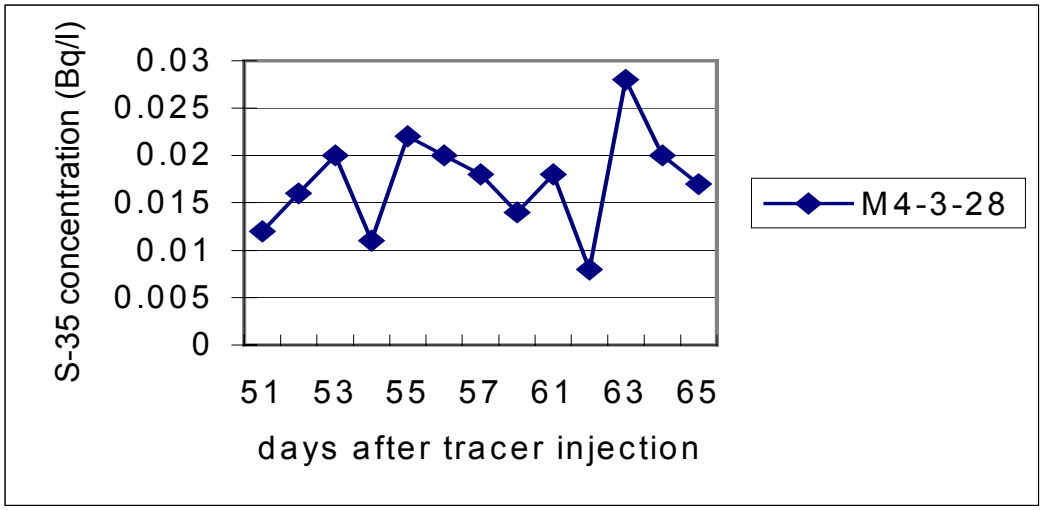

FIG. 76. Tracer response curve.

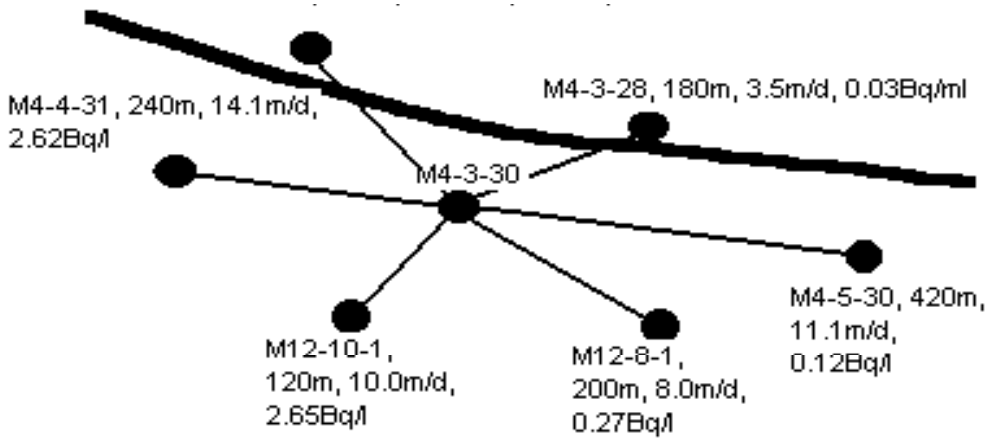

FIG.77. Tracer movement.

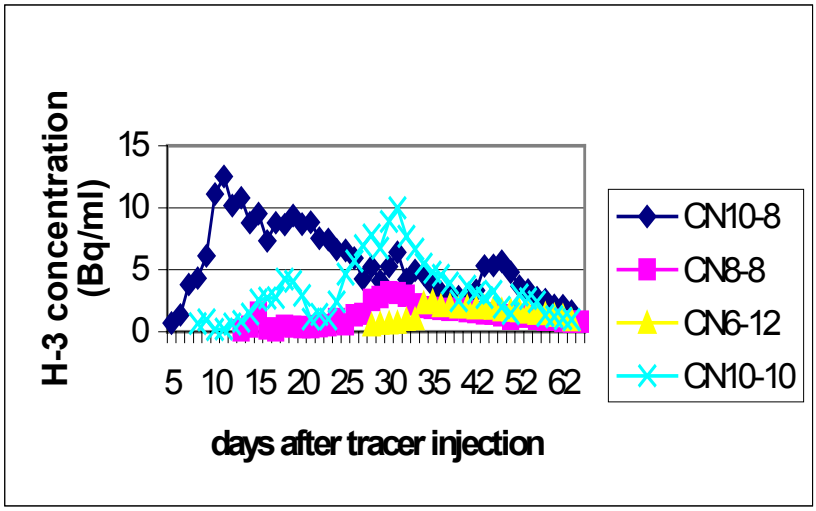

FIG. 78. Tracer response profiles, THO.

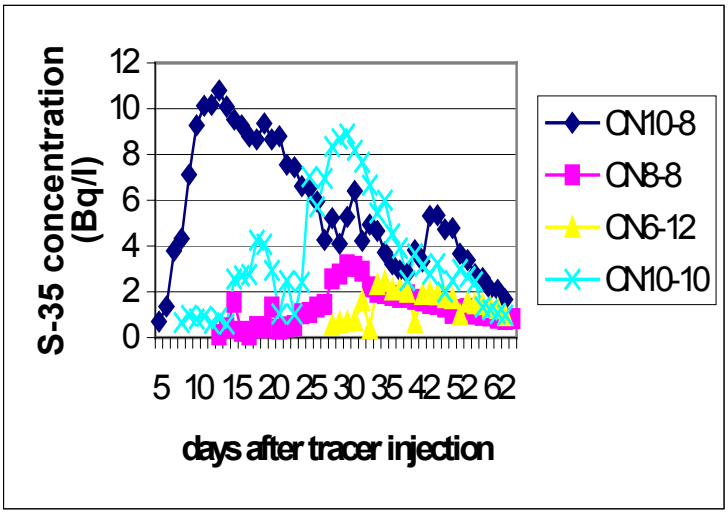

FIG. 79. Tracer response profiles, ^{35}S-$KSCN^-$.

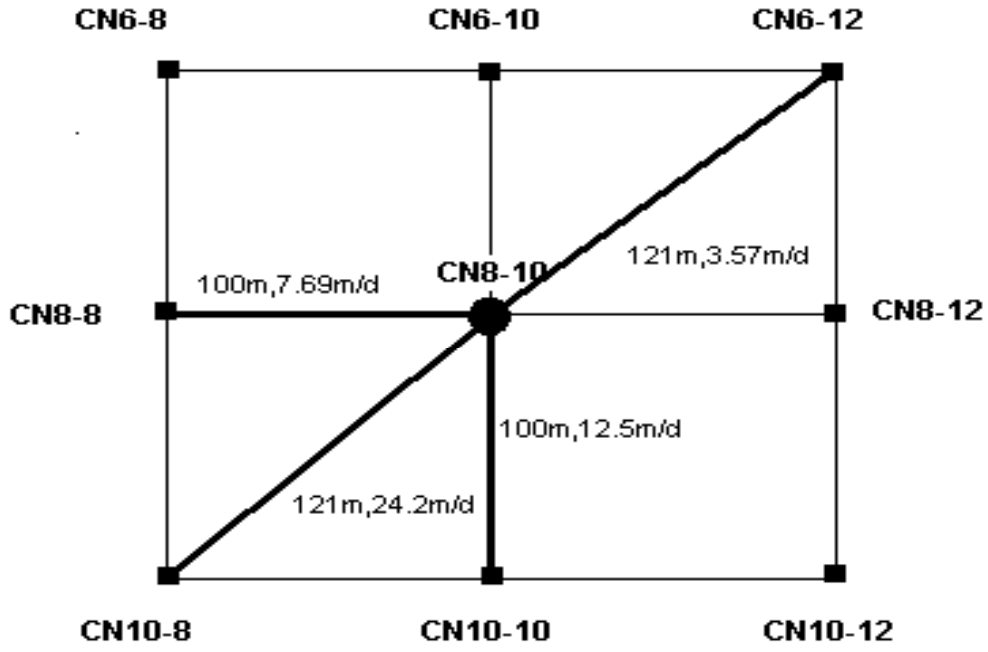

FIG. 80. Wells pattern of CN8-10 group and tracer movement.

6.9. CASE STUDY 4: FIELD TEST USING THO, $^{35}SCN^-$ AND CO-58 TAGGED $K_3[Co(CN)]_6$ AS TRACERS

The multitracer investigation ran for one year at the Tuha Oil field in China.

The purpose of this test was to evaluate waterflooding.

The well group consisted of three injectors, namely: 15–24, 14–26 and 13–26, and 11 producers, namely, 12–25, 13–25, 14–25, 15–25, 14–23, 13–28, L38, 14–27, 15–23, 16–25 and 15–27.

30 Ci of THO, 1.0 Ci of ^{35}S-KSCN and 1.0 Ci of Co-58 tagged $K_3[Co(CN)_6$ were injected separately as tracers into three injection wells of an oil field (15–24, 14–26 and 13–26). Tracers were found in producer wells successively.

Typical tracer response curves are shown in Figs 81a–81c. In the producer well 14–25, three tracers were found. It means that production well 14–25 is fed from the three injection wells 15–24, 14–26 and 13–26.

In three producer wells 15–25, 14–27 and 13–25, two kinds of tracers were found.

$^{35}SCN^-$ injected in the well 13–26 was found in the production wells 13–28 and 12–25. T and Co-58 were also found behind fault. It was found that faults located between injection and production wells are not a barrier for water movement.

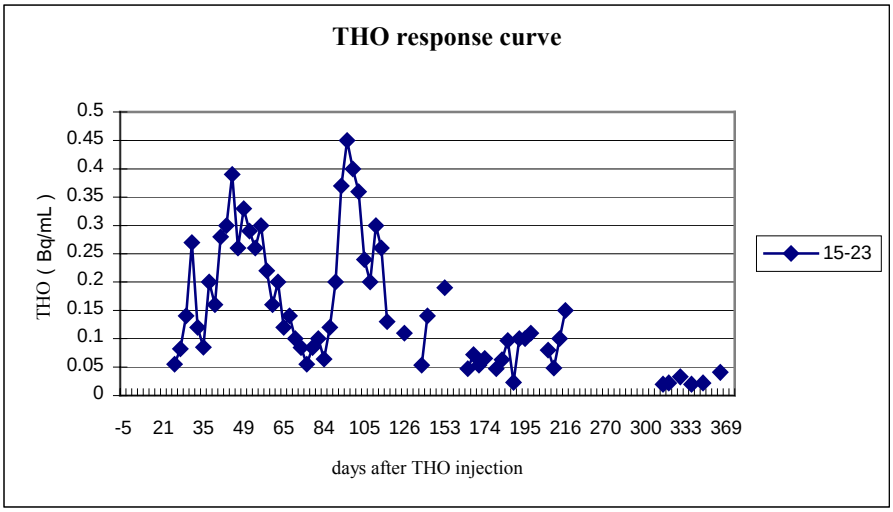

FIG. 81a. Tracer response curve, THO.

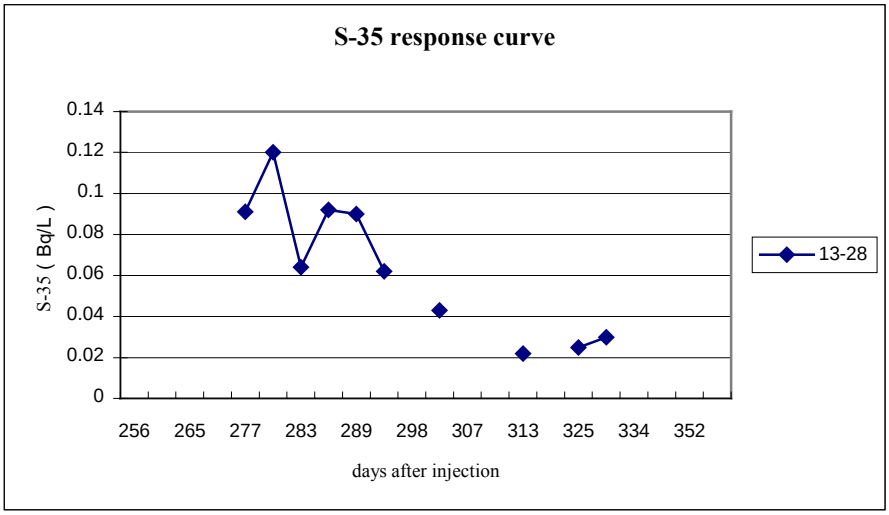

FIG. 81b. Tracer response curve, S-35.

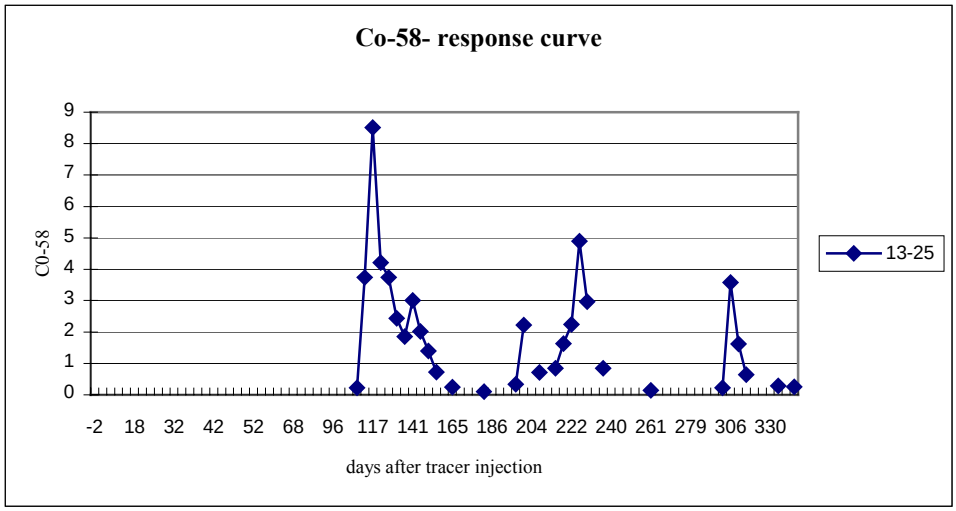

FIG. 81c. Tracer response curve, Co-58.

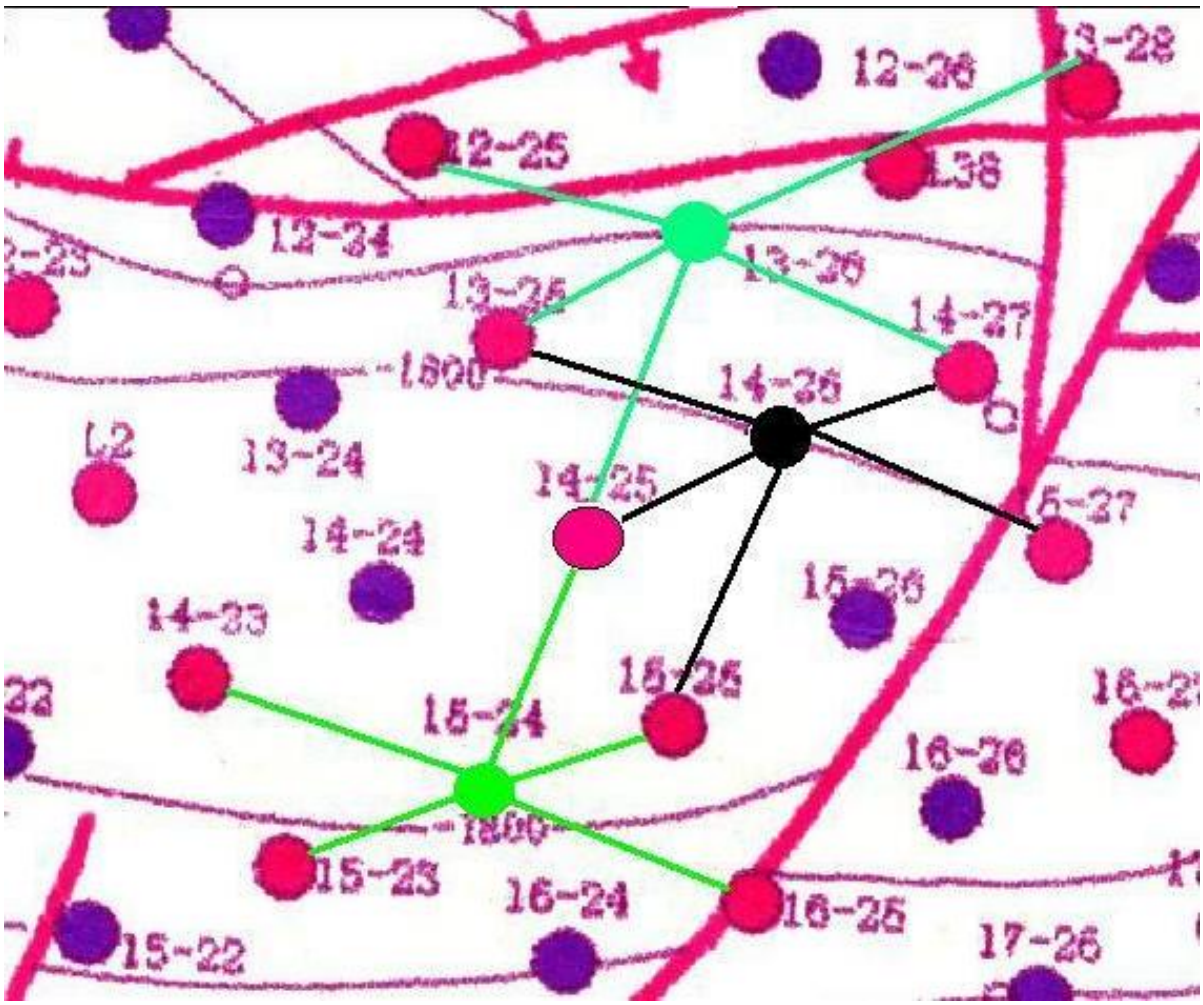

FIG. 82. Wells pattern and tracer movement in QL test.

Well position and tracer movement directions are shown in the oil field map (Fig. 82).

6.10. CONCLUSIONS

By now interwell tracer examinations are increasingly recognized as an important tool for improved reservoir evaluation, thereby contributing to optimal petroleum production. What are the prospects for further expansion?

There is, at present, a strong demand for reducing cost of petroleum production. Simultaneously, one sees an enormous increase in technical complexity of oilfield operations, especially offshore oil fields. New well concepts, remote operation, reduced manpower and increased environmental constraints call for high level and innovative technical solutions in operation monitoring. In this picture tracer technology may play an important role, both for reservoir and well monitoring, since it is relatively cheap (good value for money), and the prospects for automatization and unattended operation are present.

Presently there is good activity in the further development of interwell tracer technology. This development is concentrated in various topics including new radioactive and non-radioactive tracers for reservoir fluids, improved and new analytical techniques for tracers

in reservoir fluids, improved and new interpretation techniques including finite difference reservoir simulator modelling and innovative techniques for tracer injection and sampling.

New areas of tracer use like measurement of residual (and even remaining) oil saturation by the simultaneous use of passive water tracers and water/oil partitioning tracers will be implemented (see principle in Fig. 83) [23].

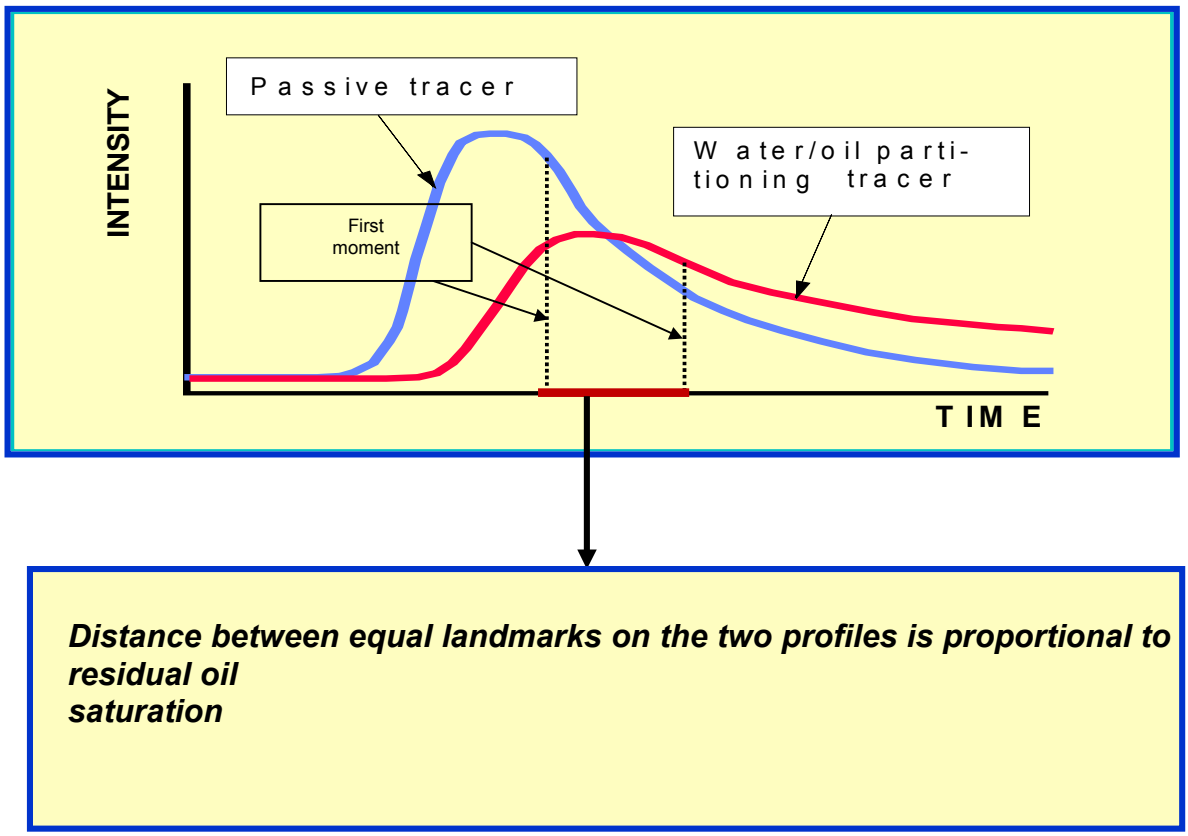

FIG.83. Principle sketch on tracer production curves of passive and phase partitioning tracers and parameters related to residual oil saturation.

A number of new non-radioactive passive and phase partitioning tracers have been developed lately and field proven for injection water (polyfluorinated benzoic acids) and injection gas (perfluorinated cyclic hydrocarbons). The development continues in different directions including experiments on polydeuterated compounds, organometallic macromolecules, complex organic sulphonic acids and even DNA-derivatives. Some of these are intended to be radiolabelled.

The future will, most probably, also see an increase in on-line and in-line analytical techniques with automatic data transfer. Zone injection of tracers will be used more.

New relations will be developed between the use of tracer data, well-test data and 4D seismic data (integrated data evaluation).

Radiotracer methodology will still have its natural and technically non-disputable position. The standard reference tracer for injection water and reservoir gas will still be

tritiated water, HTO, and tritiated methane, CH_3T, respectively. In some reservoir operations that include observation wells, gamma emitting tracers (like $^{22}Na^+$, $^{60}Co(CN)_6^{3-}$ etc.) may be preferred because of the possibility to log the flow in different zones by a normal wireline gamma ray logging tool in the observation well.

For high temperature operations (<150°C), reliable tracers are still scarce. For the moment the best choices are HTO (liquid scintillation counting), $^{22}Na^+$ (gamma ray spectrometry) and $^{36}Cl^-$ (atomic mass spectrometry, AMS) because of their simplicity and "non-reactivity" in reservoir brine.

For single well push-and-pull examination of near-well zones and for well operation monitoring, including subsea completion and fluid treatment systems and down-well operations, the use of radiotracer technology is likely to expand and develop into new applications.

7. TRENDS IN RESEARCH AND DEVELOPMENT IN RADIOTRACER METHODOLOGY AND TECHNOLOGY

Over the years the IAEA has contributed substantial funding and effort to the industrial applications of radiotracer technology. Significant progress has been made enabling IAEA Member States to introduce the technology in well defined industrial processing fields, and to establish national and private radiotracer groups with an indigenous capacity to sustain and further develop the technology.

Radiotracer technology is a unique tool in many cases for extracting valuable information about industrial processes, thereby contributing significantly to improving and optimizing their performance. Radiotracers have distinct advantages for providing reliable data which, at present, cannot be obtained by any other technique. Economic benefits of the use of radiotracers in industry are estimated to be hundreds of millions in US$ per year and are derived from:

— Troubleshooting. Radiotracer technology is used to diagnose specific causes of inefficiency in plant or process operation. In this context, it should be noted that in very many cases the benefit is derived in the form of savings associated with plant shutdown minimization and loss prevention.
— Process optimization. The radiotracer measurements provide information that facilitates improvements either in the throughput or the product quality.

Presently, there is a lively activity in further development and use of radiotracer technology. This development is concentrated on various topics including improvement in hardware and software as well as introducing innovative and interpretation techniques for flow pattern visualization and characterization.

There is a large diversity in techniques and applications. The following are the main generic trends in R&D in radiotracer methodology and technology.

7.1. INTEGRATION OF RTD TRACING WITH CFD SIMULATION FOR INDUSTRIAL PROCESS VISUALIZATION AND OPTIMIZATION

RTD method has been continuously developed and used. The treatment of RTD curves for extracting important parameters of industrial processes has achieved a good standard. Efficient RTD software was validated for modeling of various chemical engineering reactors. But RTD method still remains a global approach. RTD systemic analysis requires choice of a model, which is often semi-empirical and rather idealized (combination of perfect mixers, dead volumes, etc.). There are some situations in which the RTD approach can not be applied, i.e. no linear systems.

Industry is looking for more predictive techniques. CFD method provides detailed spatial distribution of flow fields. CFD is easily coupled with modern tools for three dimensional visualization, creating maps of velocity vectors, streamlines, iso-value contours, etc. CFD has the capacity to extrapolate to other flow conditions once it is validated. In this way a limited number of tracer experiments could be expected to cover a wide variety of flow conditions [25].

There is a need is to elaborate a combined RTD-CFD experimental computational method for obtaining reliable quantitative results about process insight in industrial vessels and process units to improve and optimize their design and efficiency. The integrated RTD-CFD method will be used to investigate typical complex chemical engineering processes in:

— heat exchangers
— crystallizers
— ore classification processes and cyclones
— mixing tanks and homogenization devices
— dryers and incinerators
— waste water treatment plants.

7.2. RADIOTRACER IMAGING TECHNIQUES FOR INDUSTRIAL PROCESS VISUALIZATION

New development is expected in introducing new radiotracers 2D and 3D imaging techniques for localization and visualization of flow patterns in multiphase systems.

Emission tomography is the last step in research and development in radiotracer methodology. The real time imaging techniques for flow pattern visualization inside vessels are important for investigating multiphase flow systems. Industrial process imaging is quite similar to nuclear medicine imaging.

Among the various techniques, single photon emission computed tomography (SPECT) method shows some promise. 2D imaging with a gamma camera is also an attractive device at a laboratory scale. Single particle tracking technique has been developed, in particular, to investigate fluidized bed reactors [26–29].

Emission tomography provides two dimensional maps of the count rates which, when properly interpreted, yield the radiotracer instantaneous concentration field. Coupled with single radioactive particle tracking, which yields the velocity field, the above techniques complement each other and provide unique means for quantification of multiphase opaque

flow fields which cannot be accomplished by any other means. The validation of radiotracer-imaging techniques for visualization of fluid patterns inside structures for industrial process design and optimization is a trend in the near future.

In fact the hardware and software related with development of radioisotope imaging techniques are very costly and industry cannot yet afford routine applications. The R&D is conducted mainly in developed country laboratories. The techniques are not yet mature to be transferred to developing countries and to end users. But the need is evident and R&D is progressing quite well.

7.3. RADIOMETRIC TECHNIQUES FOR MULTIPHASE FLOW DETERMINATION

Accurate measurement of flow in multi-phase systems (e.g. liquid-solid, solid-gas or gas/water/oil) is of great interest in many industrial processes, especially in oil, coal and mining industries, mineral ore processing, chemical and petrochemical plants, and long distance fluid transportation pipelines.

The radiotracer technique based on injection of radiotracer into the system provides accurate results mainly in mono phase flows. Radiotracer technique is used mostly for calibration of flow meters than for continuous flow rate measurements.

Gamma ray transmission technique, known as gamma ray cross correlation technique, seems attractive for on-line flow rate measurement, in particular in multiphase flows. The R&D in radiometric techniques for multiphase flow determination is going on, driven by a strong interest of end users — in oil field production, in particular.

7.4. RADIOTRACER APPLICATIONS FOR OIL RESERVOIR EVALUATION

The oil production industry remains a priority for all oil producing developing countries. Radiotracer technology has become an integrated and indispensable part of multidisiplinary investigation in oil fields for oil reservoir evaluation. Radiotracer applications can be found in almost any stage of oil field development. In many operations the application of radiotracer technology is indispensable and irreplaceable.

There is a growing consensus that research in oil reservoir technology needs to be increased in the future due to progressing difficulties in recovering remaining oil as the oil reservoirs grow mature and enter into the tail production. A good reservoir description and knowledge about the positions and concentration of remaining accumulations are imperative. There is also a growing interest in developing smaller oil fields, which will not be economically feasible with traditional technology.

Petroleum reservoirs are complex structures, and tracers help unambiguously in narrowing down interpretation possibilities. However, tracer response data need to be interpreted better. One may roughly divide the interpretation into four stages:

— extraction of qualitative and semi-quantitative data by simple calculations
— fitting the response curve with a simple dispersion function to derive quantitative information of some parameters

— streamline modeling where reservoir geological and geophysical data can be taken into account
— full finite difference or finite element modeling where all known reservoir data can be treated comprehensively, including tracer data.

The R&D programme aims to further develop and refine radiotracer methodology for oil reservoir evaluation: to prepare, test and validate new tracers, analysis and field operation techniques, as well as improve modeling and interpretation of tracer data.

Previously, much of the technology development (including tracer technology) was carried out within each of the major multinational oil companies. Thus, the technology became proprietary, and was generally not disclosed to competitors or to the scientific literature. In recent years there has been a considerable structural change by company merger and closedown of company internal research centre. This has also led to a climate change in the view on technology development. The research in tracer methodology as applied to oil field production is becoming more transparent now due to the need for new ideas and improved techniques for optimizing oil recovery from more and more complex reservoir situations. Companies are more prone to join forces in technology development (in so-called Joint Industry Projects or JIPs) where research is outsourced to external competent institutions.

In this context, IAEA may play an important role to co-ordinate generation of knowledge in this field, guarantee continuity of the technology, and transfer mature techniques to developing countries.

REFERENCES

[1] INTERNATIONAL ATOMIC ENERGY AGENCY, Guidebook on Radioisotope Tracers in Industry, Technical Reports Series No. 316, IAEA, Vienna (1990).

[2] VILLERMAUX, J., Génie de la réaction chimique; conception et fonctionnement des réacteurs, Tec&Doc, Lavoisier, Paris (1993).

[3] BLET, V., BERNE, PH., TOLA, F., VITART, X., CHAUSSY, C., Recent developments in radioactive tracers methodology, Appl. Rad. and Isot. **51** (1999) 615–624.

[4] THYN, J., ZITNY, R., KLUSON, J., CECHAK, T., Analysis and diagnostics of industrial processes by radiotracers and radioisotope sealed sources, CVUT, Prague (2000).

[5] LECLERC, J.P., CLAUDEL, S., POTTIER, O., LINTZ, H.G., ANTOINE, B., Theoretical interpretation of residence time distribution measurements in industrial processes, Oil and Gas Science and Technology — Revue de l'Institut Français du Pétrole, **55** n°2 (2000) 159–169.

[6] BERNE, PH., BLET, V., Assessment of the systemic approach using radioactive tracers and CFD (Proc. 6th International Conference on Air Distribution in Rooms, Stockholm) (1998).

[7] PROGEPI, Instruction Manual "Software DTSPRO V4.2", Nancy, France (2000).

[8] ZITNY, R., THYN, J., Residence Time Distribution Software Analysis, User's Manual, IAEA Computer Manual Series, IAEA, Vienna (1996).

[9] TOLA, F., Ecrin, code Monte-Carlo de simulation de la réponse d'un détecteur à un mélange de traceurs radioactifs uniformément distribués dans une conduite cylindrique, Internal report CEA/DTA/DAMRI/SAR/96-111/T40 (1996).

[10] FOOD AND AGRICULTURE ORGANIZATION OF THE UNITED NATIONS, INTERNATIONAL ATOMIC ENERGY AGENCY, INTERNATIONAL LABOUR ORGANISATION, NUCLEAR ENERGY AGENCY OF THE ORGANISATION FOR ECONOMIC CO-OPERATION AND DEVELOPMENT, PAN AMERICAN HEALTH ORGANIZATION, WORLD HEALTH ORGANIZATION, International Basic Safety Standards for Protection against Ionizing Radiation and for the Safety of Radiation Sources, Safety Series No. 115, IAEA, Vienna (1996).

[11] INTERNATIONAL ATOMIC ENERGY AGENCY, Occupational Radiation Protection, Safety Standards Series, Safety Guide No. RS-G-1.1, IAEA, Vienna (1999).

[12] INTERNATIONAL ATOMIC ENERGY AGENCY, Safety Assessment Plans for Authorization and Inspection of Radiation Sources, IAEA-TECDOC-1113, Vienna (1999).

[13] INTERNATIONAL ATOMIC ENERGY AGENCY, Regulations for the Safe Transport of Radioactive Material — 1996 Edition (Revised), Safety Standards Series No. ST-1, IAEA, Vienna (1996).

[14] CHARLTON, J.S., Radioisotope Techniques for Problem Solving in Industrial Process Plants, Leonard Hill, Glasgow and London (1986).

[15] SEVEL, T., PEDERSEN, N.H., GENDERS, S., "Tracing of oil, gas, and water in the oil and gas industry" (Proc. 7th ECNDT Conference) (1998).

[16] AFNOR, Mesure de débit des fluides — Conduites fermées, Recueil des Normes Françaises NF X 10–131 (1983) 7.

[17] CHMIELEWSKI, A.G., OWCZARCZYK, A., PALIGE, J., Radiotracer investigations of industrial wastewater equalizer-clarifiers, Nukleonika **43** 2 (1998) 185–194.

[18] POTIER, O., PONS, M.N., ROCHE, N., LECLERC, J.P., PROST, C., "Hydrodynamics of activated sludge channel reactor" (Proc. 16th Colloqium on Chemical Reaction Engineering, Novel Chemical Reaction Engineering for Cleaner Technologies), Hungarian Journal of Industrial Chemistry, **1**, 1, Veszprem (1999) 49–51.
[19] NIEMI, A.J., ZENGER, K., THERESKA, J., MARTINEZ, J.G., Tracer testing of processes under variable flow and volume, Nukleonika **43**, 1, Poland (1998) 73–94.
[20] ZEMEL, B., Tracers in the Oil Field, Developments in Petroleum Science, 43, Elsevier Science, Amsterdam (1995).
[21] ABBASZADEH, M., BRIGHAM, W.E., Analysis of well-to-well tracer flow to determine reservoir layering, J. Petrol. Technol. (1984) 1753–1762.
[22] ALLISON, S.B., POPE, G.A., SEPEHRNOORI, K., "Analysis of Field Tracers for Reservoir Description", J. Petrol. Sci. Eng. **5** (1991) 173–186.
[23] BJØRNSTAD, T., Selection of Tracers for Oil and Gas Reservoir Evaluation, Technical Research Report IFE/KR/E-91/009 (1991) 43 pp.
[24] NAJURIETA, H.L., MAGGIO, G.E., "Empleo de radiotrazadores en la evaluación hidrodinámica de un yacimiento de petróleo viscoso", IV Congreso de Exploración y Desarrollo de Hidrocarburos. Instituto Argentino del Petróleo y Gas. Mar del Plata (1999).
[25] DELAPLACE, G., et al., Tracer experiment — a way to validate computational fluid dynamic simulation in an agitated vessel (Proc. International Congress on Tracer and Tracing Methods), Nancy (2001).
[26] BLET, V., BERNE, PH., FORISSIER, M., LADET, O., PITAULT, I., SCHWEICH, D., Apport de la gamma-caméra à l'étude d'un réacteur agité triphasique de laboratoire (Proc. 1st French Congress on tracers and tracer methods, Nancy) (1999).
[27] KUMAR, S.B., MOSLEMIAN, D., DUDUKOVIC, M.P., Gas holdup measurements in bubble columns using computed tomography, AIChe J. **43**, 1414.
[28] LEGOUPIL, S., Tomographie d'émission gamma à partir d'un nombre limité de détecteurs, appliquée à la visualization d'écoulements, Ph.D. Thesis, Université de Caen (1997).
[29] TOYE, D., MARCHOT, P., CRINE, M., L'HOMME, G., Modelling of multiphase flow in packed beds by computer assisted tomography, Meas. Sci. Technol. **7** (1996) 436.

ABBREVIATIONS

ADC	analogue-to-digital counter
ADPE	axial dispersion plug flow with exchange
CFD	computational fluid dynamics
COD	chemical oxygen demand
DAS	data acquisition system
EDTA	ethylenediaminetetraacetate
EOR	enhanced oil recovery
IWTT	interwell tracer test
LSC	liquid scintillation counter
MCA	multichannel analyser
MDC	minimum detectable concentration
MRT	mean residence time
MSW	municipal solid waste
RTD	residence time distribution
SD	standard deviation
SPECT	single photon emission computed tomography
TBR	trickle bed reactor

CONTRIBUTORS TO DRAFTING AND REVIEW

Berne, P.	CEA/Grenoble, France
Bjørnstad, T.	Institute for Energy Technology, Norway
Chmieliewski, A.G.	Institute of Nuclear Chemistry and Technology, Poland
Farooq, M.	Pakistan Institute of Nuclear Science and Technology, Pakistan
Furman, L.	Faculty of Physics and Nuclear Techniques, Poland
Griffith Martinez, J.	Instituto Cubano de Investigaciones Azucareras, Cuba
Jentsch, T.	Fraunhofer-Institute für Zerstorungsfreie Prüfverfahren, Germany
Leclerc, J.P.	Laboratorie des Sciences du Genie Chimique- CNRS ENSIC, France
Maggio, G.E.	NOLDOR S.R.L., Investigación y Desarollo, Argentina
Najurieta, H.	Ada Elflein 3969, Argentina
Palige, J.	Institute of Nuclear Chemistry and Technology, Poland
Pant, H.	Bhabha Atomic Research Centre, India
Pendharkar, A.S.	Bhabha Atomic Research Centre, India
Sevel, T.	FORCE Institute, Mechatronic and Sensor Technology, Denmark
Thereska, J.	International Atomic Energy Agency
Thyn, J.	Czech Technical University in Prague, Czech Republic
Viitanen, P.	Technical Research Centre of FinlandFinland
Vitart, X.	CEA/Grenoble, France
Wheatley, J.	International Atomic Energy Agency
Zhang Peixin	China Institute of Atomic Energy, China
Zitny, R.	Czech Technical University in Prague, Czech Republic